



Institute for Marine and Antarctic Studies

University of Tasmania

# **Process-based delineation of the Australian continental margin**

by

Rick Porter Smith, BSc (Hons)

Submitted in fulfilment of the requirements for the Degree of

Doctor of Philosophy

November 2010

## **DECLARATION**

### **Statement of Originality**

This thesis contains no material which has been accepted for a degree or diploma by the University or any other institution and to the best of my knowledge and belief, no material published or written by another person except where due acknowledgement is made in the text of the thesis.

Signed



Rick Smith

### **Authority of Access Statement**

The publishers of the paper comprising Chapter 2 hold the copyright for that content, and access to the material should be sought from the respective journal. The remaining non published content of the thesis may be made available for loan and limited copying in accordance with the Copyright Act 1968.

Signed



Rick. Smith

## STATEMENT OF CO-AUTHORSHIP

Chapter 2 of this thesis has been prepared as a scientific manuscript, “Porter-Smith, R., Harris, P.T., Andersen, O.B., Coleman, R., Greenslade, D. and Jenkins, C.J., 2004. Classification of the Australian continental shelf based on predicted sediment threshold exceedance from tidal currents and swell waves. *Marine Geology*, 211(1-2): 1-20”.

The following people contributed to the publication of the work undertaken as part of this thesis, Rick Smith (75%), Dr. Peter Harris (5%), Dr. Ole Andersen (5%), Prof. Richard Coleman (5%), Dr. Diana Greenslade (5%) and Dr. Chris Jenkins (5%). The design, data analysis, interpretation of the results and manuscript preparation was the primary responsibility of the candidate.

Details of the other authors roles are outlined - Dr. Peter Harris (Geoscience Australia, Canberra) and Prof. Richard Coleman (Australian Research Council, Canberra) contributed to the idea, its formalisation, and development and provided advice on preliminary manuscript preparation. Dr. Ole Andersen (Kort & Matrikelstyrelsen, Geodetic Division, Copenhagen), Dr. Diana Greenslade (Bureau of Meteorology Research Centre, Melbourne) and Dr. Chris Jenkins (Institute of Arctic & Alpine, Colorado) contributed model outputs for the analysis.

We the undersigned agree with the above stated “proportion of work undertaken” for each of the above published (or submitted) peer-reviewed manuscripts contributing to this thesis:



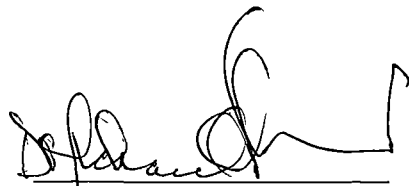
Signed:

Prof. Richard Coleman

Supervisor

IMAS

University of Tasmania



Prof. Michael Stoddart

Director

IMAS

University of Tasmania

Date: November 3, 2010

## **ABSTRACT**

This study seeks to understand and explain the present-day gross morphology of the Australian continental margin. It defines a series of robust and quantifiable process-based delineations which extend from the coastline to the foot of the continental slope through an analysis of geomorphic forms. The form and structure of the continental margin (namely the coast, shelf and slope) are the result of the interplay between geology and formative processes.

The geomorphic forms of Australia's margin are investigated with a strong emphasis on spatial and statistical analyses to define the relationships in geophysical data. Data included modelled estimates of wave and tide power, continental shelf sediment distribution, an elevation-bathymetric model and mapping of major geological structural elements and lithology. A geographical information system was used to integrate and compare these variables and map the results.

The thesis is divided into three distinct bodies of work. The first considers the relative importance of waves and tides on the Australian continental shelf to produce a delineation of wave- and tide-dominated shelves based on quantitative measures. The second investigates the development of mesoscale coastal complexity through the modulation of geomorphic form by the aforementioned marine processes over geologic time. The third examines the interactions between the continental slope and the continental shelf and deep ocean basin. A catchment-based approach is applied to characterise discrete drainage networks and the influence of marine processes at the shelf-slope interface.

The Australian continental shelf is found to be mostly dominated by tides rather than by waves. This contrasts with empirical estimations that most of the world's shelves are dominated by waves, rather than by tidal currents. Additionally, the delineation of the shelf based upon modelled wave, tide and sediment entrainment demonstrated that the results contradict the conventional, graded shelf model, which suggests that mud content increases in an offshore direction with lower energy and increasing depth. The study also confirms that these coarse-grained sediments are not in hydraulic equilibrium with the prevailing tide and wave current regime.



Terrestrial processes are the primary drivers of coastal complexity. Various geological regions respond differently to marine processes, depending on whether the lithology is homogeneous or heterogeneous. The hypothesis that wave action causes a coastline to become more complex over time is challenged by this study, which found that, for Australia, wave power is inversely proportional to coastal complexity. This is a reflection of the presence of homogenous lithology in wave-dominated waters around much of Australia and the opportunistic action of waves in attacking and eroding sections of coastline.

Submarine canyon networks are demonstrated to be similar to terrestrial drainage systems, so that a catchment-based approach to delineating these canyons is appropriate. Lengthening of canyon path and compression of canyon width indicates that the drainage morphology in that particular catchment is being impeded or affected, therefore indicating control by geological inheritance. Within each of these submarine catchments, the derived drainage networks representing the dendritic canyon systems display to a greater or lesser degree characteristics associated with geological constraints through the derivation of Horton ratios (of bifurcation length and slope ratios) highlighting regional differences.

This thesis provides crucial quantitative information about processes and form. The results of this investigation can be applied to revise the zonation of continental margins through the identification of bathomic structures, rather than the classical definitions of neritic and bathyal zonation which are currently used in regional marine planning. Consequently, this work will contribute to ongoing research in the classification of the Australian continental margin by utilising available geophysical datasets to establish process-based boundaries. There are many potential applications of such process-based, quantitative delineation to the continental margin, particularly in marine planning and management.

## ACKNOWLEDGEMENTS

Firstly, I would like to thank my supervisors, Richard Coleman whose stoic support never wavered, Vincent Lyne for his constant faith in my ability and continuing support as a colleague and mentor and Kelvin Michael without whom I would not have completed this thesis. Kelvin's pragmatic advice and support guided me through the woods.

I would like to thank the many friends who provided much support over the years including Mark Hemer, Jonathan Rhodes, Neil Klaer, Melody Puckridge, Vanessa Lucieer and many others. All of you helped me in your own way, and for this, I am indebted.

I would also like to thank the following organisations: Australian Institute of Marine Science, Geoscience Australia and CSIRO Marine and Atmospheric Research, for the opportunities and support they have provided and to the people therein for all their helpful feedback. In particular Peter Harris who was an inspiration.

A special thank you to my mother Anna and brothers Dave, Drew and Steve, whose continual support and belief in me has been an inspiration throughout all these years. Similarly, love and hugs to my two beautiful sons, Mark and Michael - I want them to be half as proud of me, as I am of them.

Finally, to my primary school teacher Miss McColl - "not bad for a starling!"

Rick Smith (November 2010)

**To Mamie**

**CONTENTS**

**Declaration ..... i**

**Statement of co-authorship ..... ii**

**Abstract..... iii**

**Acknowledgements .....v**

**Contents..... vii**

**List of Figures..... xi**

**List of Tables .....xv**

**1. Chapter 1 Introduction ..... 1**

1.1 Overview.....1

1.2 Bathomes .....2

1.3 Aims and objectives .....4

1.4 Geospatial approach.....6

1.5 Datasets used.....7

1.6 Geophysical background .....8

1.6.1 Continental shelf.....8

1.6.2 Australian coastline..... 10

1.6.3 Continental slope ..... 11

1.7 Structure of thesis..... 12

**2. Chapter 2 Shelf Dominance ..... 13**

2.1 Abstract..... 13

2.2 Introduction..... 13

2.2.1 Shelves dominated by storms ..... 16

2.2.2 Shelves dominated by tides ..... 17

2.2.3 Shelves dominated by intruding ocean Currents ..... 18

2.3 Methods ..... 19

2.3.1 Threshold exceedance due to swell waves..... 19

2.3.2 Australian wave model..... 19

2.3.3 Estimation of wave threshold exceedance..... 21

2.3.4	Sediment grain size distribution on the Australian continental shelf .....	22
2.3.5	Threshold exceedance due to tidal currents .....	23
2.3.6	Australian tide model .....	23
2.3.7	Assimilated altimetry and tide gauge data .....	24
2.3.8	Estimation of tidal current threshold exceedance .....	25
2.3.9	Relative significance of wave versus tidal current threshold exceedance .....	26
2.4	Results .....	27
2.4.1	Waves.....	27
2.4.2	Threshold exceedance due to swell waves.....	28
2.4.3	Tides .....	30
2.4.4	Threshold exceedance due to tides .....	31
2.5	Discussion.....	32
2.5.1	Derivation of a new shelf regionalisation .....	32
2.5.2	Regions of zero sediment mobilisation .....	34
2.5.3	Mean grain size in relation to wave-only and tide-only mobilisation regions .....	35
2.5.4	Sediment mobility and benthic biological habitats .....	41
2.6	Conclusion .....	41
2.7	Addendum .....	42
<b>3.</b>	<b>Chapter 3 Coastal complexity .....</b>	<b>45</b>
3.1	Abstract .....	45
3.2	Introduction.....	46
3.2.1	Characteristic length scales.....	47
3.2.2	Causes of complexity .....	48
3.2.3	Limitations of broad-scale approach .....	48
3.3	Regional setting.....	50
3.3.1	Coasts dominated by storms and tides.....	50
3.3.2	Geology of Australia .....	51
3.4	Methods .....	52
3.4.1	Wave and tide models .....	53
3.4.2	Elevation-bathymetric variables .....	55
3.4.3	Geological variables.....	56
3.4.4	Quantifying coastal complexity ( $C_x$ ) .....	58
3.4.5	Aggregating to geological regions .....	60
3.4.6	Cluster analysis of $C_x$ .....	62
3.4.7	Similarity matrix of physical variables .....	63
3.4.8	Correlating $C_x$ to physical variables.....	63

3.5	Results .....	63
3.5.1	Geological regions and length scales .....	63
3.5.2	Geological regions and physical variables.....	67
3.5.3	Hierarchical cluster of $C_X$ values.....	70
3.5.4	Correlation of hierarchical $C_X$ table and physical variables.....	71
3.6	Discussion.....	75
3.6.1	Coastal complexity.....	75
3.6.2	Wave and tide dominated coasts.....	76
3.6.3	Lithological control .....	79
3.7	Conclusion .....	79
<b>4.</b>	<b>Chapter 4 Canyon classification.....</b>	<b>81</b>
4.1	Abstract .....	81
4.2	Introduction.....	81
4.2.1	Background.....	81
4.2.2	Canyon systems.....	86
4.2.3	Past classification of canyons.....	88
4.2.4	Catchment-based approach.....	88
4.2.5	Depth structure.....	89
4.3	Methods .....	90
4.3.1	Drainage analysis.....	90
4.3.2	Continental shelf break and foot of slope .....	91
4.3.3	Catchment zonation .....	92
4.3.4	Geomorphic measures of drainage network .....	93
4.4	Results .....	96
4.4.1	Continental shelf and slope boundaries .....	96
4.4.2	Continental slope catchments.....	100
4.4.3	Drainage networks.....	103
4.4.4	Bathomic structure .....	109
4.5	Discussion.....	110
4.5.1	Classifying catchments .....	110
4.5.2	Bathomic classification .....	112
4.5.3	Other issues .....	112
4.6	Conclusion .....	113
<b>5.</b>	<b>Chapter 5 Conclusion.....</b>	<b>116</b>
5.1	Key findings.....	116

5.2	Detailed assessment of objectives .....	117
5.3	Summary .....	122
5.4	Implications .....	123
5.5	Future work .....	126
<b>References .....</b>		<b>127</b>
<b>Publications of the author .....</b>		<b>142</b>
Journals.....		142
Conference Abstracts and Papers .....		142
Reports .....		145

## LIST OF FIGURES

Fig. 1.1: Map of Australia showing geographic locations cited in the text.....	9
Fig. 1.2: Schematic diagram showing cross section of a continental margin. ....	9
Fig. 2.1: Division of the Australian shelf (after Harris, 1995) into regions indicating sediment transport is caused mainly by tidal currents (17.4% of the shelf area), currents derived from tropical cyclones (53.8%), ocean swell and storm generated currents (28.2%) and intruding ocean currents (0.6%). Contours representing tropical cyclone frequency are from the Bureau of Meteorology ( <a href="http://www.bom.gov.au">http://www.bom.gov.au</a> ) and contours for significant wave height percentage exceedance from McMillan (1981). Mean spring tidal ranges along the coastline are from the Australian National Tide Tables. ....	15
Fig. 2.2: Mean grain size of sediments on the Australian continental shelf derived from the auSEABED database (Jenkins, 2000). ....	22
Fig. 2.3: Mean annual wave power ( $\text{kW/m}^2$ ) for the period March 1997 to February 2000 inclusive. ....	27
Fig. 2.4: Maximum wave power ( $\text{W/m}^2$ ) for the period March 1997 to February 2000 inclusive..	28
Fig. 2.5: Wave-induced exceedance for observed grain size distribution on Australian continental shelf for the period March 1997 to February 2000, inclusive. ....	29
Fig. 2.6: Mean spring tidal current speed ( $\text{m/s}$ ) on the Australian continental shelf. ....	30
Fig. 2.7: Tide-induced exceedance for observed grain size distribution on Australian continental shelf. ....	31
Fig. 2.8: Regionalisation of the Australian continental shelf for observed grain size distribution based on ratio of wave and tidal exceedance estimates.....	33
Fig. 2.9: Scatter plots of mean grain size versus: (A) $\log_2$ of maximum wave power ( $\text{W/m}^2$ ) for the period March 1997 to February 2000, inclusive; and (B) mean tidal current speed ( $\text{m/s}$ ).....	37
Fig. 2.10: Map of the northern Australia continental shelf, showing the mud content of surficial sediments in relation to the direction of maximum tidal current vectors. Muddy sediments	



appear to be associated with landward and along-shelf vectors whereas low mud content is associated with off-shelf oriented vectors.....	38
Fig. 2.11: A time series of wave power for four locations (shown in Fig. 2.2) (A) Marion Plateau; (B) Gulf of Carpentaria; (C) Bass Strait; and (D) Rottneest Shelf, southwest Australia. The 18 kW/m <sup>2</sup> wave power peak on the Marion Plateau occurs in March 1997 at the same time that tropical cyclone Justin was active over the Coral Sea and Queensland coast (X1 in Fig. 2.5). Wave power attained 10 kW/m <sup>2</sup> in the central Gulf of Carpentaria in December 1997, coincidental with Tropical cyclone Sid (X2 in Fig.2.5). This result is > 20 times the mean wave power at this location.....	40
Fig. 3.1: Geological regions of Australia representing major structural elements (based on Blake and Kilgour, 1998).....	52
Fig. 3.2: Australian continental margin - bathymetry and elevation (Geoscience Australia, 2008).	55
Fig. 3.3: Diagram of 3 x 3 cell grid demonstrating how $R_g$ is calculated. ....	56
Fig. 3.4: Maximum age of terrestrial geology. ....	57
Fig. 3.5: Lithology of the Australian continent.....	58
Fig. 3.6: Calculation of complexity using the 'angled measurement technique'. The length scale (S) is measured forward (AB) and backwards (AC) of a randomly chosen point (A) on the mapped coastline. The measure of complexity is the angle CAD (supplementary angle of CAB).....	59
Fig. 3.7: Geological regions of Australia, as classified by Blake and Kilgour (1998), adjacent to the coastline. ....	62
Fig. 3.8a: Boxplots of $C_x$ expressed in degrees (°), at varying length scales (2.5 – 100 km) for geological regions of Albany, Arafura, Bonaparte, Cairns, Canning, Carnarvon, Carpentaria Lowlands, Coen, Eucla, Fraser, Gawler and Gippsland geological regions. The horizontal bar in the middle of each boxplot indicates the median value of length scale, with the top and bottom of these boxes capturing the 75 <sup>th</sup> and 25 <sup>th</sup> percentile, also referred to as the interquartile range. The whiskers indicate the full range of data, while the circles represent the outliers. Outliers are values more than 1.5 times the interquartile range above the 75 <sup>th</sup> or below the 25 <sup>th</sup> percentile (Crawley, 2005). The y-axis represents the $C_x$ measured in degrees and the x-axis represents the length scale ranging from 2.5 km - 100 km. ....	65
Fig. 3.9: Rugosity ( $R_g$ ) expressed in percentiles for each Geological Region. ....	67

Fig. 3.10: Elevation expressed in percentiles for each Geological Region. ....	68
Fig. 3.11: Geological age expressed in percentiles for each Geological Region. ....	68
Fig. 3.12: Lithology expressed in percentiles for each Geological Region. ....	69
Fig. 3.13: Wave power ( $W_g$ ) acting on the coastline expressed in percentiles for each Geological Region. ....	69
Fig. 3.14: Tide power ( $T_g$ ) acting on the coastline expressed in percentiles for each Geological Region. ....	70
Fig. 3.15: Hierarchical structure of the cluster analysis for the geological regions based on Euclidian distance. ....	71
Fig. 3.16: Graph demonstrating inverse linear relationship of wave power ( $W_g$ ) vs. coastal complexity ( $C_x$ ). ....	77
Fig. 4.1: Discharge in terrestrial systems based upon precipitation and catchment area. Marine systems are dependant upon slope gradient sediment reservoir on adjacent continental shelf edge. ....	85
Fig. 4.2: Location diagram showing the extent of the continental shelf (coloured grey). ....	87
Fig. 4.3: The Bass Canyon amphitheatre is the largest canyon amphitheatre in Australia and consists of several shelf-incised and slope confined canyons that converge into the main tributary of Bass Canyon. The ridgeline defining the Bass Canyon catchment is outlined in black. ....	87
Fig. 4.4: The continental slope is shown in green and adjacent to areas of wave and tide-dominated shelves. The continental slope is characterised by having numerous dendritic canyon networks that transfer sediment to the abyssal plain and nutrients onto the continental shelf. ....	97
Fig. 4.5: Boxplots of northeast, northwest, southeast and southwest differences of gradient shelf break and foot of slope. The horizontal bar in the middle of the boxplot indicates the median value of length scale. The top and bottom of the box indicate the 75 <sup>th</sup> and 25 <sup>th</sup> percentile respectively, marking the interquartile range inside which 50% of the data lie. The whiskers indicate the range of data. The circles represent the outliers, which are values more than 1.5 times the interquartile range above the 75 <sup>th</sup> or below the 25 <sup>th</sup> percentiles (Crawley, 2005). ....	98

- Fig. 4.6: Histograms of northeast, northwest, southeast and southwest differences showing a) the gradient shelf break against depth, b) the distance of gradient shelf break to the 200 m isobath, c) the foot of slope against depth and d) the distance of foot of slope from the gradient shelf break. .... 99
- Fig. 4.7: Approximately 257 catchments are derived on the continental slope from the current available bathymetric data. The catchments slope angles are percentile ranked and in 20% bins ranging from 'very shallow' to 'very deep'. The slope angles are  $0^{\circ}$  -  $1.1^{\circ}$ ,  $1.1^{\circ}$  -  $2.0^{\circ}$ ,  $2.0^{\circ}$  -  $3.2^{\circ}$ ,  $3.2^{\circ}$  -  $4.8^{\circ}$  and  $4.8^{\circ}$  -  $10.6^{\circ}$ . The area of wave- and tide-dominated shelves around Australia is  $\sim 1.1$  million  $\text{km}^2$  and  $\sim 1.3$  million  $\text{km}^2$  respectively ..... 101
- Fig. 4.8: Derived sub-catchments within for the Bass Canyon catchment. These sub-catchments are typically elongated demonstrating the steepness of slope. .... 102
- Fig. 4.9: Drainage off Bass Strait and western Tasmania showing parallel channels (possibly pre-canyon rills) particularly on the upper slope. The resultant drainage analysis of the elevation-bathymetric grid has revealed paleo Bass Lake that was flooded by rising sea level  $\sim 15,000$  years ago. The drainage pattern indicates possible terrestrial – shelf – slope relationships. .... 104
- Fig. 4.10: The canyons west of Tasmania according to the 'Geomorphic map of Australia's EEZ' (Heap and Harris, 2008) drafted in green with the derived drainage analysis (in blue) superimposed. .... 105
- Fig. 4.11: Drainage density on continental margin. The catchments are percentile ranked in 20% bins ranging from "Little density" to "Very dense". .... 106
- Fig. 4.12: Location diagram of selected catchments to compare statistical characteristics..... 107
- Fig. 4.13: a). Drainage density vs. slope and semi-log plots of the Horton ratios for b) bifurcation ( $R_b$ ), c) length ( $R_l$ ) and d) slope ( $R_s$ ) for the six catchments.  $R^2$  is the correlation coefficient for best-line fit (derived from Table 4.1). Figures b), c) and d) for bifurcation, length and slope show a linear regression indicating that there is a relationship between stream orders. .... 108

**LIST OF TABLES**

Table 1.1: Hierarchical structure of Australian continental margin (Lyne et al., 1998; Butler et al., 2001; Last et al., 2005; Lyne et al., 2009). Last et al., (2010) proposed a new term ‘bathome’, in preference to ‘biome’, the larger-scale, pelagic-based, global units as defined by Longhurst (1998).....4

Table 1.2: Datasets used in analysis.....7

Table 2.1: Delineated shelf categories and associated carbonate, grainsize, mud-content, and sorting percentages..... 33

Table 3.1: Outputs for complexity ( $C_x$ ), wave ( $W_g$ ) and tidal power ( $T_g$ ) recorded for each random point location on the coastline. .... 60

Table 3.2: Coastal complexity ( $C_x$ ), marine variables ( $W_g$ ,  $T_g$ ,  $WT_{dom}$ ) and rugosity ( $R_g$ ), height, age and lithology aggregated for each geological region. .... 61

Table 3.3: Physical variables driving the structure of groupings..... 72

Table 4.1: Attributes defined for each submarine catchment. .... 95

Table 4.2: Metrics from six catchments demonstrating morphological differences. .... 109

Table 4.3: Standardised bioregions/bathomic structure (Last et al., 2005; Williams et al., 2008). Showing area (km<sup>2</sup>), median angle (°) and variability (std (°))..... 110

# CHAPTER 1 INTRODUCTION

## 1.1 Overview

There are a variety of modern pressures on the Australian coastline including increasing population, tourism, fishing, and urban development. Given the suite of environmental issues associated with global warming, Australia is facing changes in weather patterns, drought and sea level rise. Environmental planning is crucial to audit and mitigate these coastal pressures. However, mitigation is only effective when considered with an understanding of coastal and marine forms and the processes involved. The land and sea are intimately connected at the coast. These domains (terrestrial and marine) must be considered in tandem in dealing with the mitigation strategies.

This thesis adopts this holistic approach to quantify and analyse how both terrestrial and marine processes influence form and regional variation of the coast, continental shelf and slope vary regionally. It has long been established that the main marine processes influencing the continental shelf are waves and tides; however, their relative dominance on the Australia continental shelf remains unquantified. Similarly, there is a lack of clarity on the formative processes responsible for the variations in complexity of coastal morphology. In addition, despite their importance in sediment and nutrient transfer, the drainage patterns along the continental slope, in the form of submarine canyons, remain unclassified. By investigating these areas, this work provides clarity on regional variation along the continental margin: the coast, continental shelf and slope and their important interfaces. Therefore, it is feasible to use estimates of modelled wave/tide along with physical variables to define and investigate these boundaries.

Classifications are constantly being refined based on new methodologies and available data, particularly with the advent of remote sensing technologies, such as multibeam swath data. These new data are continuously revising what is known about geomorphic form and the formative processes. There have been attempts to refine marine demarcation boundaries using multivariate techniques and analysis. This can rely upon unsupervised classification,

where the researcher has limited control over the ordination process. Similarly, the choice of appropriate variables for the ordination can be arbitrary.

One application of this work is to enhance the accuracy and relevance of the bathomic structures (Table 1.1). By providing a better quantitative understanding of the land-sea interface, it will assist in determining and auditing form and process for Australia's continental margin, which in turn should assist better management practices at national and regional levels. Similarly, it hopes to enhance the spatial accuracy of some 'geomorphic units' (Heap and Harris, 2008). This research complements and extends work already undertaken by CSIRO Marine and Atmospheric Research in Australian environmental management (CSIRO, 1996; IMCRA, 1998; Lyne et al., 1998; Butler et al., 2001; Commonwealth of Australia, 2005; Last et al., 2005; Heap and Harris, 2008; Williams et al., 2008).

## **1.2 Bathomes**

Last (2010) proposed the term 'bathome' as a replacement for 'biome' to avoid confusion with the other marine unit of the same name defined by Longhurst (1998). Originally developed in the realm of terrestrial ecology, biomes refer to major regional ecological communities of plants and animals (Abercrombie et al., 1951). The rationale for their adoption to describe biogeographical structure in the marine environment was to accommodate the fact that evolutionary pressures and physical conditions are not homogenous throughout the oceans, or even within a marine province (Last et al., 2010). For the marine environment, bathomes (biomes, also referred to as environmental regions or zones (Hedgepeth, 1957)) are generally depth-related strata in which distinctive biotic assemblages are thought to exist.

Temperature, light and pressure vary enormously on the continental slope (Gage and Tyler, 1991). Bathomes are a useful way to capture depth-related structure within provinces. The spatial scales of bathomes are large, generally exceeding 1000 km (Last et al., 2010). Survey data suggest that bathomes are important large-scale units of marine biodiversity (Last et al., 2010). For instance, depth has a strong correlation with fish community structure in deep Australian marine environments (Williams and Bax, 2001; Last et al., 2005). These

bathomes can correlate with large-scale geological features, possibly due to constraints which have affected the evolution of the biota (Last et al., 2010). Therefore, there are strong associations between biogeographical and geophysical structures.

Marine geologists describe depth zonations through physical terms, *e.g.* continental shelf break, continental slope and abyssal plain. Benthic ecologists are likely to describe the same features as neritic and bathyal zones (Hedgepeth, 1957). The 200 m isobath (or more appropriately, the greatest gradient change between the shelf and slope) is generally accepted as the boundary between the neritic (coastal) and bathyal (oceanic) zones (Marshall, 1979). This also delineates the fuzzy boundary between shelf and deep water masses (Longhurst, 1998). The neritic zone can be subdivided into four primary bathomes: namely estuarine, coastal marine, demersal shelf and pelagic shelf. The bathyal zone extends from the top of the continental slope to the continental rise (Fairbridge, 1966) and consists of three primary benthic or demersal bathomes (continental slope, abyssal, and hadal).

Table 1.1: Hierarchical structure of Australian continental margin (Lyne et al., 1998; Butler et al., 2001; Last et al., 2005; Lyne et al., 2009). Last et al., (2010) proposed a new term 'bathome', in preference to 'biome', the larger-scale, pelagic-based, global units as defined by Longhurst (1998).

Level	Name	Scale (approx. size)	Examples
1	Provinces	province (1000s of km)	Broad-scale geological units such as continental blocks and abyssal plains. May include distribution data of fish assemblages.
2	Bathomes (previously Biomes)	regional (100s of km)	Broad-scale gross geomorphology nested within Provinces, e.g. coast, continental shelf, slope and abyssal plain. It has neritic and oceanic zones with the boundary at the continental shelf break. The neritic zone has four primary bathomes: estuarine, coastal marine, demersal shelf and pelagic shelf.
3	Geomorphic Units	local (10s of km)	Areas characterised by similar seabed geomorphology e.g. submarine canyons, sand-waves, rocky outcrops, incised valleys, flat muddy seabeds, seamounts, oceanic ridges and troughs on the shelf, slope and at abyssal depths.
4	Primary Biotopes	local (10s of km)	Low-profile reefs; substrate - soft, hard or mixed with their associated biological communities.
5	Secondary Biotopes	site (<10 km)	Generalised types of biological and physical substrate within the soft, hard or mixed substrate, e.g. limestone, granite, shell sands.
6	Biological Facies	site (<10 km)	Biological indicator or suite of species used as a surrogate for a community, e.g. seagrass species.
7	Microcommunities	site (<10 km)	Assemblages of species that depend on member species of the biological facies.

### 1.3 Aims and objectives

The main research question can be summarised as: is it feasible to use estimates of modelled wave/tide along with physical variables to redefine boundaries, particularly those used in regional marine planning? And can these quantitative process-based delineations provide a relevant framework for other classifications? An obvious application would be to add value to the bathomic structures that are currently in use (Lyne et al., 1998; Butler et al., 2001; Last et al., 2005; Lyne et al., 2009; Last et al., 2010).

Marine processes on the shelf (Chapter 2) adjoin the coastline (Chapter 3) and continental slope (Chapter 4). This study is concerned with quantitative measures that define these processes on a continental-wide scale in order to detect regional differences. It will also



focus on underlying geophysical constraints and form of the coastline to submarine catchments on the continental slope that are influenced by geological inheritance and marine processes. The scale primarily addressed in Chapters 2, 3, and 4 is the bathymic scale (previously biomes). This scale range is nested between the Province level and large geomorphic features (Table 1.1).

**Objective (1)** is to delineate continental shelves based on the relative dominance of marine processes such as swell waves and tides and to define the physical relationship between mobilising processes and shelf sediments.

This work was done to gain an understanding of the relationships between relative domination of waves and tides on the continental shelf. It was also calculated as an input to define the relationship to coastline complexity and submarine catchments around the continental margin. Using modelled estimates of tidal current speed and significant wave height and period, the Australian continental shelf will be categorised into wave- and tide-dominated shelf environments. The results will provide a predictive, process-based understanding of wave and tide domination that has applications to the other chapters as the combination of wave and tidal processes have implications for the coastline and submarine canyon systems on the continental slope.

**Objective (2)** is to quantify coastline complexity and establish the relationship between the varying length scales, geological structure and influence from various marine shelf processes.

This chapter investigates drivers of coastal complexity (in the form of depositional and erosive processes modulated by marine processes over geologic time) by examining the influence of geology and those marine processes quantified in chapter 2 at the land-sea interface. The challenge is to identify coastline complexity that develops in response to geological inheritance, terrestrial and ocean processes, as well as determine the characteristic length scales at which they operate. By examining the complexity of the coastline and its relationship to geological regions of the Australian continental platform, the complexity of the coastline will be quantified at various length scales and the results compared to various mappings of geophysical variables that control coastline formation and structure. Some hypotheses dictate that waves provide the greatest influence on coastline complexity (Sapoval et al., 2004). However, many areas of the Australian shelf are

tide-dominated. This section will examine the difference between wave- and tide-dominated shelves to explore if waves alone drive coastal processes that form the resultant crenulations and complexity.

**Objective (3)** is to classify the continental slope into discrete submarine catchments and to derive metrics from both the drainage analysis and associated catchments.

This chapter will demonstrate a methodology to automatically and rapidly define submarine catchments and associated drainage networks on the continental slope to investigate how the continental shelf interfaces with the deep ocean basin, leading to a better geological understanding through the extraction and analysis of associated metrics. This catchment-based approach enables the investigation of the influence of marine processes defined in chapter 2 at the shelf-slope interface. Similarly, adopting this catchment-based approach highlights the contributions of sediments from the continental shelf that can be so important in submarine canyon evolution.

All these bodies of work will contribute to the establishment of more accurate process-based boundaries that can be utilised in regional marine planning thereby providing a better framework for further research.

## 1.4 Geospatial approach

The datasets used in this study came from many sources - some were freely available, others were derived through spatial analysis techniques and model outputs. Ultimately, these data were manipulated, analysed and visualised in a Geographic Information System (GIS). However, the purpose of the project was to concentrate on addressing scientific questions, rather than demonstrating GIS procedures and outputs. The GIS merely enabled the complex data forms to be integrated onto a common platform. The analysis was completed using national datasets and avoided any disadvantages of truncating them at regional boundaries or at the shelf edge (Butler et al., 2001). Arguably, one of the most important datasets was the elevation-bathymetric model of the Australian continental margin (Buchanan, 1998; AGSO, 1999; Petkovic and Buchanan, 2002). This three-

dimensional model held many clues as to the form and processes that dominate regions of the Australian continental margin.

## 1.5 Datasets used

Table 1.2: Datasets used in analysis.

Name	Chapter/s	Comments
Modelled estimates of wave power	2, 3 & 4	The AusWAM hindcast time series provides estimates of wave height and period, and wave direction. Estimates of wave power (or energy flux) were derived from the modelled wave height and period (Greenslade, 2001)
Modelled estimates of tide power	2, 3 & 4	Outputs for tidal processes were generated using the linearised, shallow-water (Andersen et al., 1995) tide model described by Egbert et al. (1994). Estimates of tide power (or energy flux) were derived from these outputs.
Sediment distribution	2	The observed mean grain size of sediment on the Australian continental shelf extracted from the sediment database auSEABED (Jenkins, 2000)
Elevation-bathymetric model	3 & 4	The elevation-bathymetric model topography grid dataset (Petkovic and Buchanan, 2002), resampled to a resolution of 0.01° and merged with a second Geoscience Australia dataset (Buchanan, 1998; AGSO, 1999).
Coastline 1:100 k	3	The GEODATA Coast 100k is a vector dataset representation of Australia's coastline at 1:100 000 scale (Geoscience Australia, 2004).
Geological regions.	3	The major structural elements of the Australian continent as summarised by Blake and Kilgour (1998) and used to define geological regions.
National geology dataset	3	Geoscience Australia's 1:2,500,000 national geology dataset (AGSO, 1998).

## 1.6 Geophysical background

### 1.6.1 Continental shelf

The continental shelf is defined as an offshore extension of the continent that has a gentle slope of  $< 1^\circ$  towards the top of the continental slope (Fig. 1.1; Fig. 1.2). The shelf itself is part of the continent during glacial periods and corresponding lower sea level. During interglacial periods, the shelves are part of the sea, but technically they are the flooded margins of the continent (Gross, 1972; Pinet, 1996). The Australian shelf is highly variable in character; its morphology varies in width, depth, gradient and profile. The distance from the coastline to the edge of the shelf (shelf break) can vary from 10 - 500 km. The depth of the shelf break varies between 75 - 750 m - although 200 m is an accepted depth (Condie and Harris, 2005). The northern Australian shelf is generally broad and can be as much as 500 km wide, encompassing part of the Arafura Sea (Church and Craig, 1998). The northwest shelf is narrower at  $\sim 150$  km, while the southeast shelf is narrower still at  $\sim 20$  km (Church and Craig, 1998) (Fig. 1.1). The Gulf of Carpentaria is an epicontinental sea with a maximum depth of 70 m. It is bordered to the west by the Arafura Sea and to the east by Torres Strait, which is approximately 12 m deep. Torres Strait forms a natural restriction between the Gulf and the Coral Sea. During times of low sea level (Quaternary), the Gulf of Carpentaria was a completely isolated basin (Lake Carpentaria) separated from the Indian and Pacific Oceans (Chivas et al., 2001). The modern Gulf of Carpentaria forms a broad shallow shelf area which is hundreds of kilometres from the shelf edge (Church and Craig, 1998). Other broad shelf regions include Bass Strait, which was the site of a perched Pre-Holocene Lake. Bass Strait is situated in a shallow sea region ( $\sim 80$  m) and exposed to extreme temperate storms (Fig. 1.1).

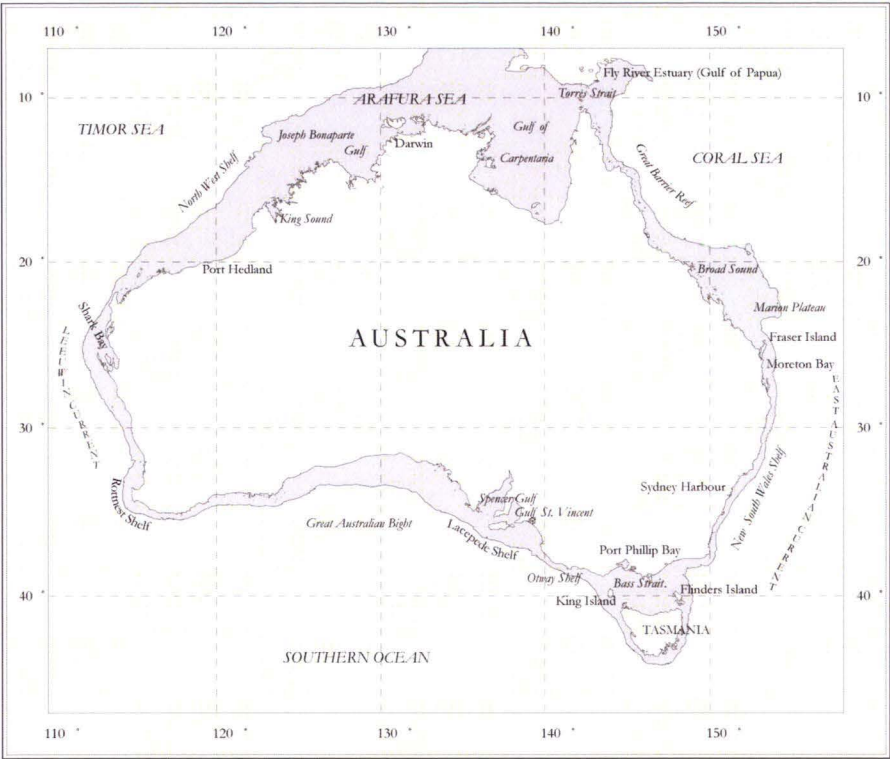


Fig. 1.1: Map of Australia showing geographic locations cited in the text.

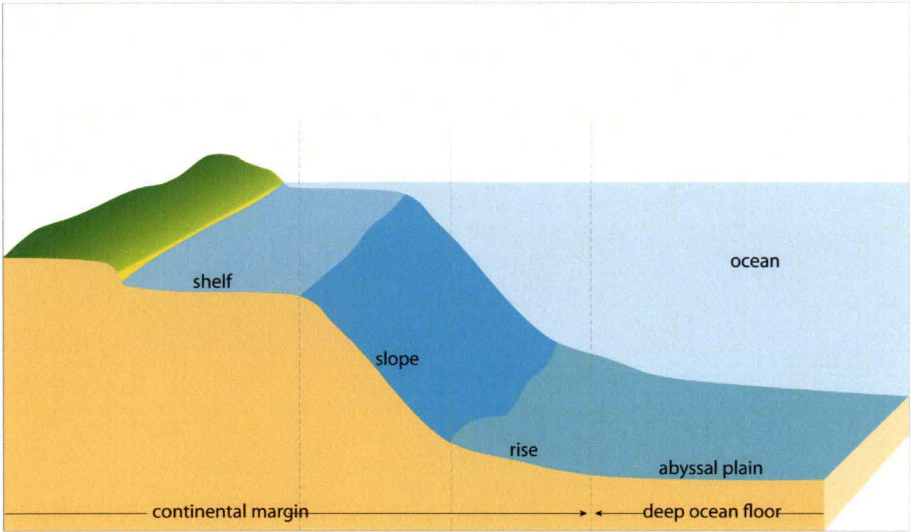


Fig. 1.2: Schematic diagram showing cross section of a continental margin.

It has been suggested that about  $\sim 80\%$  of the world's shelves are dominated by storm-waves,  $\sim 17\%$  by tidal currents and  $\sim 3\%$  by ocean currents (Walker, 1984; Swift *et al.*, 1986). Terrigenous sediments derived from erosion of the land account for 60 - 70%, though these are generally relic deposits from the last ice age when sea level was  $\sim 120$  m

lower (Gross, 1972; Pinet, 1996). Sediment can be transported on the shelf in many directions by marine processes: onshore, offshore or alongshore (Short and Woodroffe, 2009).

Temperate waves in southern latitudes are different from the episodic, catastrophic cyclonic storm events of the tropics (Porter-Smith et al., 2004). These marine processes are postulated to determine coastline form and sediment gravity flows down the continental slope.

### **1.6.2 Australian coastline**

During the northward drift, fluctuating climate over the last few million years and sea level have caused a series of depositional and erosional events (Short and Woodroffe, 2009). The modern coastline comprises both unconsolidated sediments and rocky substrate due to processes such as rivers depositing sediment and building deltas, waves building beaches and the erosion of rocky coastlines (Short and Woodroffe, 2009). Additionally, the Australian continent, being relatively tectonically stable, enables rising and falling sea level to stay within a fairly narrow elevation range, activating and deactivating marine processes that over time have sculpted the coastline (Short and Woodroffe, 2009).

Formation processes through deposition and erosion are generally caused by waves and tides (Davidson et al., 2002). Tidal range can determine the height of the shoreline over which deposition or erosion takes place. Additionally, coastline formation and character is influenced by the hardness and grain direction of the lithology (Davidson et al., 2002). For instance, geological structure can have an influence. Bands of rock running parallel to the shore can promote cove formation (concordant coastline) (Whitlow, 1984). A coastline where the rock grain runs perpendicular tends to create inlets or bays where the least resistant rock is broken down by waves. The more resistant rocks remain as headlands (discordant coastline) (Whitlow, 1984).

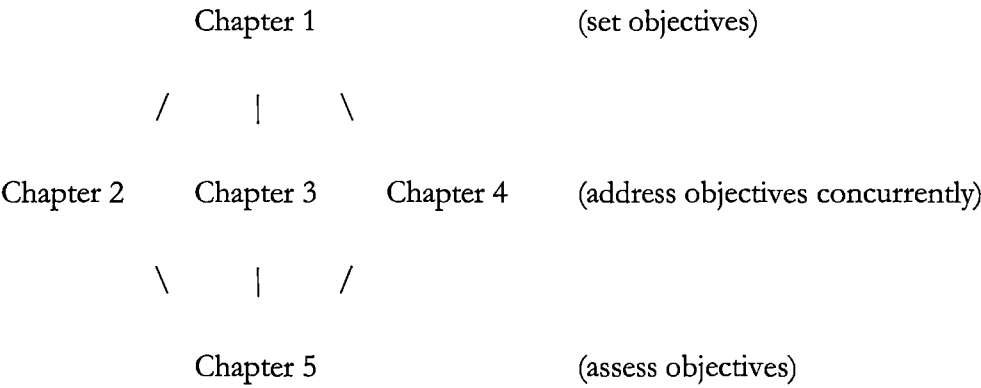
### 1.6.3 Continental slope

Beyond the continental shelf is the slope, typified by an increasing slope angle from  $1^\circ$  to generally between  $2 - 5^\circ$ , but ranging as low as  $1^\circ$  or as high as  $10^\circ$  extending towards the abyssal zone or plain (Whitlow, 1984). Increased gradient on the continental slope affects and promotes submarine canyon evolution through periodic gravity currents. The continental slope is often heavily indented with channels and submarine canyons, although their distribution around the continental slope is variable (Gross, 1972; Pinet, 1996).

Australia has several major canyon systems, such as the Perth and Horseshoe canyons in the southwest and southeast respectively. The continental slope is terminated by the continental rise (or apron). The continental rise has a slope angle approximately  $0.5 - 1^\circ$  and starts at a depth of around 1800 - 2000 m. It consists of thick sediments deposited by turbidity currents from the continental shelf and slope. The rise extends down to the abyssal zone or plain, typically at depths of about 4000 metres (Whitlow, 1984).

Gravity currents, consisting of a dense mixture of water and sediment, periodically flow down the slope transferring large quantities of material onto the abyssal plain (Whitlow, 1984). These periodic events erode channels on the slope and cause canyoning that is dependent on slope gradient, the availability of sediment, base geological tectonics as well as the presence of energetic oceanographic processes (such as interactions with eddies). There is a clear analogy to terrestrial catchment systems. As the location of the slope is variable around the Australian margin, an important part of classifying the slope correctly is defining the continental shelf break and foot of slope. This is preferably based on change in gradient as opposed to the more arbitrary 200 m isobath. Similar to terrestrial catchment systems, continental slope catchment areas channel the erosive gravity flows. Sediment transport processes on the slope and shelf are very different in nature, distribution, frequency and quantity.

1.7 Structure of thesis



The thesis comprises five chapters. Chapters 1 and 5 are the introduction and conclusion chapters respectively. The middle three are independent and each one addresses one of the stated objectives in turn.

**Chapter 2** provides an estimation of continental shelf dominance by either wave and/or tidal currents as they affect dominant processes on the Australian continental shelf. This chapter was published as ‘Porter-Smith, R. et al., 2004. Classification of the Australian continental shelf based on predicted sediment threshold exceedance from tidal currents and swell waves. *Marine Geology*, 211(1-2): 1-20’.

**Chapter 3** quantifies coastline complexity and establishes the relationship between the varying length scales, geological structure and influence from various marine shelf processes.

**Chapter 4** focuses on classifying the continental slope using a catchment-approach and associated depth zones, and then deriving metrics from both the drainage analysis and associated catchments.

**Chapter 5** concludes the previous chapters and synthesises the findings. Suggestions and recommendations are made towards further research.



## CHAPTER 2 SHELF DOMINANCE

### 2.1 Abstract

Estimates of significant wave height and period, together with tidal current speed over a semi-lunar cycle, were used to predict the area on the Australian continental shelf over which unconsolidated sediment was mobilised (threshold exceedance). These sediment-entraining processes were examined independently to quantify their relative importance on the continental shelf. Using observed grain size data, mobilisation occurred from swell waves on  $\sim 31\%$  and tidal currents on  $\sim 41\%$  of the continental shelf. Swell wave energy is sufficient to mobilise fine sand (0.1 mm diameter) to a water depth of 142 m on the Otway Shelf near the western entrance to Bass Strait. Tidal currents in King Sound (Northwest Shelf) are capable of mobilising large areas of medium sand (0.35 mm diameter) 100% of the time. Superimposing the distribution of threshold exceedance by wave and tidal currents indicates that there are areas on the shelf where either wave-induced or tidal currents dominate, some areas where waves and tides are of relatively equal importance and still other areas where neither is significant. We define six shelf regions of relative wave and tidal energy: zero (no mobility); waves-only, wave-dominated, mixed, tide-dominated and tides-only. Our results provide a predictive, process-based understanding of the shelf sedimentary system that has applications to marine engineering projects and to regional studies of pollution dispersal and accumulation where significant shelf sediment mobilisation is a factor.

### 2.2 Introduction

An unanswered question in continental shelf sediment research is "What percentage of the Earth's continental shelves are subject to hydrodynamic processes strong enough to mobilise the bed sediment (Swift and Thorne, 1991)?" Although it has been suggested that about  $\sim 80\%$  of the world's shelves are dominated by storm waves,  $\sim 17\%$  by tidal currents and  $\sim 3\%$  by ocean-current interactions (Walker, 1984; Swift et al., 1986), there is

currently no published quantitative analysis of continental shelves to determine the spatial distribution of dominant sediment transport processes. The main limitation has been the practical difficulties involved in collecting enough data over the shelf. In a first attempt at quantifying the influence of the global wave climate on sediment mobility, Harris and Coleman (1998) used wave data generated by a global climate model. They found that the wave climate was capable of mobilising 0.1 mm diameter quartz sand over 41.6% of the Earth's continental shelves on at least one occasion during a 3-year period from July 1992 to July 1995.

For the Australian continental shelf, Harris (1995) proposed a classification based on the relative influence of storms (including tropical cyclones), swell waves, tidal currents and intruding ocean currents. According to this scheme (Fig. 2.1), the Australian shelf may be subdivided into areas where storm processes dominate in the mobilisation of sediments (82% of the shelf), where tidal currents dominate (17.4%), and where intruding ocean currents dominate (< 1%).

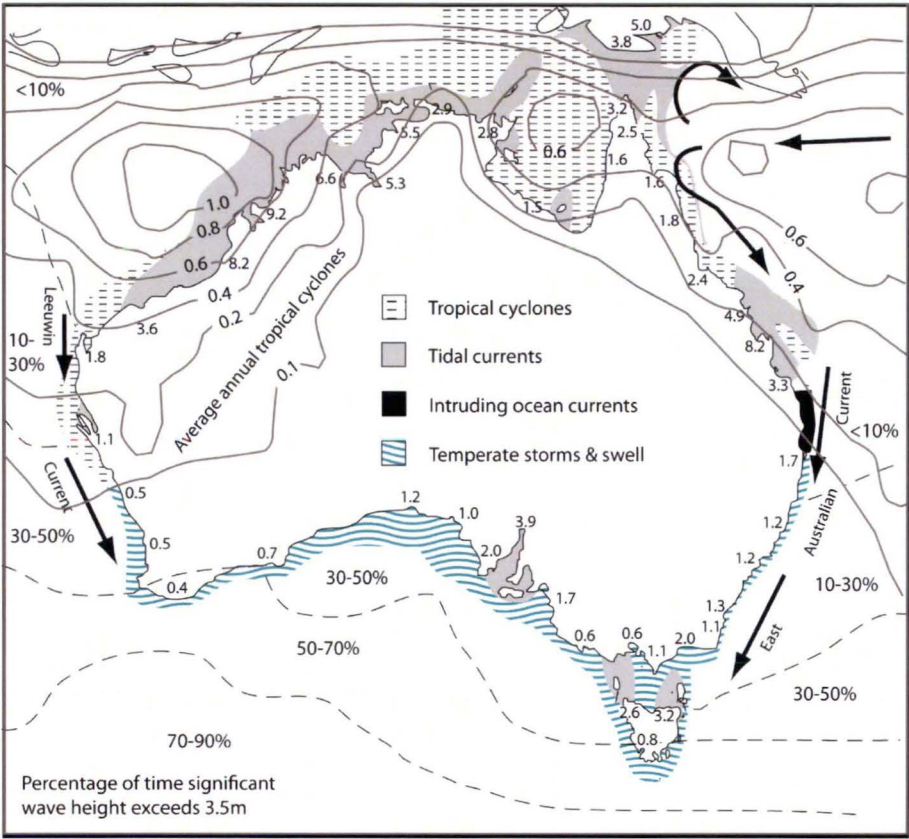


Fig. 2.1: Division of the Australian shelf (after Harris, 1995) into regions indicating sediment transport is caused mainly by tidal currents (17.4% of the shelf area), currents derived from tropical cyclones (53.8%), ocean swell and storm generated currents (28.2%) and intruding ocean currents (0.6%). Contours representing tropical cyclone frequency are from the Bureau of Meteorology (<http://www.bom.gov.au>) and contours for significant wave height percentage exceedance from McMillan (1981). Mean spring tidal ranges along the coastline are from the Australian National Tide Tables.

The aims of the present study are twofold. Firstly, our aim is to extend the work of Harris and Coleman (1998) for the Australian region by incorporating a finer resolution wave climatology data set, together with a similar spatial resolution shelf tide model. This will allow a more detailed assessment of the relative spatial distribution of wave- and tide-dominated portions of the Australian continental shelf. Secondly, our aim is to use observed sediment data to examine the relationship between mean grain size ( $D_{50}$ ) and current velocity ( $U_{max}$ ) produced from tides and waves. It is acknowledged that other processes such as continental shelf waves have the potential to mobilise sediment on the continental shelf (Freeland et al., 1986), however for this study it has been decided to concentrate on the two main processes of tidal currents and swell waves.

### 2.2.1 Shelves dominated by storms

Storm-dominated regions of the Australian shelf may experience one or several storm events per year, which cause sediment-transporting flows. Currents produced during the passage of storm events control the erosion and transport of unconsolidated sediment over an estimated 82% of the Australian shelf surface area (Harris, 1995). Storms occur in the form of tropical cyclones and temperate low-pressure systems. The energy expended and the amount of sediment transported during one storm event may equal many months (or years) of fair-weather transport (Swift and Thorne, 1991). Even on highly dynamic, tidally influenced shelves, the effect of a storm event is to initiate sediment movement at even greater water depths and at greater rates in shallower depths than is experienced under fair-weather conditions.

Significant wave height data obtained from satellite altimeters illustrates that, although significant wave heights are less than 1.5 m for 50 - 70% of the time in northern Australia, they are larger than 3.5 m for 30 - 50% of the time along much of the southern Australian shelf (McMillan, 1981; Young and Holland, 1996.) (Fig. 2.1). Storm events influence not only the initiation of sediment movement, but also the deposition of sediment. Examples of studies in Australia which have documented the development of shelf storm deposits include those of the Rottneest Shelf (Collins, 1988), the Lacepede Shelf coast (James et al., 1992), the New South Wales Shelf (Davies, 1979) and the Gippsland Shelf (Black and Oldman, 1999). In these locations (Fig. 1.1), long-period swell waves cause nearly continuous reworking of sediment on the inner shelf, winnowing away fine grains and leaving a sorted, sandy deposit. On the New South Wales shelf, mud is deposited in water depths of between 60 to 130 m (Gordon and Hoffman, 1986) while on the higher energy Lacepede shelf mud is deposited below 140 m (James et al., 1992). On the southern parts of Australia's shelf, the sediment is arranged in zones parallel to the coast (James et al., 1992), reflecting the dominance of ocean swell waves and storms (Fig. 2.1).

Tropical cyclones are the cause of storm events in much of northern Australia (Lourensz, 1981) (Fig. 2.1). The sections of the northern shelf most frequently affected by cyclones include the Northwest Shelf, Gulf of Carpentaria and the Great Barrier Reef. Information on the frequency of tropical cyclones can be found on the Bureau of Meteorology's site (BoM, 2007). These shelf areas experience generally small (< 1.5 m significant wave height)

ocean swell waves (Fig. 2.1). Tropical cyclones induce strong currents, which erode and transport sediment over a wide area (Gagan et al., 1990). Current meter measurements, obtained in the Gulf of Carpentaria during one tropical cyclone, recorded near-bed currents that attained hourly speeds up to 6 times larger than during fair-weather conditions (Church and Forbes, 1983). In the Great Barrier Reef, Cyclone Winfred produced a mixed terrigenous-carbonate storm layer averaging 6.9 cm thick on the middle shelf, and transported sediment alongshore and northward a minimum distance of 15 km (Gagan et al., 1990). Modelling studies by Hearn and Holloway (1990) on the Northwest Shelf have shown that, under the influence of tropical cyclones, strong westward-flowing coastal and inner shelf currents are established between the eye of the cyclone and the coast. Such cyclone-induced currents are clearly a significant factor affecting sediment movement on cyclone-dominated shelves, but they may also influence the long-term (net) sediment movement on some otherwise tidally-dominated sections of the shelf (Harris, 1995).

## 2.2.2 Shelves dominated by tides

Tidally-dominated, macrotidal shelves occur where the mean spring tidal range measured along the coast exceeds 4 m (Walker, 1984). Around Australia, tidal ranges > 4 m occur along the Northwest Shelf between Port Hedland and Darwin (Fig. 1.1), and attain 12.5 m in King Sound (Fig. 2.1 and Fig. 1.1). The southern Great Barrier Reef platform is also macrotidal, with a maximum tidal range of 8.2 m in Broad Sound (Fig. 1.1). In the Fly River Delta (Gulf of Papua; Fig. 1.1) tidal ranges are up to 5 m (Harris et al., 1993). Tidal currents are also an important sand-transporting mechanism in mesotidal (2 - 4 m tidal range) regions such as Torres Strait, Bass Strait and Moreton Bay (Fig. 1.1). Tidal currents are capable of controlling sand transport in microtidal regions (tidal range < 2 m) in restricted cases, where coastal geometry affords shelter from ocean-generated swell and wind-driven currents (Harris, 1994). Such is the case in many bays (e.g. Shark Bay), the approaches to some major ports (e.g. Port Phillip Bay, Melbourne) and in partly enclosed gulfs (e.g. Spencer Gulf, Gulf St. Vincent and the Gulf of Carpentaria). Tidal currents are accelerated as they flow over and between shelf edge barrier reefs, thus sediment transport is affected by tides along the shelf edge over much of the Great Barrier Reef (Fig. 2.1). In

total, tidal currents are estimated to dominate sediment transport on about 17.4% of the Australian shelf (Fig. 2.1; Harris et al., (1995)).

Generally, tidally-dominated shelves display discrete zones of seabed scouring and erosion coinciding with regions of the shelf subject to maximum tidal bed stress (Harris et al., 1995). An important distinction from storm-dominated shelves is that the facies on tidally-dominated shelves have boundaries that are aligned more or less at right angles to the coast (Walker, 1984). Sediment facies are arranged in a divergent pattern that reflects an increasing supply of sand of decreasing grain size with increasing distance away from the scour zone (Harris et al., 1995). Such diverging bedload transport patterns are known as bedload partings (Johnson et al., 1982). Regions of the Australian continental shelf where tidal currents have produced strong bedload parting facies include the Torres Strait, the Gulf of Carpentaria (Harris, 1994) and Whitsunday Islands (Heap, 2000). In these regions, tidal currents are accelerated as they flow through constricted channels located between islands and reefs. The zones of maximum tidal current speed are sometimes related to tidal amphidromic points. These are a type of standing wave node in which sea level change is small but current speeds are large; two such amphidromic points are found in the Gulf of Carpentaria (Harris, 1994).

### 2.2.3 Shelves dominated by intruding ocean Currents

Intrusive ocean currents that cause sediment transport (Fig. 2.1) affect less than 1% of the Australian shelf. These currents are dominant offshore from Fraser Island, where the southward-flowing East Australian Current intrudes onto the shelf and a coarse-grained rhodolith gravel pavement has been deposited (Harris et al., 1996). Sidescan sonar and seabed photographs, obtained during the 1980 cruise of the German research vessel *Sonne* to the northern NSW and southern Queensland region, reveal large subaqueous dunes at water depths as great as 80 m (Jones and Kudrass, 1982). Dune morphologies indicate a general southward transport of sand, which Gordon and Hoffman (1986) attributed to the East Australia Current. The Leeuwin Current has a similar effect over parts of the Western Australia shelf (Pearce and Pattiaratchi, 1997).

## 2.3 Methods

### 2.3.1 Threshold exceedance due to swell waves

Using Airy, first-order wave theory (Komar and Miller, 1973), we have estimated the wave-induced threshold of sediment for observed grain size distribution around the continental shelf. Currents produced by the passage of a shallow water wave are reduced to backward and forward motions, having an orbital diameter  $d_o$ . Over the wave period  $T$ , the velocity at a fixed point on the bed will vary from zero to a maximum  $U_{max}$  according to the relationship.

$$U_{max} = \frac{\pi d_o}{T} = \frac{\pi H}{[T \sinh(2\pi h/\lambda)]} \quad (1)$$

where  $H$  is the wave height (m),  $h$  is the water depth (m) and  $\lambda$  is the wavelength of the surface gravity wave (m) (Komar and Miller, 1973). When the near-bed current accelerates from zero towards a maximum value ( $U_{max}$ ), it may exceed the threshold value ( $U_{cr}$ ) where a specific sediment grain size is mobilised. Although more accurate estimates of  $U_{max}$  are possible by using a spectral wave current model (Madsen, 1994), the necessary wave data are not available. Estimates of  $U_{max}$  derived from Equation (1) give an accurate result away from the shoreface zone in water depths greater than 5 m and under the near-threshold and deep water shelf conditions that are of interest in the present study (Hardisty, 1994).

### 2.3.2 Australian wave model

In this study, surface wind speed estimates generated by the Australian Bureau of Meteorology's regional atmospheric model provided input to the wave model, WAM (Hasselmann et al., 1988; Komen et al., 1996) to yield estimates of mean wave height and period. The output data are 6-hourly predictions of significant wave height (SWH), period and mean wave direction, gridded at  $0.1^\circ$  spatial resolution, for the period March 1997 to February 2000, inclusive. The WAM model is run operationally at many forecasting centres around the world, including a version at the Australian Bureau of Meteorology. When

compared to observations of SWH from wave-rider buoys around the Australian coast, the root mean square (RMS) error of forecast SWH is approximately 0.5 m. The source terms and propagation terms are integrated every 5 minutes. In terms of the wave spectrum, the directional resolution is  $15^\circ$  and there are 25 frequency bins ranging from 0.0418 Hz to 0.4114 Hz. This represents wave periods from approximately 24 - 2.5 s.

This high-resolution wave model ( $0.1^\circ$ ) was nested within a regional wave model ( $1^\circ$ ), which spans the oceans around Australia, ranging from latitudes  $60^\circ$  S to  $12^\circ$  S and longitudes  $69^\circ$  E to  $180^\circ$  E. The spectral resolution was the same for both models. The regional wave model ( $1^\circ$ ) provided the boundary conditions for input to the high-resolution wave model ( $0.1^\circ$ ). This regional wave model, in turn, was nested within a global model ( $3^\circ$ ).

Although we are concerned here with the impact of the water waves on the bed sediment, the seafloor in turn affects the form and propagation of surface waves. The major impact on the modelled wave height due to the water depth is that when  $h < \lambda/4$ , an extra source term must be included in the wave models, representing the dissipation of wave energy due to bottom friction. Other shallow water effects, such as depth-induced breaking, are not included in WAM, and for this reason, a water depth of approximately 20 m is considered to be the shallowest depth for which it is possible to run WAM successfully (Booij et al., 1999).

In Equation (1), water depth ( $h$ ) was approximated from Geoscience Australia's (formerly the Australian Geological Survey Organisation) bathymetry database. This bathymetric model was interpolated to a grid spacing of  $0.01^\circ$ . The high-resolution wave model outputs were then combined with the bathymetry grid, and Equations (1 - 3) were solved at six-hourly intervals. The number of times that the threshold value was exceeded at each bathymetric grid point was then summed to produce threshold exceedance maps of Australia's continental shelf region for observed grain size.



To quantify the synergy of wave height and period around Australia, wave power  $P$  was calculated as follows:

$$P = \frac{\rho g^2 H^2 T}{32\pi}, \quad (2)$$

where  $\rho$  is the density of seawater ( $\text{kg/m}^3$ ),  $g$  where  $g$  is gravity ( $9.8 \text{ m/s}^2$ ),  $H$  is significant wave height (m), and  $T$  is the wave period (seconds). Wave power ( $P$ ) units are measured in  $\text{W/m}^2$ .

### 2.3.3 Estimation of wave threshold exceedance

The threshold speed ( $U_{cr}$ ) is a function of the wave period, boundary layer thickness, bed roughness, grain density and shape, water viscosity and whether or not the grains are cohesive or cemented (Grant and Madsen, 1979; Hammond and Collins, 1979; Grant and Madsen, 1986; Hardisty, 1994). Simplified empirical threshold equations have been published by Clifton and Dingler (1984), for flat-bed, spherical, cohesionless, quartz silt and fine sand. For silt and fine sand and grain size  $D < 0.05 \text{ cm}$  in diameter the threshold speed is given by:

$$U_{cr} = 33.3(TD)^{0.33}, \quad (3)$$

and for coarse sand and gravel ( $D > 0.05 \text{ cm}$ ):

$$U_{cr} = 71.4(TD^3)^{0.143}, \quad (4)$$

Although the viscosity of water varies with temperature and salinity, these are held constant in Equations 3 and 4 (Clifton and Dingler, 1984).

2.3.4 Sediment grain size distribution on the Australian continental shelf

The observed mean grain size of sediment on the Australian continental shelf was provided from the sediment database auSEABED (Jenkins, 2000) (Fig. 2.2). The grid representing sediment grain size for the shelf was generated from the September 2000 data content at a resolution of 0.01°. In total, there were in excess of 180,000 sites made up of both descriptive and quality controlled analyses. The descriptive data from known sites were parsed and used along with the analyses to glean as much information as possible about the distribution of sediment grain sizes on the shelf. The statistical confidence of these descriptions is documented (Jenkins, 2000). To convert these data from auSEABED into a grid, the mean grain size data were converted from *phi* to millimetres and linearly interpolated to give a continuous surface. It is acknowledged that values on some areas of the shelf are not as reliable as others, due to the spatial distribution of sample sites. This is particularly true in the Gulf of Carpentaria and parts of the Northwest Shelf.

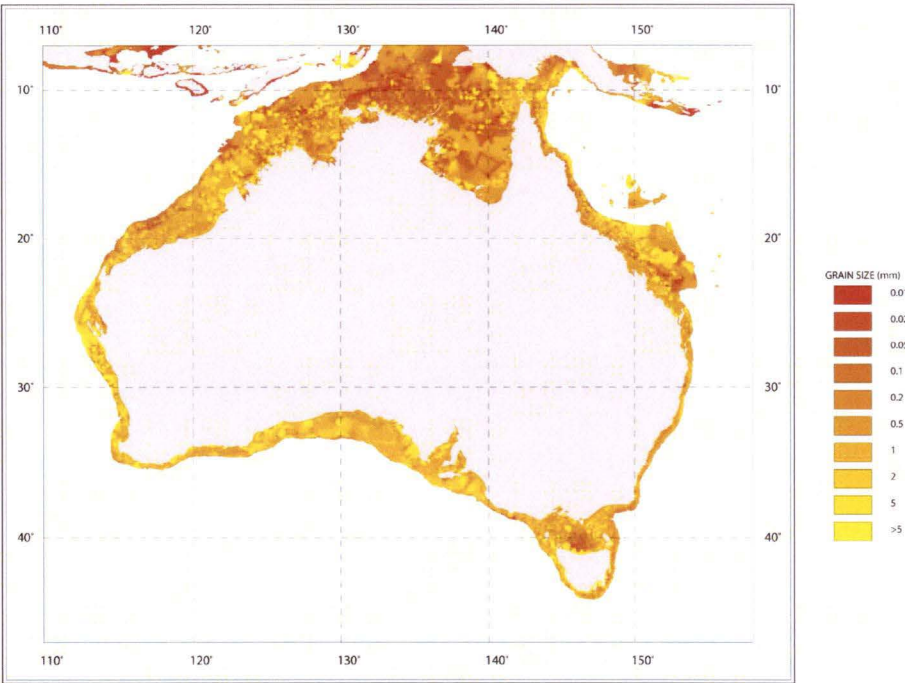


Fig. 2.2: Mean grain size of sediments on the Australian continental shelf derived from the auSEABED database (Jenkins, 2000).

### 2.3.5 Threshold exceedance due to tidal currents

Threshold exceedance was estimated for unidirectional, steady flow conditions using the empirical curves (Miller et al., 1977). This graph is based on the results of selected open-channel, straight-sided flume experiments conducted by various investigators, using standard laboratory conditions (i.e., an initial flat bed, cohesionless quartz spheres under steady, fresh water flow at 20° C). The data specify an empirical formula which gives threshold exceedance for quartz spheres less than or equal to 2 mm under the above described laboratory conditions, as:

$$U_{100} = 122.6D^{0.29}, \quad (5)$$

where  $U_{100}$  is the threshold current speed referenced to 1 m above the seabed and  $D$  is the grain diameter in mm. Hourly-averaged, tidal current speeds were estimated using a hydrodynamic tidal model for the Australian shelf, derived specifically to meet the spatial-temporal requirements of the present study.

### 2.3.6 Australian tide model

An ocean tide model for the Australian shelf was set up for the region limited by 0° S to 45° S and 109° E to 160° E (Harris et al., 2000). The resolution of the model is 0.067° in both latitude and longitude; correspond to 7.4 km at the equator and 5.2 km at the southern-most latitude of the model domain. In the latitude direction, it corresponds to 7.4 km.

The linearised, shallow-water, tide model described by Egbert et al. (1994) was used. Dissipation was approximated using a quadratic expression with depth ( $h$ )

$$K = \frac{K_0}{(\max(h, h_0))^2}, \quad (6)$$

where  $K_0$  is the bottom drag coefficient at depth  $h_0$ . At shallower depth, dissipation is equal to  $K_0$ . A parameter choice of  $K_0 = 0.05$  and the minimum depth of  $h_0 = 20$  m was made

after extensive testing as it worked well for most regions. In Bass Strait, the model tidal amplitudes were too small, which was subsequently compensated for by the data assimilation (see below).

Geoscience Australia's bathymetry on a 1 minute (1.8 km) grid was used and re-interpolated onto the 15 minute resolution grid used for the model. However, this database suffers from frequent loss of coverage for several regions in the deep ocean. In these regions it was supplemented with data obtained from the National Geophysical Data Center (NGDC) bathymetry model (Smith and Sandwell, 1997).

The tidal model includes the eight major constituents  $M_2$ ,  $S_2$ ,  $N_2$ ,  $K_2$ ,  $K_1$ ,  $O_1$ ,  $Q_1$ , and  $P1$ . The solution was obtained using time stepping on an Arakawa C-grid by applying periodic forcing and time stepping from homogenous initial conditions. The solution was achieved in 10,000 time steps using a step length of 15 seconds. This corresponds to running the model for roughly two days. Along the open boundaries around the edges of the model a global ocean tide model AG95.1 (Andersen et al., 1995) was used to provide boundary elevations (Shum et al., 1997).

### 2.3.7 Assimilated altimetry and tide gauge data

Satellite observations of sea surface height were initially used to derive harmonic constituents at the location of observations. The altimetry observations were derived from the NASA ocean altimeter Pathfinder products for the TOPEX/POSEIDON satellite. A full description of the data sets, their editing and processing can be found at <http://neptune.gsfc.nasa.gov/ocean.html>. A total of 179 crossover solutions obtained from TOPEX/POSEIDON altimetry were located inside the domain of the model.

The Australian National Tidal Facility provided a set of harmonic constituents for 57 primary ports in Australia. Harmonic constituents from 16 of these ports were used to supplement the altimetry, resulting in 195 tidal constituent sets, which were "blended" into the hydrodynamic tide model as described below. Harmonic constituents from the remaining 41 ports were used to tune and validate the tidal model.

Altimetry and tide gauge data at these 195 locations within the model domain were incorporated into the hydrodynamic model using a simple assimilation procedure called blending. The technique is similar to the method introduced to tidal modelling for a global case (Kantha, 1995).

In this procedure, the predicted tidal height at the 195 locations is substituted by a weighted mean of the predicted tidal height ( $H_{pred}$ ) by the model and the observed height ( $H_{obs}$ ) by the satellite or tide gauge, as:

$$Ht = wH_{obs} + (1 - w)H_{pred} , \quad (7)$$

where the prediction weight  $w$  is determined for each constituent individually. The modified height  $Ht$  is subsequently used to calculate the velocities for the subsequent timestep.

The weights for the blending were determined to ensure that the model is spatially smooth around the location of the blending. For diurnal constituents obtained from altimetry,  $w = 0.85$  and for diurnal constituents  $w = 0.75$ . For harmonic constituents derived at tide gauge ports a weight of 0.97 was used. The blending was only performed at each 10<sup>th</sup> timestep because of the way that the asymptotic model is sampled to obtain the harmonic constituents.

### 2.3.8 Estimation of tidal current threshold exceedance

The problem of calculating the bottom stress using modelled current speeds is that the effect of the benthic boundary layer is difficult to model in deep water (Pingree and Griffiths, 1979). The tidal model used here generated depth-averaged, hourly-averaged currents, and ignores the effects of bottom roughness elements and other bathymetric features affecting the velocity profile.

The Australian shelf model was subsequently time-stepped through a spring-neap cycle (roughly two weeks) at hourly intervals. The tidal current speeds were bilinearly interpolated to a grid spacing of 0.01° to conform to the swell wave exceedance calculations. Based on the threshold curve for unidirectional currents (Miller et al., 1977)

(Eq. 5), occurrences of threshold exceedance were tallied for the hourly current speed at each grid point to then generate a percentage of threshold exceedance map of the Australian continental shelf. As with the wave model, the observed grain size data for the Australian continental shelf was provided from the sediment database auSEABED (Jenkins, 2000).

### **2.3.9 Relative significance of wave versus tidal current threshold exceedance**

Waves or tides (or both) may affect sediment mobilisation on continental shelves, but the question posed here is which process is dominant on the Australian continental shelf? For the purpose of our analysis, threshold exceedance by waves occurring during any 6-hour period is registered as an “event”. The number of events per year yields a percentage of time for wave threshold exceedance for a given grid point.

For tides, threshold exceedance by the hourly-averaged bottom stress over a spring-neap cycle implies that movement occurs at least every fortnight (or 26 times per year). Thus, the main difference between wave and tidally-affected shelf areas is that, whereas tidal exceedance is periodic (fortnightly), the wave exceedance is episodic and/or seasonal. The sources of error in the analysis are thus also different for each case.

Below we assess the relative importance of waves and tides in mobilising the unconsolidated seabed sediments on the Australian continental shelf by accounting for the percentage of time that each process exceeds the threshold for mobilising the observed mean grain size. The analysis is carried out for each modelled grid point and the data are used to generate maps showing the spatial distribution of wave- and tide-dominated threshold exceedance.



## 2.4 Results

### 2.4.1 Waves

Around Australia, annual mean wave power is greater in the southern waters than in the northern waters (Fig. 2.3). The largest and longest-period (most powerful) waves occur off the west coast of Western Australia, in the Great Australian Bight and off western Tasmania (Fig. 2.4). Low mean wave heights and shorter wave periods occur on the Northwest Shelf, the Arafura Sea and in the Gulf of Carpentaria (Fig. 2.3). This pattern of wave climate is generally consistent with previous studies of waves on the continental shelf around Australia (Louis and Radok, 1975; McMillan, 1981; Wolanski, 1985).

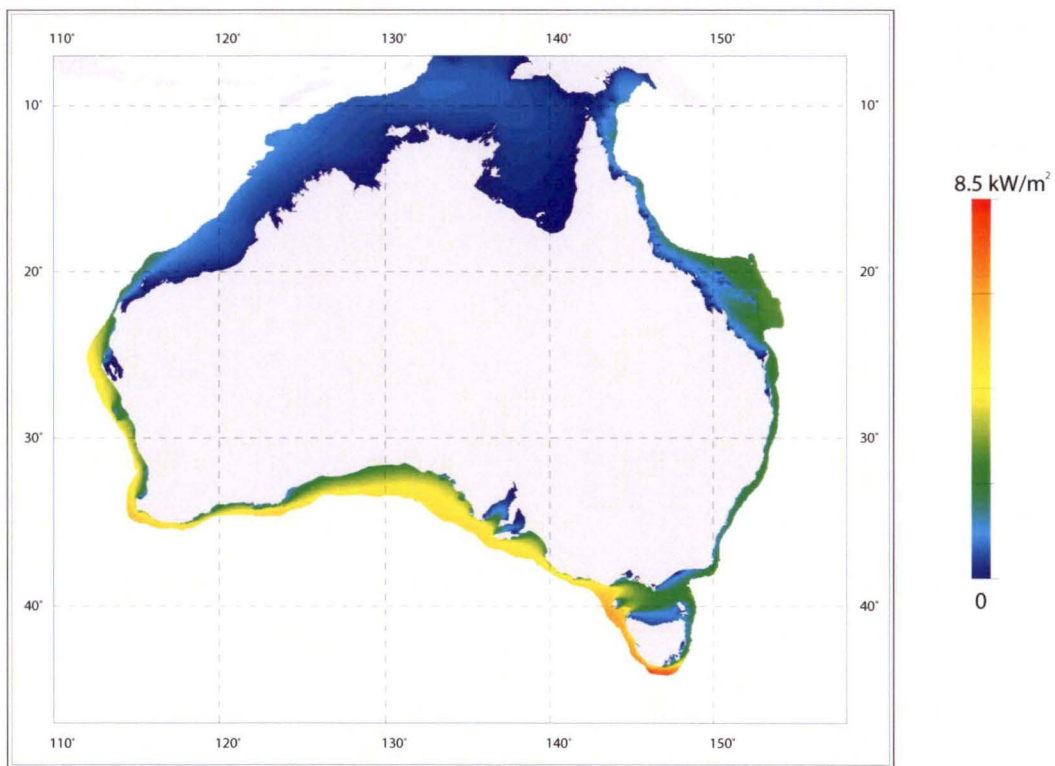


Fig. 2.3: Mean annual wave power ( $\text{kW/m}^2$ ) for the period March 1997 to February 2000 inclusive.

Maximum wave power peaks at  $2 \text{ MW/m}^2$  in the southern Great Barrier Reef, close to the Marion Plateau (Fig. 2.4), associated with waves generated by tropical cyclone conditions. Wave power attained  $0.76 \text{ kW/m}^2$  in the central Gulf of Carpentaria associated with

Cyclone Sid, which is nearly 200 times the mean wave power at this location (Fig. 2.3 and Fig. 2.4).

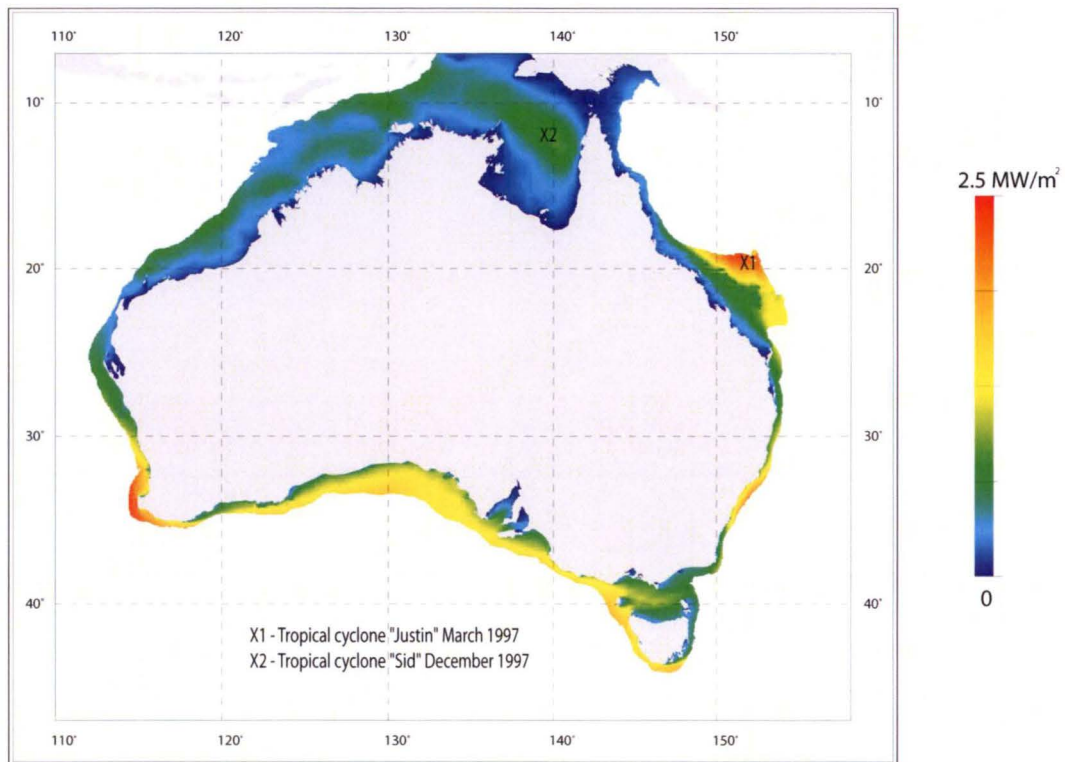


Fig. 2.4: Maximum wave power ( $\text{W/m}^2$ ) for the period March 1997 to February 2000 inclusive.

A feature of our prediction (Fig. 2.3 and Fig. 2.4) is the occurrence of quiet zones on the lee sides of islands and within protected embayments including King and Flinders Islands in Bass Strait (Fig. 2.3) which are protected from the prevalent weather. However, diffraction and refraction are not accounted for in the wave model used here, and so these protected zones are probably overestimated to a certain extent.

## 2.4.2 Threshold exceedance due to swell waves

The results indicate that threshold for mean grain size was exceeded over  $\sim 31\%$  of the shelf by waves between 1997 - 2000. The coarsest sediment appears to be in the temperate regions (Fig. 2.2). There is generally a landward succession of zones of increasing threshold exceedance, which is particularly clear on broad shelves such as the Great Barrier Reef, Gulf of Carpentaria, Lacepede Shelf and the Gulf of Papua (Figs. 2.2 and 2.6).



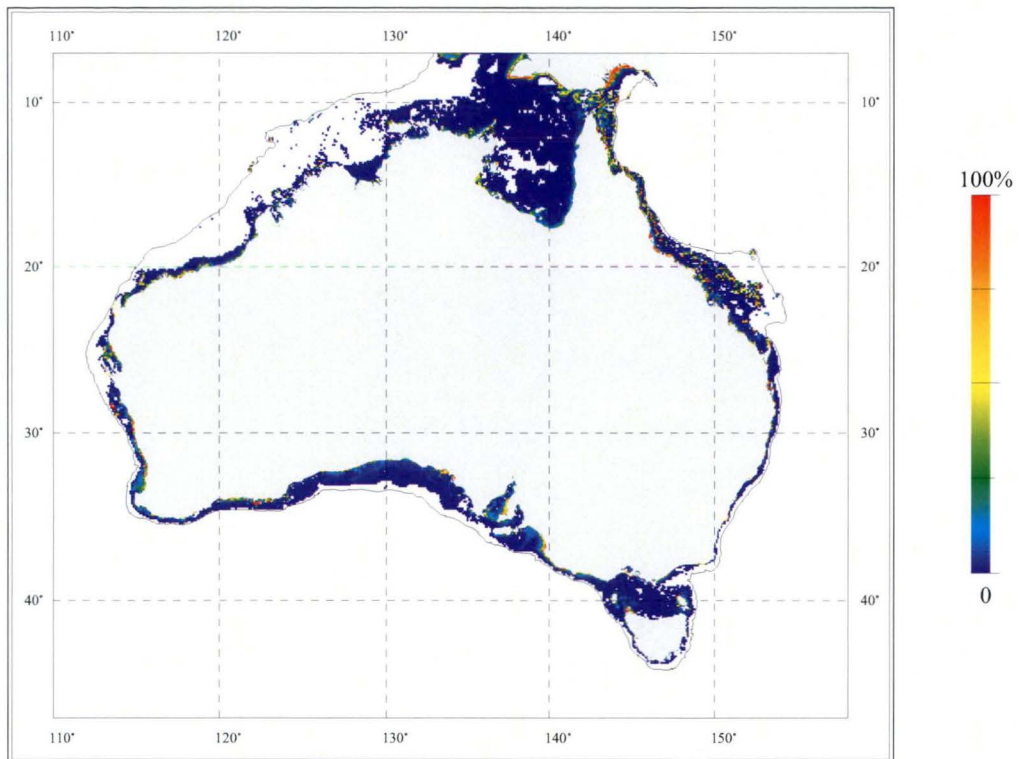


Fig. 2.5: Wave-induced exceedance for observed grain size distribution on Australian continental shelf for the period March 1997 to February 2000, inclusive.

The precise locations where the most powerful waves in the oceans around Australia are found vary from year to year; depending on the frequency/duration of storms and prolonged high wind speeds over a large fetch (Vincent, 1986; Harris and Coleman, 1998). The maximum wave height and period occurring on the shelf translates into a maximum water depth of potential shelf sediment mobilisation (depending on grain size). During the three years of modelled wave power, the maximum occurred in the southwest off Cape Leeuwin and eastern Marion Plateau. The deepest sediment mobilised was 0.005 mm on the Marion Plateau at a depth of greater than 300 metres.

### 2.4.3 Tides

Generally, the strongest tidal currents occur on macrotidal shelf areas (Fig. 2.6). Along the northwestern coastline of Australia, a maximum spring tidal range of 12.5 m is reached in King Sound (Easton, 1970) (Fig. 1.1). On the shelf adjacent to King Sound, our modelling results show maximum tidal current speeds ranging up to around 1.5 m/s. For eastern Queensland, our modelling results show the shelf is characterised by relatively high maximum tidal currents in the Torres Strait and Broad Sound areas (Fig. 1.1). Broad Sound has a tidal range of up to 8.2 m (Cook and Mayo, 1978).

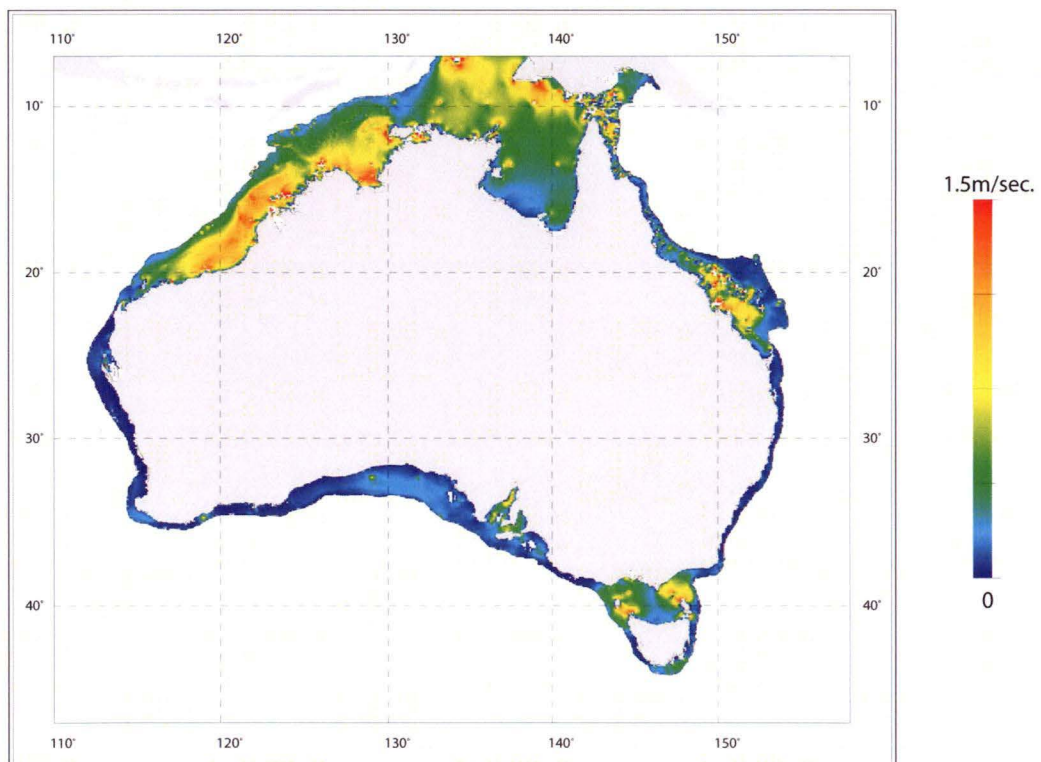


Fig. 2.6: Mean spring tidal current speed (m/s) on the Australian continental shelf.

Tidal currents are also relatively strong in some mesotidal and microtidal gulfs and shelf seaways, such as the Gulf of Carpentaria, Spencer Gulf, Gulf of St. Vincent, Bass Strait and Torres Strait. Amphidromic points located in the Gulf of Carpentaria, Joseph Bonaparte Gulf and in Bass Strait (Harris, 1994) are locations of tidal current maxima (Fig. 2.6).

2.4.4 Threshold exceedance due to tides

Tidal currents exceed the threshold speed for the mean grain size over ~ 41% of the shelf. The spatial distribution of tidal threshold exceedance (Fig. 2.7) illustrates that tidal currents are capable of mobilising finer sediments in the silt to fine sand range over most of the northern and northeastern sections of the shelf, including Bass Strait, Shark Bay and in Spencer Gulf. In contrast, gravel is locally mobilised mainly on the inner shelf at the sites of strongest tidal flows such as Torres Strait. In macrotidal King Sound, sand of up to 0.35 mm in diameter is mobilised 100% of the time.

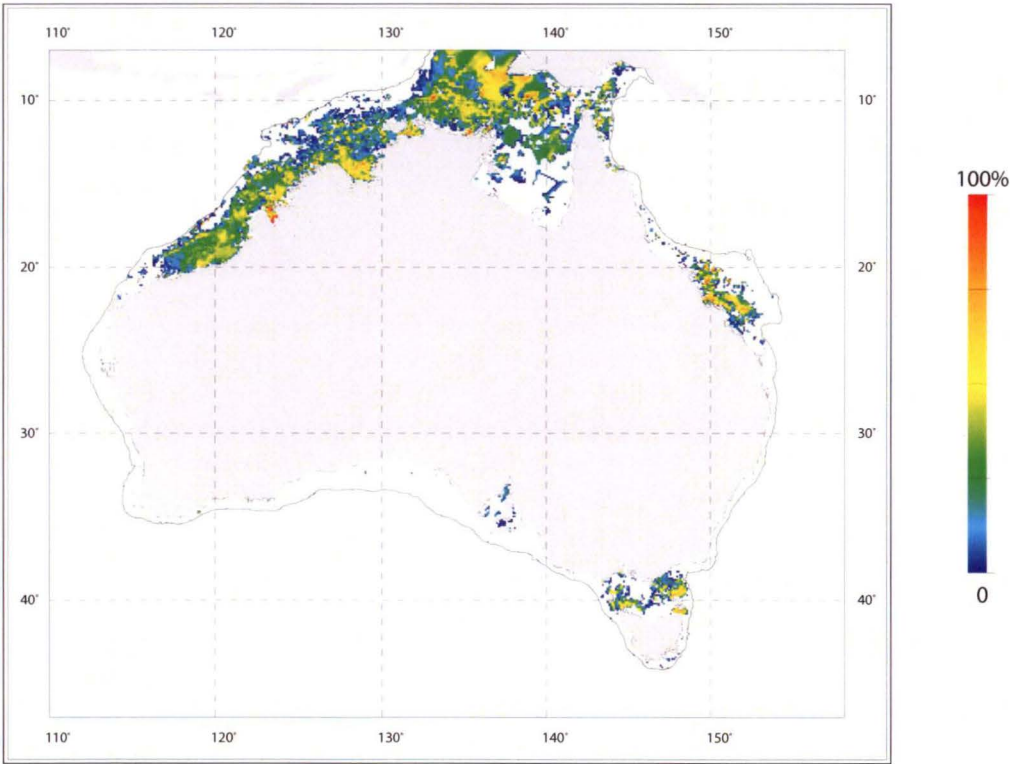


Fig. 2.7: Tide-induced exceedance for observed grain size distribution on Australian continental shelf.

## 2.5 Discussion

### 2.5.1 Derivation of a new shelf regionalisation

Combining the wave and tidal exceedance estimates into a ratio allows an assessment of the relative spatial importance of these two mechanisms in mobilising bottom shelf sediments (observed mean grain size, Fig. 2.2). Based on this approach, we have defined six separate categories of continental shelf region. Shelf regions where neither wave nor tidal currents were capable of mobilising bottom sediment are classified as "zero-mobility" regions. Shelf regions where either waves or tides mobilised the bottom sediment are classified as "wave only" or "tide only". Shelf regions where both waves and tides are capable of mobilising sediment are classified as "wave-dominated", "tide-dominated", or "mixed" depending upon the relative amount of time that each process is competent in mobilising the bed sediment. Our definition of "wave-dominated" applies to locations where the percentage of time of wave mobilisation is greater than 3 times the percentage of time of tide mobilisation. "Tide-dominated" applies to locations where the percentage of time of tidal mobilisation is greater than 3 times the percentage of time of wave mobilisation. Finally, "mixed" regions are defined here as occurring where the ratio of wave/tidal percent time exceedance is between 1/3 and 3. This concept of mixed wave and tidal current energy in mobilising bottom sediments is well established in the literature (Grant and Madsen, 1979; Pattiaratchi and Collins, 1985; Lyne et al., 1990).

The spatial distribution of our six regions (Fig. 2.8) indicates that they are not equal in surface area (Table 2.1). However, increasing or decreasing the value of the thresholds ratios from 1/3 and 3 only results in the increase of some regions at the expense of others. For example, wave-dominated and mixed areas are both small ( $\sim 0.5\%$  and  $\sim 2\%$  of the shelf, respectively; (Table 2.1), and the area of one of these regions can only be increased at the expense of the other. The spatial extent of the wave-only region ( $\sim 30\%$  of the shelf) and the tide-only region ( $\sim 22\%$  of the shelf; (Table 2.1) are mutually exclusive and their surface area is not affected by the definition of wave-dominated, tide-dominated or mixed regions.



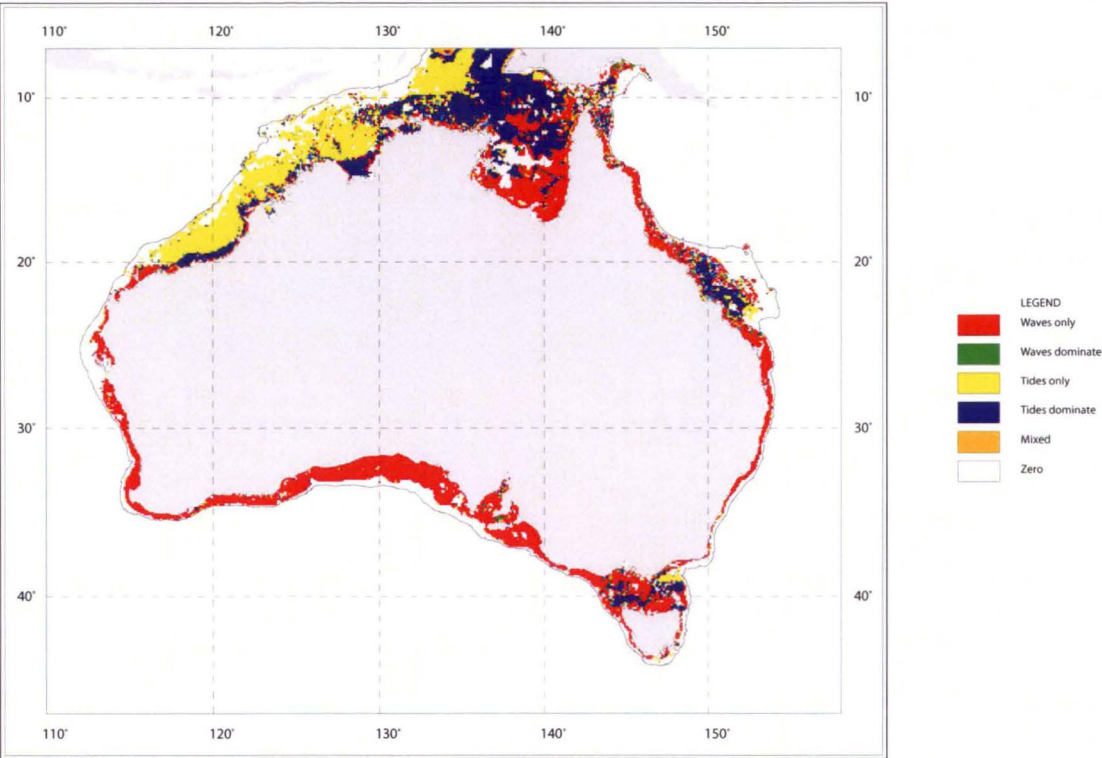


Fig. 2.8: Regionalisation of the Australian continental shelf for observed grain size distribution based on ratio of wave and tidal exceedance estimates.

Table 2.1: Delineated shelf categories and associated carbonate, grainsize, mud-content, and sorting percentages.

Regime	km <sup>2</sup>	Shelf (%)	Depth (m)	Carb. cont%	Grainsize(mm)	Mud cont. %	Sorting
Wave only	768508	30.22	48.55	72.66	0.88	13.32	1.36
Wave dominated	12345	0.49	22.63	63.79	0.39	26.86	1.72
Tide only	571559	22.47	47.98	72.69	0.29	40.96	2.16
Tide dominated	466144	18.33	111.32	76.93	0.57	24.21	1.61
Mixed	48403	1.90	24.85	70.56	0.43	25.53	1.66
Zero mobility	676199	26.59	188.78	83.65	1.95	14.67	1.52

Overall, there is a good spatial correspondence between our modelling results (Fig. 2.8) and the intuitive shelf classification proposed by (Harris (1995); Fig. 2.1), although there are some disparities. For example, our results show Spencer Gulf is “wave-dominated” and mixed (Fig. 2.8), whereas Harris (1995) predicted that this region was dominated by tidal currents (Fig. 2.1).

### 2.5.2 Regions of zero sediment mobilisation

Although we have focussed on near-bed currents generated by tidal and swell-wave processes, shelf currents occur over a broad range of spatial and temporal scales: at the scale of turbulence (0.2 - 5 sec); at the scale of wave orbital currents (5 - 20 sec); at the scale of tidal currents (6 hours); and at the scale of storm events (6 - 10 days). Superimposed upon these "events" will be other currents, such as intruding ocean currents, which may flow at a steady rate for weeks or months without changing significantly in speed or direction. The current regime in any given area is the product of a combination of different current components, although one type may be dominant locally (Swift et al., 1971). There are also areas of the shelf where the total energy available to mobilise the bottom sediment is very low.

The results indicate that the region of zero mobility accounts for ~ 27% of the shelf. Combined wave and tidal currents are capable of mobilising and transporting quartz grains of a given size in deeper water, or in shallow water more frequently. Furthermore, in shallow areas with a large tidal range, swell waves are most effective at mobilising sediment towards low water (i.e. when the water depth is at a tidal minimum). Under these circumstances, sea level variations must also be taken into account in the estimation of sediment mobilisation under combined flows. However, our interest is in the relative importance of waves and tides (i.e. determining areas of tide- versus wave-dominated transport) rather than the absolute value of transport intensity under combined flow conditions.

Although oceanographic processes other than waves and tides may influence sediment mobilisation, to a first approximation the zero-mobility regions defined here may be expected to behave as low-energy, depositional environments. In the present study, sediments deposited in zero-mobility regions occur at the greatest mean water depth (mean of 189 m) and are found to be more coarse-grained (mean size of 1.95 mm), higher in carbonate content (83.7%) and relatively lower in mud content (14.7%) in comparison to other shelf regions (Table 2.1). This finding contradicts the concept of a graded shelf (Swift and Thorne, 1991) and Aigner's "proximity" diagram (Aigner, 1985), in which mud content and the rate of bioturbation increase in an offshore direction (with lower energy and increasing depth). The explanation is that widespread occurrence of coarse, carbonate

sediments on outer portions of the Australian continental shelf has been attributed in many areas to their relict origin (Jones, 1973; Davies, 1979; Jones and Davies, 1983). These relict deposits appear generally not to have been buried by fine-grained, muddy sediments, probably because of the small volume of sediment discharge by Australian rivers, much of which is trapped within coastal depositional environments (Harris et al., 2002).

In conclusion, we find that Australia's deep-water, outer-shelf sediments are not in equilibrium with modern tide and wave hydrodynamic processes. Previous researchers have shown that in at least a few locations (i.e. off Fraser Island and sections of the east Australian margin) the deposition of coarse-grained carbonates is affected by strong ocean boundary currents. The question remains as to how much of the zero-mobility region is influenced by such ocean currents. Further field-research and modelling studies are required to find the answer to this question.

### **2.5.3 Mean grain size in relation to wave-only and tide-only mobilisation regions**

The results of our analysis allow comparisons between the areas of the Australian continental shelf where sediment mobilisation is affected by swell waves or tidal currents, and the associated water depth, carbonate content and grain size distribution (Table 2.1). The associations between regions of zero-mobility and water depth, carbonate content and grain size distribution were described above.

The wave-only and tide-only regions have nearly identical mean water depths ( $\sim 48$  m) and mean carbonate contents (both 73%) but very different mean grain size properties. Sediments in wave-only regions are coarser, lower in mud content and better sorted than sediments in tide-only regions (Table 2.1). A plot of mean grain size versus wave power and tidal current speed provides further insight (Fig. 2.9). This figure shows that, whereas there is a weak relationship between increasing tidal current speed and increased grain size ( $R = 0.38$ ; Fig. 2.9A), there is no evident correlation between mean grain size and increasing wave power (Fig. 2.9B). Apparently, wave-only regions are more efficient at winnowing and dispersing mud and finer-grained sediment, leaving a coarse, sorted lag deposit. In contrast, some tide-only regions appear to trap fine sediment particles, as

supported by previous observations of tidal turbidity maxima at several locations around Australia, including Gulf of St. Vincent (Phillips and Scholz, 1982), King Sound (Semeniuk, 1982) and Torres Strait (Harris and Baker, 1991). The results of our analysis of tidal currents and bottom sediments in tide-only regions indicates that areas of the Northwest Shelf and Bonaparte Gulf (Fig. 2.1) featuring bottom sediments with high mud-content are associated with peak tidal current vectors directed landwards and along the coastline (Fig. 2.10). In contrast, areas of low mud content are associated with seaward-directed maximum tidal current vectors. In regions where tidal processes control sediment transport, mud appears to be trapped on flood-dominated shelves but not on ebb-dominated shelves.



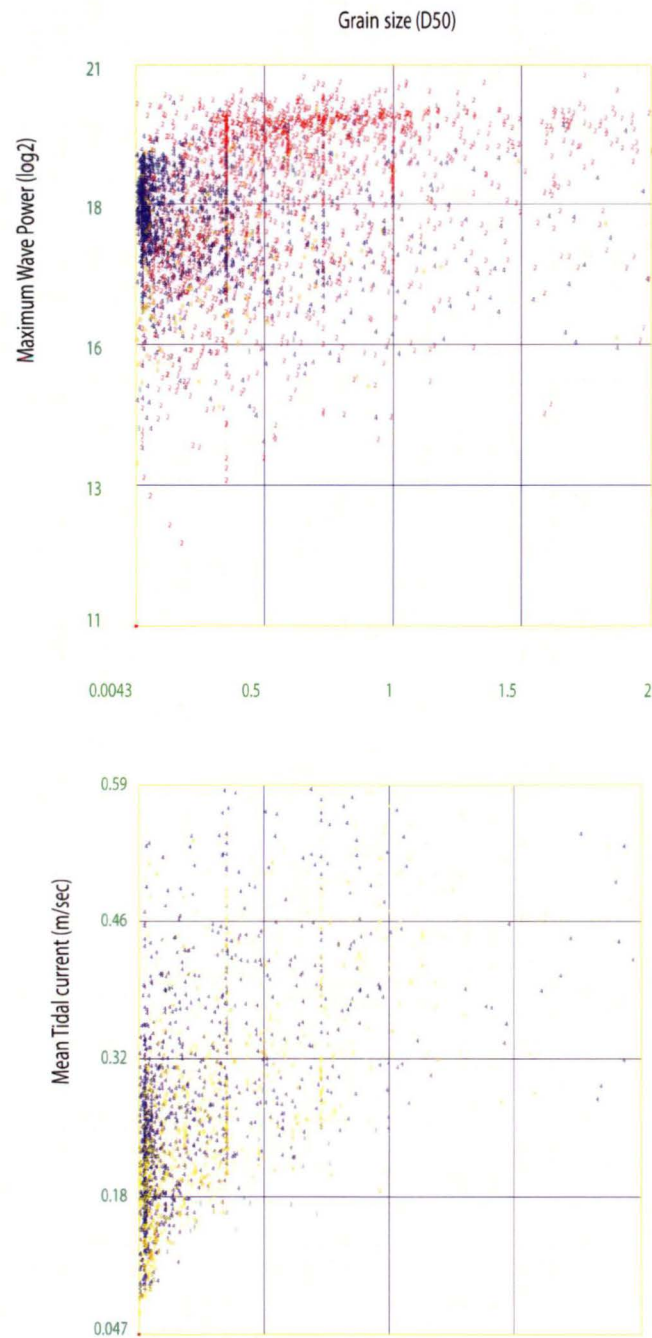


Fig. 2.9: Scatter plots of mean grain size versus: (A)  $\log_2$  of maximum wave power ( $\text{W/m}^2$ ) for the period March 1997 to February 2000, inclusive; and (B) mean tidal current speed (m/s).

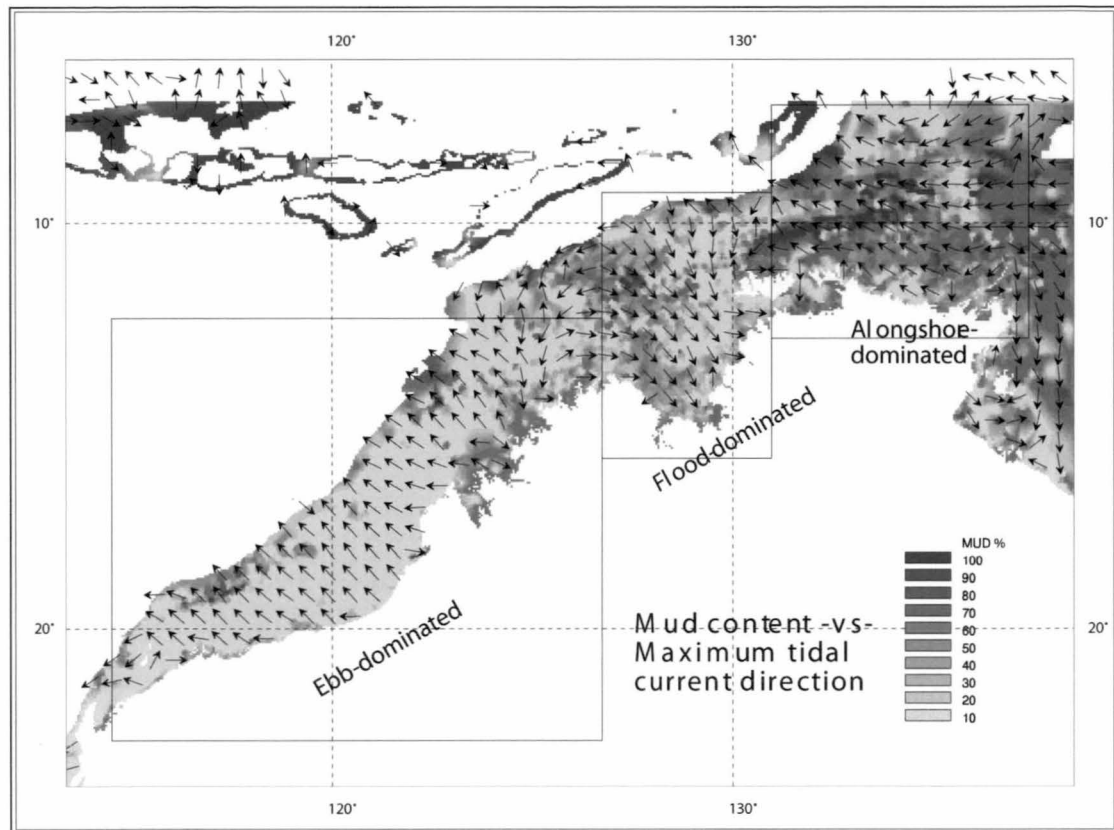


Fig. 2.10: Map of the northern Australia continental shelf, showing the mud content of surficial sediments in relation to the direction of maximum tidal current vectors. Muddy sediments appear to be associated with landward and along-shelf vectors whereas low mud content is associated with off-shelf oriented vectors.

Calcareous detrital silt is also generated in tidal shelf environments by the disintegration of soft carbonate grains as they are transported during bedload transport (Harris, 1994), which explains the high mud content (41%) of tide-only regions (Table 2.1). This high mud content is potentially of interest to environmental managers because heavy metals are commonly absorbed onto the surfaces of fine-grained sediments (Bourg, 1987). For example, the highest concentrations of heavy metals are found in the muddy deposits of Spencer Gulf (Harbison, 1984) and Torres Strait (Baker and Harris, 1991).

Tropical regions of Australia are prone to rare cyclone storm events. The sections of the shelf most frequently affected by cyclones are the Northwest Shelf (with an average of 10 cyclones per decade), the Gulf of Carpentaria (6 cyclones per decade) and the Great Barrier Reef (4 - 5 cyclones per decade) (Fig. 2.1). Tropical storms are episodic and infrequent (Fig. 2.1) with the time between events being measured in years. Between these violent storm

events, amounts of fine sediment are likely to accumulate and are only mobilised when another event occurs.

In contrast with the tropics, temperate regions experience frequent low-pressure systems and related storm events (Fig. 2.11). Large swell waves in temperate regions (Fig. 2.3) are the result of a continual series of cold fronts passing eastwards across the Southern Ocean. They are responsible for gale force winds producing large amplitude, long-period swell waves in places like southwest Australia and Bass Strait (Fig. 2.3). The propagation direction of storms in this region is usually towards the east. For example, the profile of a large storm in southwest Australia during October 1997 can be seen a few days later in Bass Strait (Fig. 2.11).

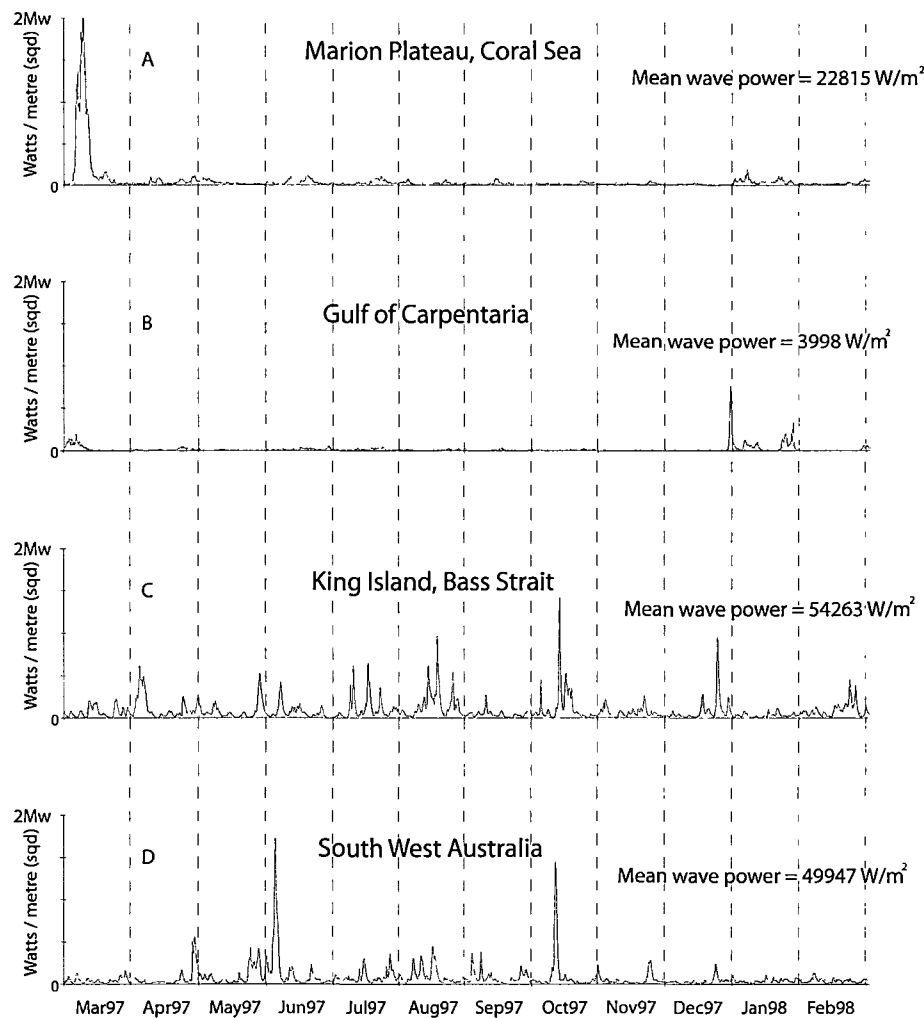


Fig. 2.11: A time series of wave power for four locations (shown in Fig. 2.2) (A) Marion Plateau; (B) Gulf of Carpentaria; (C) Bass Strait; and (D) Rottnest Shelf, southwest Australia. The 18 kW/m<sup>2</sup> wave power peak on the Marion Plateau occurs in March 1997 at the same time that tropical cyclone Justin was active over the Coral Sea and Queensland coast (X1 in Fig. 2.5). Wave power attained 10 kW/m<sup>2</sup> in the central Gulf of Carpentaria in December 1997, coincidental with Tropical cyclone Sid (X2 in Fig.2 5). This result is > 20 times the mean wave power at this location.

Currents produced by swell waves winnow away fine sediments, leaving a sorted layer of coarser sediment, which armours the seabed against further mobilisation. The equilibrium is only broken when a storm is violent enough to remove the armoured layer to allow the winnowing process to start again. For this reason, wave-only regions of the Australian shelf (Fig. 2.8) are associated with the coarsest-size sediments (0.88 mm; Table 2.1) and coarser sediments generally coincide with the largest maximum wave power (Fig. 2.9).

### **2.5.4 Sediment mobility and benthic biological habitats**

Sedimentologists generally focus on the preserved fossil assemblage and rarely consider the entire suite of living organisms that may be associated with a given core site or sedimentary environment. Biologists are equally biased in their research, as much more has been published on ecosystems associated with hard substrates (e.g. rocky shores and coral reefs) than ecosystems associated with unconsolidated sediment (Gray, 1981). Some studies have illustrated links between the texture and composition of bottom sediment and the distribution and abundance of benthic species (Somers, 1987; Long et al., 1995; Kostylev et al., 2001). It has been demonstrated that biodiversity and abundance of benthic species is inversely related to the mobility of the substrate (Shepherd, 1983; Poiner and Kennedy, 1984), with the lowest abundance and diversity associated with bedforms.

From this perspective, the high energy, mixed and tide-dominated zones of eastern and western Bass Strait comprise coarse-grained carbonate dunes (also termed ‘sandwaves’), which coincide spatially with a large part of scallop trawl-grounds (Kailola et al., 1993). It follows, therefore, that on sediment-mantled continental shelves, benthic habitats can be distinguished by sediment composition and grain size properties, together with the rate of sediment transport, and the frequency of the resuspension of detritus during storm and current events (Todd et al., 2000). On such continental shelves, measurements of sediment mobility can provide the basis for predicting the spatial and temporal nature of benthic habitats.

## **2.6 Conclusion**

Using estimates of tidal current speed and significant wave height and period, we have generated a new regionalisation of the Australian continental shelf, differentiating between wave- and tide-dominated shelf environments. The relative distribution of these regions is not dissimilar from the conceptually-based regionalisation previously proposed (Harris, 1995).

Our models, applied to the observed mean grain sizes, predict that sediments are mobilised by waves on  $\sim 31\%$  of the continental shelf and by tidal currents on  $\sim 41\%$  of the shelf. Thus, mobilisation of sediment on the Australian continental shelf is due mostly to tides rather than waves, in contrast to earlier models. Although the wave-only and tide-only regions of sediment mobilisation are found in similar water depths (mean depth of around 48 m) and the sediments have comparable carbonate content (mean of about 73%) the grain distributions are quite dissimilar. Tide-only regions have a mean grain size of 0.29 mm, and a mean mud content of 41%, compared with 0.88 mm and 13%, respectively, for wave-only mobilisation regions. We attribute these grain size patterns to differential winnowing and trapping of fine sediments by wave and tidal processes, and in particular, to the more efficient generation of calcareous silt by the fracturing of soft carbonate particles in tide-only regions. Trapping of mud on the shelf is associated with landward and along-shelf oriented maximum tidal current vectors, whereas off-shelf directed current vectors are associated with low mud content deposits.

The zero mobility regions, located in deep water (189 m mean depth) is characterised by coarse-grained, calcareous sediments having low mud content. This contradicts the conventional, graded shelf model (Aigner, 1985) but is consistent with earlier reports of widespread relict sediment deposits on the outer shelf and upper slope (Jones, 1973; Davies, 1979; Jones and Davies, 1983). These coarse-grained, relict carbonates are not in hydraulic equilibrium with the prevailing tide and wave current regime, but are known to be influenced in some locations by strong ocean boundary currents. Further research is needed to establish the spatial extent of ocean current influence on sediment mobilisation over Australia's continental shelf.

## **2.7 Addendum**

Since this chapter was accepted for publication in 2004, other studies have conducted further research into wave- or tide- dominated regions, sediment mobility and wave power distribution on Australia's continental shelf (Hemer et al., 2006; Griffin et al., 2008; Hughes and Heap, 2010). These models have been used to quantify sediment entrainment on the Australian continent (Porter-Smith et al., 2004; Hemer, 2006; Hughes and Heap, 2010) and

regionally (Griffin et al., 2008) and delineate the shelf on dominant processes. However, there were subtle differences between these models, for instance, how they treat mobilising currents, calculated sediment mobilisation and deriving estimates of sediment distribution.

Chapter 2 (Porter-Smith et al., 2004), provides a regionalisation of wave and tide dominance, based on an analysis of the ratio between wave and tide energy, and treating these processes proportionately but independently. The sediment mobilisation thresholds were calculated (Clifton and Dingler, 1984) by using simple calculations of maximum bed velocities due to wave and tidal currents, and the frequency with which sediments were mobilised by waves or tides were expressed as a percentage, allowing different regions of Australia's shelf to be classified as wave- or tide-dominated as appropriate. In contrast, other techniques such as the GeoMac model (Hemer, 2006; Hughes and Heap, 2010) have considered combined (vectorially-added) interactions between waves and currents (tidal and ocean), and then deriving the magnitude and frequency of these combined-flow bed shear stresses.

Another area of difference between models is the derivation and estimation of sediment distribution. The model described in Chapter 2 uses linearly-interpolated mappings of mean grainsize distribution over the shelf (Porter-Smith et al., 2004) from the auSEABED database (Jenkins, 2000). Other researchers (Hemer, 2006; Griffin et al., 2008) used specific site data from Geoscience Australia's Marine Samples (MARS) database (Passlow et al., 2005) and whose computations were restricted to locations where specific sediment samples were collected. The rationale was to reduce potential error resulting from interpolation anomalies, but the disadvantage is limited and sometimes patchy coverage resulting from the variability in data collection density. Other studies (Griffin et al., 2008) have refined the treatment of sediment quantification to include more multiple grainsize classes to counteract the over-simplification of using mean grainsize. One disadvantage of using mean grainsize is that it does not account for bi-modal grain sizes or poorly sorted sediment (Griffin et al., 2008). In assuming a singular grain size, finer grain sizes in the sediment matrix could be mobilised resulting in a potential underestimation of sediment mobilisation (Griffin et al., 2008).

One of the results of Chapter 2 was that present day physical sediment distribution was not in hydraulic equilibrium with mobilising processes. This was confirmed by the subsequent study of Hemer (2006) stating that low energy zones, particularly on the outer shelf,

corresponded with regions of zero mobility previously described in Chapter 2, confirming that processes in these regions of the Australian continental shelf were insufficient to mobilise sediment on the shelf (Hemer, 2006).

In conclusion, the results in Chapter 2 stand up well when compared to more recent studies (Hemer, 2006; Griffin et al., 2008). Chapter 2 explains most of the variability in the areas of wave and tide shelf domination, sediment-mobility and wave power distribution and is therefore relevant. In addition, Chapter 2 demonstrated a methodology that is ideal for continental-wide studies (Griffin et al., 2008) where data can be disparate. Additionally, this approach allows wave and tide processes to be assessed independently, which is more consistent with the other chapters of this thesis. A fuller description of comparative aspects of these models are well-documented in Griffin et al. (2008) and Hemer (2006).



## CHAPTER 3 COASTAL COMPLEXITY

### 3.1 Abstract

This study investigates Australia's planform coastline complexity to establish the relationship between geological inheritance, terrestrial and ocean processes, as well as determine the characteristic length scales at which they operate. Each of Australia's geological regions displays discrete complexity signatures indicating a strong correlation of coastal complexity to geology. These mesoscale complexity signatures vary enormously, over a range of length scales, indicating that geological inheritance is not the sole cause of complexity and that terrestrial and marine processes may well be significant factors. An angled measurement technique was used to quantify the coastal complexity at varying length scales. Estimates of coastal complexity were aggregated to each coastal geological region. Modelled estimates of wave and tide power and physical variables were compared to analyse the relative importance for each geological region in the formation of coastal complexity. These predictor variables included wave power, tidal power, elevation, rugosity, geological age and lithology. For each geological region, a correlation coefficient ( $\rho$ ) was calculated between coastal complexity and the predictor variables. Results show that lithological mix to be an important factor and coastlines of a homogeneous lithology tend to be straighter than coastlines of mixed lithology. The results further demonstrate that wave action promotes a straight coastline if the lithology is homogeneous and a complex one if the lithology is heterogeneous. This study found that lithological characteristics primarily determine the coastal complexity signature, which in turn determines the type of modification by wave action. This indicates that lithological makeup is an important determinant and that geological inheritance has the major influence in determining the control over variability represented by the characteristic length scales.

## 3.2 Introduction

A substantial amount of research has gone into quantifying planform coastal complexity but little done as to the reasons, and there are many hypotheses as to why some coasts are complex while others are not. One hypothesis is that coastal complexity is due to geological inheritance, and that the natural evolution for a coastline is to become more complex over time (Langford-Smith and Thom, 1969; Bishop and Cowell, 1997) - while others argue that coastlines can become straighter over time (Scheidegger, 1983). The coastal geological regions of the Australian mainland display visibly different types of crenulations. This implies that geological inheritance is an important factor. The main aim of this study was to investigate the relationship of coastal complexity to terrestrial and marine variables.

Mandelbrot's original assertion, that natural phenomena should be self-similar and the complexity across length scales should be constant, gives rise to the concept that a single value should, in theory, be descriptive of that particular landform (Mandelbrot, 1967). For a two-dimensional shape like a coastline, the fractal dimension ( $D_f$ ) can be expressed between 1 and 2, ranging from a straight line to an extremely complex line, respectively. There have been many attempts to correlate  $D_f$  to geomorphic form and process phenomena (D'Alessandro et al., 2006). For example, D'Alessandro et al. (2006) averaged the values of  $D_f$  for individual sectors along Italy's coastline, in an attempt to differentiate between tectonic dominance and erosive processes. They noted that several geological regions shared similar fractal values of  $D_f \sim 1.03$  and concluded that tectonic processes were the major influence in these regions and that where  $D_f > 1$ , secondary processes such as wave action were responsible for the complexity of the coastline. Although this work and many others (e.g. Klinkenberg and Goodchild (1992); Xu et al. (1993)) produced great advances in understanding the empirical relationships of the geomorphic form, the physical meaning of these calculated values remains elusive.

There is a difficulty in trying to directly link  $D_f$  of landforms to underlying geomorphic processes as there is no one-to-one relationship (Gao and Xia, 1996). The challenges of trying to relate a single fractal value to the summation of many characteristics is not the only impediment in the use of fractal geometry to measure and interpret landforms (Andrle, 1996). There is an inability to differentiate between large- and small-scale features (Goodchild, 1980; Mark and Aronson, 1984; Lam and Quattrochi, 1992; Bartley et al.,

2001). Geographical features and form are categorised by definitive measurements (Pentland, 1984; Duckham and Drummond, 2000). Ringrose (1994) considered an area of interest subject to a hierarchy of processes with different length scales, and concluded that a single fractal dimension will fail to pick up the inter-relationships of the processes and the scales at which they operate. Natural phenomena ultimately cannot be captured by a single value (Ringrose, 1994), and an attempt to do so may cause a process or form to be missed or misinterpreted (Andrle, 1996). Therefore, an appreciation of the variability of complexity evident at different length scales is fundamental. As such, the challenge is to try to quantify the relationship between form and process.

### **3.2.1 Characteristic length scales**

To study this relationship, it is necessary to adopt a methodology that accounts for scale variation as most geomorphologists recognise that there are characteristic length scales operating in landscapes and that geomorphic forms become most complex when approaching a dominant scale (Goodchild and Mark, 1987; Lam and Quattrochi, 1992; Andrle, 1994; Andrle, 1996). If dominant length scales apply to forms and processes relating to complexity on the coastline, it is vital to identify the scale at which these forms and processes are operating (Andrle, 1996).

Along the Australian coastline, discrete structural signatures appear to correlate to its geology, suggesting that geological structure may dictate the spatial variability. However, the complexity varies enormously, over a range of length scales, indicating that geological inheritance is not the sole cause of complexity and that terrestrial and marine processes may well be significant factors. Therefore, variations in the coastline complexity ( $C_x$ ) may hold an important clue to understanding the processes responsible for coastal form over different length scales. Notably, however, some variation may remain unexplained through investigations into  $C_x$  alone as, for example, prograding coastlines, such as deltas and strandplain coasts; owe nothing of their morphology to the inherited bedrock structure they overlie.

### 3.2.2 Causes of complexity

Some researchers have attributed  $C_x$  to the intersection of the sea surface with the bathymetric profile, stating that  $C_x$  is a two-dimensional indication of rugged shelf topography (Jiang and Plotnick, 1998; Zhu et al., 2004). As an example, the bathymetric profile of the Atlantic coast of North America is more complex than the Pacific coast and, therefore, has a more complex coastline (Jiang and Plotnick, 1998; Zhu et al., 2004). Other researchers have theorised that rocky coastline morphology is a function of the hydraulic pressure from wave action and the structural strength of the rocks (Sunamura, 1992; Fairbridge, 2004; Sapoval et al., 2004; Dickson and Woodroffe, 2005). However, a complex coast may also be the product of long-term terrestrial erosion (Phillips, 1986; Gao and Xia, 1996). Currently, there is no singular conclusive explanation as to why coastlines become complex. Certainly, the removal of material along the coastline is controlled by both wave action and mechanical erosion (Whitlow, 1984; Fairbridge, 2004; Finkl, 2004; Dickson and Woodroffe, 2005); however, this does not explain the resultant complexity at varying length scales.

### 3.2.3 Limitations of broad-scale approach

This study investigates coastal complexity relevant to mesoscale geological regions, based on the hierarchical scale described in Table 1.1. Geological regions reflect distinct, but cohesive, geological assemblages that differ significantly geologically from the adjoining regions (Blake and Kilgour, 1998). Visual examination of the geological regions shows that coastal complexity signature is quite distinct from region to region providing a first-order explanation of coastal complexity. Within each geological region the lithological mix within was examined, the rationale being that lithology is an important factor in erosion control and chemical weathering intensity (Biro, 1970; Summerfield, 1991b; Ludwig et al., 1996; Summerfield, 2000; Durr et al., 2005) and therefore possibly an important determinant of the resultant coastline morphology.

Some of the limitations of this broad-scale approach include the assumption of homogeneous geological structure (fracturing, jointing, faultline and folding) within each of

the geological regions (100s of km). The broad scale approach generalises the processes operating in a geological region, making it more difficult to attribute a specific process to form. Even coastlines within a lithological typology (therefore with similar lithology, aspect and processes) can exhibit considerable variation at a finer scale due to their different underlying structural geology. If a fine-scale approach was considered, it would likely lead to a greater variability of coastal complexity due to detailed consideration of the structural geology (fracturing, jointing, faultline and folding), sediment distribution, and morphology as these are important variables controlling form.

One assumption of this broad-scale approach is that the rock type as depicted on the small-scale geological map of Australia extends to the water line, ignoring beaches and exposures of sediment. In reality, these marginal features restrict interaction between waves and tides on the described bedrock where marine processes are opportunistic in attacking and eroding sections of coastline. It is acknowledged that this does represent a limitation of the analysis, however, as this is designed to operate at a broad scale, it is not practical to try to include these fine-scale coastal interactions.

A detailed field study of a smaller section of coastline would provide information on the relative influences of structural geology, sediment cover, local slope and aspect at a fine scale. However, such analysis along a section of Australia's coastline with a length of say 50 km would be time-consuming to say the least, and would represent a large project in its own right, requiring a combination of detailed photography and shape analysis of the coastline, as well as comprehensive geological sampling and digital terrain modelling. Even if such an analysis had been completed as a component of this study, its impact would not have been dramatic, as the length of the coastline of the Australian mainland alone is approximately 36,000 km. The extrapolation of a detailed analysis of a small section of coastline to the whole coastal margin would at best be regarded as highly optimistic.

It is acknowledged that the broad-scale approach undertaken in this thesis is unlikely to directly impact upon site-specific coastal management, which necessitates detailed assessment of small segments of coastline. However, this study is best regarded as a major step towards a conceptual hierarchical framework for the Australian continental margin. This approach will allow resource allocation to be assessed for areas of coastline with environmental significance. However, investigation at the level of reserve system design is beyond the scope of this study.

Although one of the advantages of the angled measurement technique is that it can be reliably quantify a planform coastline at varying length scales, another potential for error is the dependence upon data quality. For instance, sampling below the horizontal accuracy of a mapped coastline (rather than returning an angle of complexity), returns constant zeros or repetitive numbers, indicating lack of detail at these resolutions. Similarly, the choice of sample resolution is important and can potentially lead to the exclusion or separation of key geomorphic features.

In conclusion, although the technique for capturing coastal complexity is applicable to smaller sections of coastline, is a useful measure, and is repeatable at broad and fine scales, there are implications of data homogeneity and heterogeneity that are dependent on the scale being addressed.

### **3.3 Regional setting**

#### **3.3.1 Coasts dominated by storms and tides**

The Australian shelf and regional seas experience a wide range of climatic and oceanic conditions. The tropics experience episodic catastrophic cyclones, in contrast to temperate regions which experience frequent low-pressure storms (Porter-Smith et al., 2004; Condie and Harris, 2005; Church et al., 2006). Around Australia, annual mean wave power is greater in the southern waters than in the northern waters. The largest and longest-period (most powerful) waves occur off the southwest coast of Western Australia, in the Great Australian Bight and off western Tasmania. Low mean wave heights and shorter wave periods occur on the Northwest Shelf, the Arafura Sea and in the Gulf of Carpentaria. Maximum wave power generated by tropical cyclone conditions can increase the local mean wave power be nearly 200 times (Porter-Smith et al., 2004).

A number of tidal conditions occur around the Australian coast, as summarized by Easton (1970). Tide-dominated, macro-tidal shelves occur where the mean spring tidal range measured along the coast exceeds 4 m. The highest tidal ranges are on the Northwest Shelf (> 8 m) and the southern Great Barrier Reef platform with a tidal range > 7 m in Broad

Sound (Church and Craig, 1998). Outside the tropics, tidal ranges are generally micro-tidal ( $< 2$  m), with the exception of Spencer Gulf and Bass Strait (Easton, 1970; Church and Craig, 1998; Condie and Harris, 2005). Tidal currents can be significant in the previously mentioned high tidal range areas (Church and Craig, 1998). However, tidal currents are also relatively strong in some mesotidal regions (2 – 4 m), micro-tidal gulfs, and shelf seaways, such as the Gulf of Carpentaria. The strong tidal currents in Torres Strait and parts of the Great Barrier Reef are influenced by the narrow channels and shallow seas (Condie and Harris, 2005).

### **3.3.2 Geology of Australia**

The major structural elements of the Australian continent have been used by Blake and Kilgour (1998) to define geological regions. These regions comprise geological assemblages that differ significantly from adjoining regions with respect to age and lithology type (Fig. 3.1). Their classification is based on the underlying bedrock alone, not the superficial cover of unconsolidated material. This classification provides a spatial representation of the major crustal blocks (Scheibner, 1976; Plumb, 1979) and a framework for examining  $C_x$ . The geological regions range from Archaean (3500 ma) to Cainozoic (65-0 ma), and stark contrasts exist in their coastal complexity, even between adjacent regions. Lithology is an important factor in erosion control and the intensity of chemical weathering (Biro, 1970; Summerfield, 1991a; Ludwig et al., 1996; Summerfield, 2000; Durr et al., 2005) and may, therefore, play an important role in determining coastline morphology (Langford-Smith and Thom, 1969), particularly in response to different terrestrial and marine processes (Bishop and Cowell, 1997).

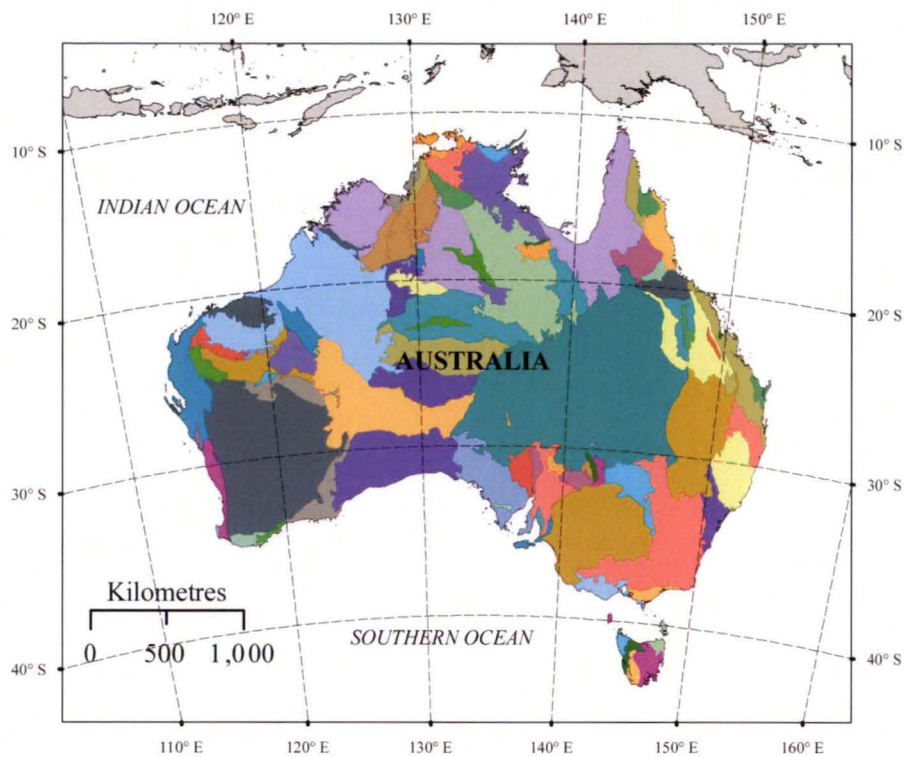


Fig. 3.1: Geological regions of Australia representing major structural elements (based on Blake and Kilgour, 1998)

### 3.4 Methods

The methodology chosen to capture  $C_x$  as a quantitative measurement was the angled measurement technique (Andrle, 1996). Complexity was measured at varying length scales of 2.5 km, 5 km, and 10 – 100 km at 10 km increments. The predictor variables included wave power, tidal power, coastal elevation, rugosity, geological age and lithology. Estimates of  $C_x$  and the predictor variables were aggregated at the above varying length scales to each coastal geological region (Fig. 3.1) for analysis.

The GIS used was Arc/Info (ESRI, 1996). This software allows for the assimilation of large complex datasets to be efficiently handled and has many vector and raster functions embedded in its software. The scripts for processing the large datasets were written in Arc Macro Language (AML) allowing a consistent methodology and procedure for optimising



and processing. Statistical analysis was carried out using the R package (Ihaka and Gentleman, 1996; R Development Core Team, 2004).

### 3.4.1 Wave and tide models

The wave model for the Australian region (AusWAM) used for this study was previously documented in Porter-Smith et al., (2004). Estimates of wave power or energy flux acting on the coastline were derived from wave height and period generated with the wave model (Greenslade, 2001), and used to quantify forcing from waves on the Australian coastline. The Australian wave model, whose boundaries are confined to 46°S to 07°S and 100°E to 156°E with a spatial resolution of 0.1°, is a high-resolution application of the WAM wave model (Hasselmann et al., 1988; Komen et al., 1996). This hindcast model is used to yield six-hourly predictions of significant wave height ( $H_s$ ), mean period ( $T$ ) and mean direction ( $D$ ). Model outputs used in this study were for the period March 1997 to February 2003, inclusive. Other investigations used additional years from the AusWAM hindcast time series in their investigations (Hemer, 2006; Hughes and Heap, 2010), eight and eleven years respectively. Their outputs were very similar indicating capture of most of the variability with the possible exception of decadal trends.

Wave power or wave energy flux ( $W_{ef}$ ), measured in W/m<sup>2</sup> is calculated from the wave model outputs using the formula (Holthuijsen, 2007):

$$W_{ef} = \frac{1}{16} \rho g H_s^2 C_g, \quad (1)$$

where  $\rho$  is the average density of seawater (kg/m<sup>3</sup>),  $g$  is gravity (9.8 m/s<sup>2</sup>),  $H_s$  is significant wave height (m), and  $C_g$  is the wave group velocity (m/s).  $C_g$  is determined using the equation  $C_g = n\lambda/T$ , where  $\lambda$  is wavelength of the wave and  $T$  is wave period. To determine the wave dispersion relationship  $n$  is (Holthuijsen, 2007):

$$n = \frac{1}{2} \left( 1 + \frac{4\pi h/\lambda}{\sinh(4\pi h/\lambda)} \right), \quad (2)$$

which varies from  $n = 1/2$  for deep water, and  $n = 1$  for very shallow water,  $h$  is water depth.

The tide model used for this study was previously documented in Porter-Smith et al., (2004). For estimations of the tidal processes acting on the continental shelf and on the coastline, outputs for tidal processes were generated using a tide model, namely the linearised, shallow-water (Andersen et al., 1995) tide model described by Egbert et al. (1994). The model boundaries were 0°S to 45°S and 109°E to 160°E, and the resolution was 0.067° for both latitude and longitude. The model output provides sine and cosines of the easterly and northerly components of the four main tidal (semi-diurnal and diurnal) constituents of  $M_2$ ,  $S_2$ ,  $K_1$  and  $O_1$ . The tidal power (or energy flux) was calculated for one half-lunar cycle from the tidal model outputs using the shallow water wave formulae (Dean and Dalrymple, 1990).

$$T_{ef} = \frac{1}{16} \rho g H_s^2 \sqrt{gh}, \quad (3)$$

where  $\rho$  is the average density of seawater ( $\text{kg/m}^3$ ),  $g$  is gravity ( $9.8 \text{ m/s}^2$ ),  $H_s$  is significant wave height (m), and  $h$  is the water depth (m). Tide power or energy flux ( $T_{ef}$ ) are measured in  $\text{W/m}^2$ .

The detailed criterion for quantifying the influence of waves and tides over the continental shelf is outlined in Porter-Smith (2004). Shelf regions where either waves or tides mobilised the bottom sediment are classified as ‘wave-dominated’ or ‘tide-dominated’. However, both waves and tides could be acting in synergy; so, the definition of wave-dominated is applied to locations where the percentage of time of wave mobilisation is greater than 3 times that of tide mobilisation. Correspondingly, tide-dominated applies to locations where the percentage of time of tidal mobilisation is greater than 3 times that of wave mobilisation. Areas where the ratio of wave/tidal percentage time exceedance falls between 1/3 and 3 are classified as mixed. This concept of mixed areas is well documented (Grant and Madsen, 1979; Pattiaratchi and Collins, 1985). The classification of wave- and tide-dominated areas used in this study corresponds to the intuitive shelf classification proposed by Harris (1995).

### 3.4.2 Elevation-bathymetric variables

To extend the study area to include the Gulf of Carpentaria and the far north, Geoscience Australia's Australian bathymetry and topography grid dataset (Petkovic and Buchanan, 2002) was resampled to a resolution of  $0.01^\circ$  and merged with a second Geoscience Australia dataset (Buchanan, 1998; AGSO, 1999). The topography above sea level originated from Geoscience Australia's (formerly AUSLIG) second edition digital elevation model for Australia. The new elevation-bathymetric model extended from  $45^\circ\text{S}$  to  $09^\circ\text{S}$  and  $109^\circ\text{E}$  to  $156^\circ\text{E}$  with a spatial resolution of  $0.01^\circ$  (Fig. 3.2).

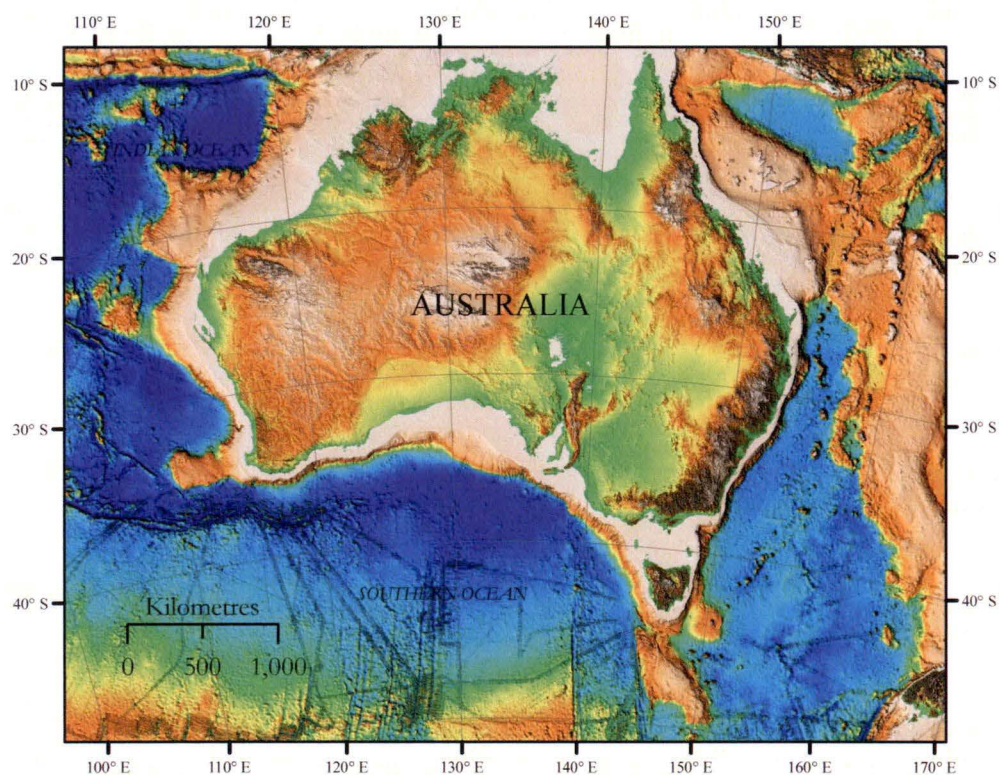


Fig. 3.2: Australian continental margin - bathymetry and elevation (Geoscience Australia, 2008).

This elevation-bathymetric model was used to extract rugosity ( $R_y$ ). Rugosity ( $R_y$ ) is in essence a measure of topographic unevenness and can be used to investigate the underlying geophysical processes that would not be apparent from a simple elevation model (Herzfeld, 2008). It is scale dependent, defining relief, rather than capturing the changes in elevation alone (Herzfeld, 2008). This method gives a quantitative metric that calculates the root mean square of height difference between a centre cell and its surrounding eight adjacent

neighbours (Fig. 3.3). This was calculated at a resolution of  $0.01^\circ$  for every cell (Błaszczynski, 1997; Riley et al., 1999).

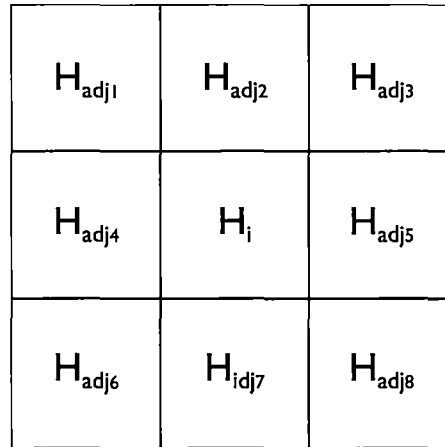


Fig. 3.3: Diagram of 3 x 3 cell grid demonstrating how  $R_g$  is calculated.

Rugosity index ( $R_g$ ), can be defined as,

$$R_g = \sqrt{\frac{\sum (H_i - H_{adj})^2}{n}}, \quad (4)$$

where  $H_i$  is a cell in a grid and  $H_{adj}$  are the adjacent cells around  $H_i$ .

The  $R_g$  for the Australian continental margin was derived from the Australian bathymetric and topographic models described previously (Fig. 3.2).

### 3.4.3 Geological variables

Geological variables used in this study included age and lithology. These variables were derived from Geoscience Australia's 1:2,500,000 national geology dataset (AGSO, 1998). This dataset gives an approximate maximum age in millions of years (Fig. 3.4) as well as stratigraphy and dominant lithological groupings (Fig. 3.5) of rock units for continental Australia (Shaw et al., 1999; Hillis and Müller, 2003). The dominant lithological associations include; sedimentary rocks, mafic volcanics, dolerites and gabbros, felsic volcanics, granites,

intrusive complexes (non-granitic), amphibolite-facies metamorphics, serpentinites, mafic-ultramafic intrusives, felsic to mafic volcanics and granulite-facies metamorphics.

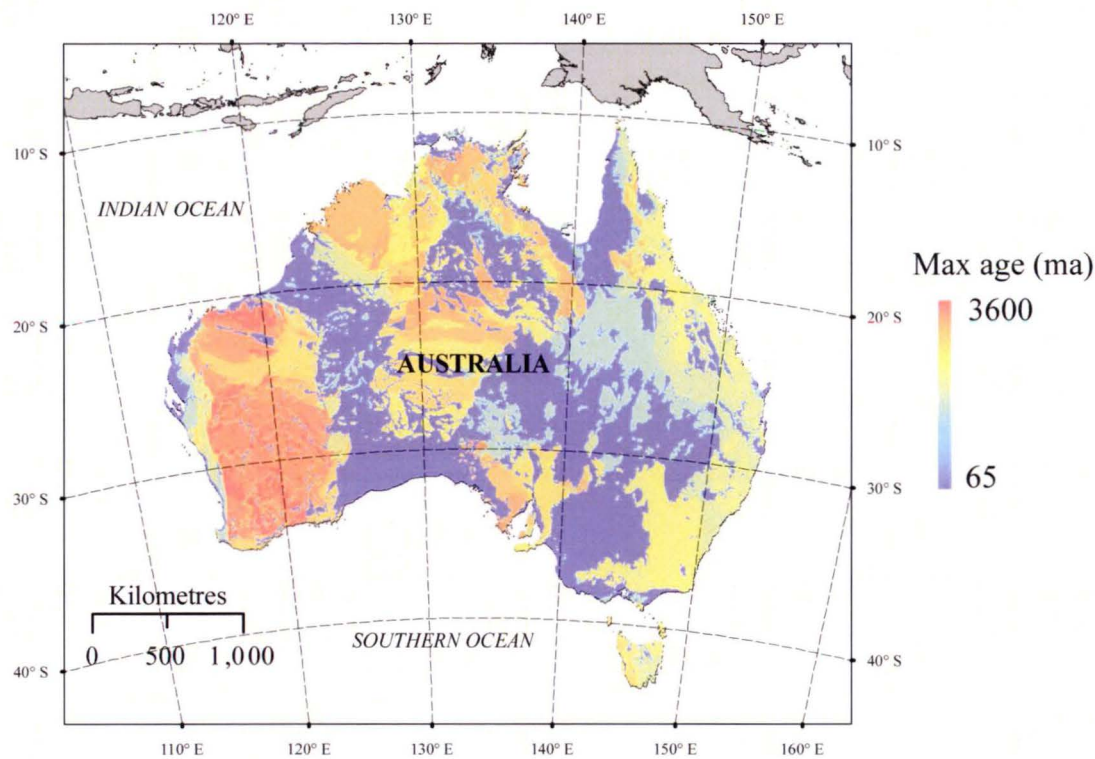


Fig. 3.4: Maximum age of terrestrial geology.



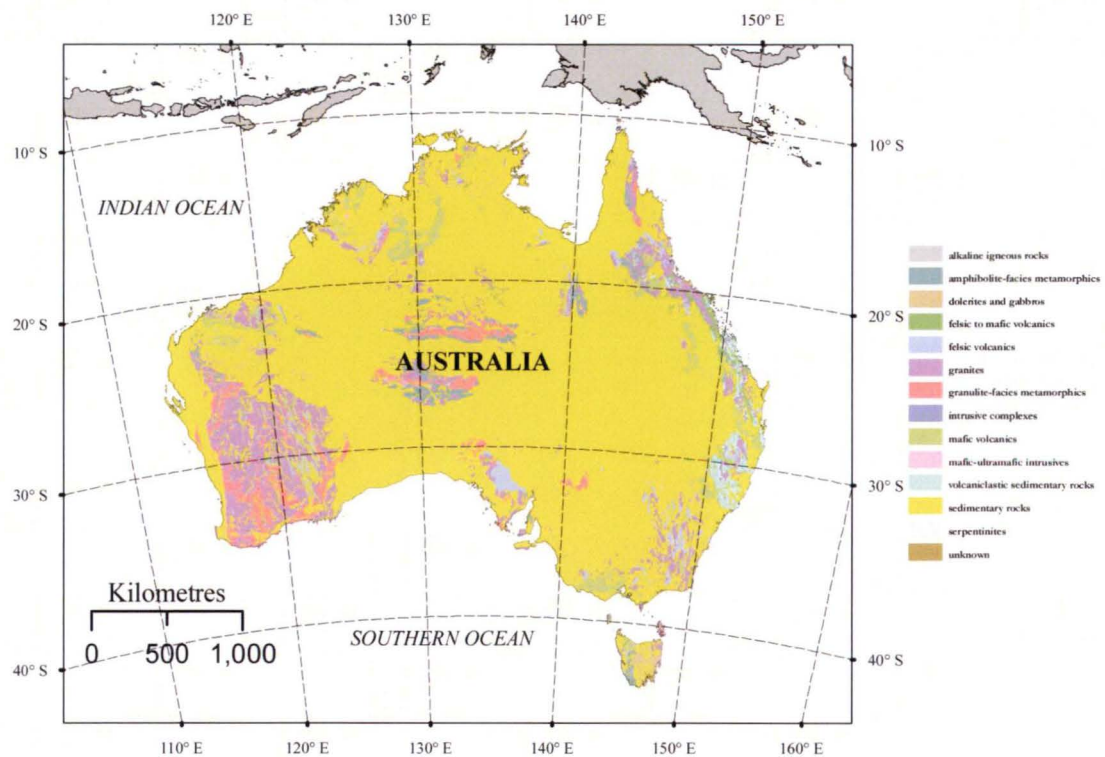


Fig. 3.5: Lithology of the Australian continent.

The dataset representing lithology is categorical. As such, a quantitative measure for each geological region is derived to represent the diversity of lithology therein. To quantify the lithology within each geological region, the Shannon index (also known as the Shannon-Weaver Index) was used (Shannon, 1948; Shannon and Weaver, 1949). This index extracts information on the entropy of a distribution of categorised data.

### 3.4.4 Quantifying coastal complexity ( $C_x$ )

The angled measurement technique (AMT) was used to quantify coastal complexity at various length scales (Andrle, 1994). AMT is well suited for geomorphic classification because it can differ with scale without making any assumptions about statistical self-similarity. To calculate this, the mapped coastline at a 1:100,000 scale was used. Random nodes along the coast were selected (e.g. Fig. 3.6) and the Euclidean distance of a length scale ( $S$ ) was measured out forward (AB) and backward (AC) of each random point (A). The angle CAD, (the supplementary angle of CAB), was measured, and used to quantify  $C_x$  for that particular segment of coastline (Andrle, 1994; Bartley et al., 2001). To identify

characteristic scales, a number of length scales or resolutions were chosen (scales of 2.5 km, 5 km, and 10 – 100 km at 10 km increments). At each of these nodes, several variables were recorded (Table 3.1).

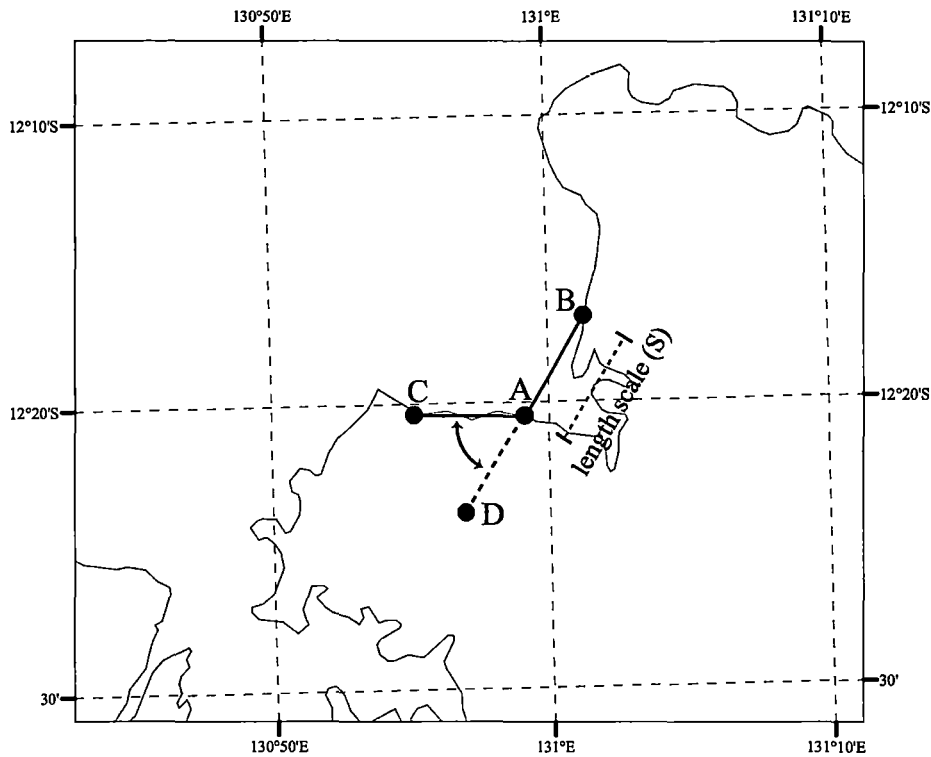


Fig. 3.6: Calculation of complexity using the 'angled measurement technique'. The length scale ( $S$ ) is measured forward ( $AB$ ) and backwards ( $AC$ ) of a randomly chosen point ( $A$ ) on the mapped coastline. The measure of complexity is the angle  $CAD$  (supplementary angle of  $CAB$ )

The number of random nodes selected around the Australian coastline was 2373; the maximum distance between each node was never greater than 20 km. and the measure of complexity ( $CAD$ ) ranged between 0 - 135°.

Table 3.1: Outputs for complexity ( $C_x$ ), wave ( $W_{ef}$ ) and tidal power ( $T_{ef}$ ) recorded for each random point location on the coastline.

Variables	Definitions	Methods
X-coord	Longitude of random point	Arc/Info ARC
Y-coord	Latitude of random point	Arc/Info ARC
RegName	Geological Region	Arc/Info ARC
$C_x$ 2.5	Length scale of 2.5 km (°)	Arc/Info GRID
↓	↓	↓
$C_x$ 100	Length scales of 100 km (°)	Arc/Info GRID
$W_{ef}$	Wave power or energy flux (kW/m <sup>2</sup> )	Arc/Info GRID
$T_{ef}$	Tidal power or energy flux (kW/m <sup>2</sup> )	Arc/Info GRID
$WTdom$	Wave and tide dominated shelves	Arc/Info GRID

3.4.5 Aggregating to geological regions

The random point data from Table 3.1 were aggregated to each geological region along with estimates of  $R_g$ , height, age and lithology. By aggregating the median values of  $C_x$  and the marine and physical variables to geological regions (Table 3.2), it was possible to investigate the relationship of a coastline to terrestrial and marine processes. The geological regions examined were reduced from 38 to 24, due to a paucity of representative numbers of random sample points within 14 of the geological regions.



Table 3.2: Coastal complexity ( $C_x$ ), marine variables ( $W_{ef}$ ,  $T_{ef}$ ,  $WT_{dom}$ ) and rugosity ( $R_g$ ), height, age and lithology aggregated for each geological region

Variables	Definitions	Methods
RegName	Geological region	Arc/Info ARC
$C_x 2.5$	Length scale of 2.5 km (°)	Arc/Info GRID
↓	↓	↓
$C_x 100$	Length scales of 100 km (°)	Arc/Info GRID
$W_{ef}$	Wave power or energy flux (kW/m <sup>2</sup> )	Arc/Info GRID
$T_{ef}$	Tidal power or energy flux (kW/m <sup>2</sup> )	Arc/Info GRID
$WT_{dom}$	Wave and tide dominated shelves	Arc/Info GRID
$R_g$	Median zonal rugosity ( $R_y$ )	Arc/Info GRID
Height	Median zonal height (m)	Arc/Info GRID
Age	Median zonal dominant age (ma/yr)	Arc/Info GRID
Lithology	Median Shannon Diversity Index of lithology	Arc/Info GRID

The Arc/Info GRID platform was used to analyse the geological regions using functions available within the software (ESRI, 1996). Values within 100 km of the coastline were selected, as distances greater than this allowed interior geology to overly influence results (Fig. 3.7). Median values of all variables were calculated and mapped according to percentile ranges for each geological region. The terrestrial variables included  $R_g$ , height, age and the Shannon diversity index for lithology. The variables representing marine processes were represented by  $W_{ef}$  and  $T_{ef}$ .

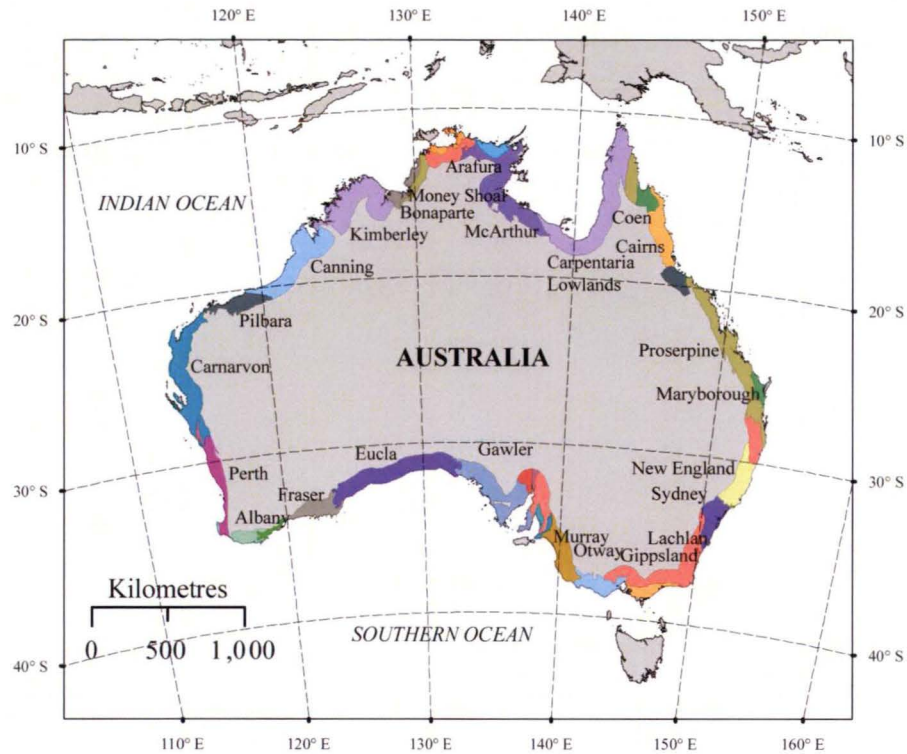


Fig. 3.7: Geological regions of Australia, as classified by Blake and Kilgour (1998), adjacent to the coastline.

### 3.4.6 Cluster analysis of $C_x$

To determine the hierarchical relationship between the geological regions, based on  $C_x$ , a similarity matrix was constructed using only the  $C_x$  length scales ( $L_m$ ) (Clarke et al., 2001). A dendrogram was constructed from these results highlighting the Euclidean distance between each region. This hierarchical clustering method is agglomerative, starting at individual geological regions and successively merging regions based on the linkage criteria.

An advantage of clustering the  $C_x$  variables exclusively is that there is no ambiguity as to what variables are relevant for this ordination. In this way, all variables are the same, differing only in length scale measure, eliminating the need to standardise the data or debate the validity of variables included.

### 3.4.7 Similarity matrix of physical variables

The remaining physical variables ( $W_{sp}$ ,  $T_{sp}$ ,  $R_{sp}$ , height, age and lithology) were transformed to a dimensionless scale to accommodate the many data ranges and a similarity matrix was constructed based on their Euclidean distance ( $V_m$ ).

### 3.4.8 Correlating $C_x$ to physical variables

Spearman rank correlation is a non-parametric method that can be applied to data that do not meet the assumptions about normality, homoscedasticity and linearity (McDonald, 2009). A Spearman rank correlation was implemented between the respondent  $C_x$  length scales ( $L_m$ ) and the predictor physical variable ( $V_m$ ) matrices. By rank correlating the two similarity matrices, a measure of agreement ( $\rho$ ) was computed for all possible combinations of each variable (Clarke and Ainsworth, 1993; Clarke et al., 2001).

The Spearman rank coefficient  $\rho$  is given by,

$$\rho = 1 - \frac{6}{N(N^2 - 1)} \sum_{i=1}^N (d_i)^2, \quad (5)$$

where  $d_i = L_m - V_m$  = the difference between the ranks of corresponding similarity matrices of length scales ( $L_m$ ) and physical variables ( $V_m$ ) and  $N$  = the number of values in each data set (Kendall, 1970; Clarke and Warwick, 1994).

## 3.5 Results

### 3.5.1 Geological regions and length scales

The characterisation of geological regions based on  $C_x$  at varying length scales is given in Fig. 3.8. The graphs for each geological region reflect the varying levels of complexity, and

provide a visual representation of modal characteristics. Each geological region displays a characteristic  $C_x$ , enabling correlations and classifications to be made between them. For example, the Eucla geological region (Fig. 3.8a) has a very low degree of complexity for all length scales, in contrast to the Kimberley region, which has high levels of complexity and variability, particularly at shorter length scales.

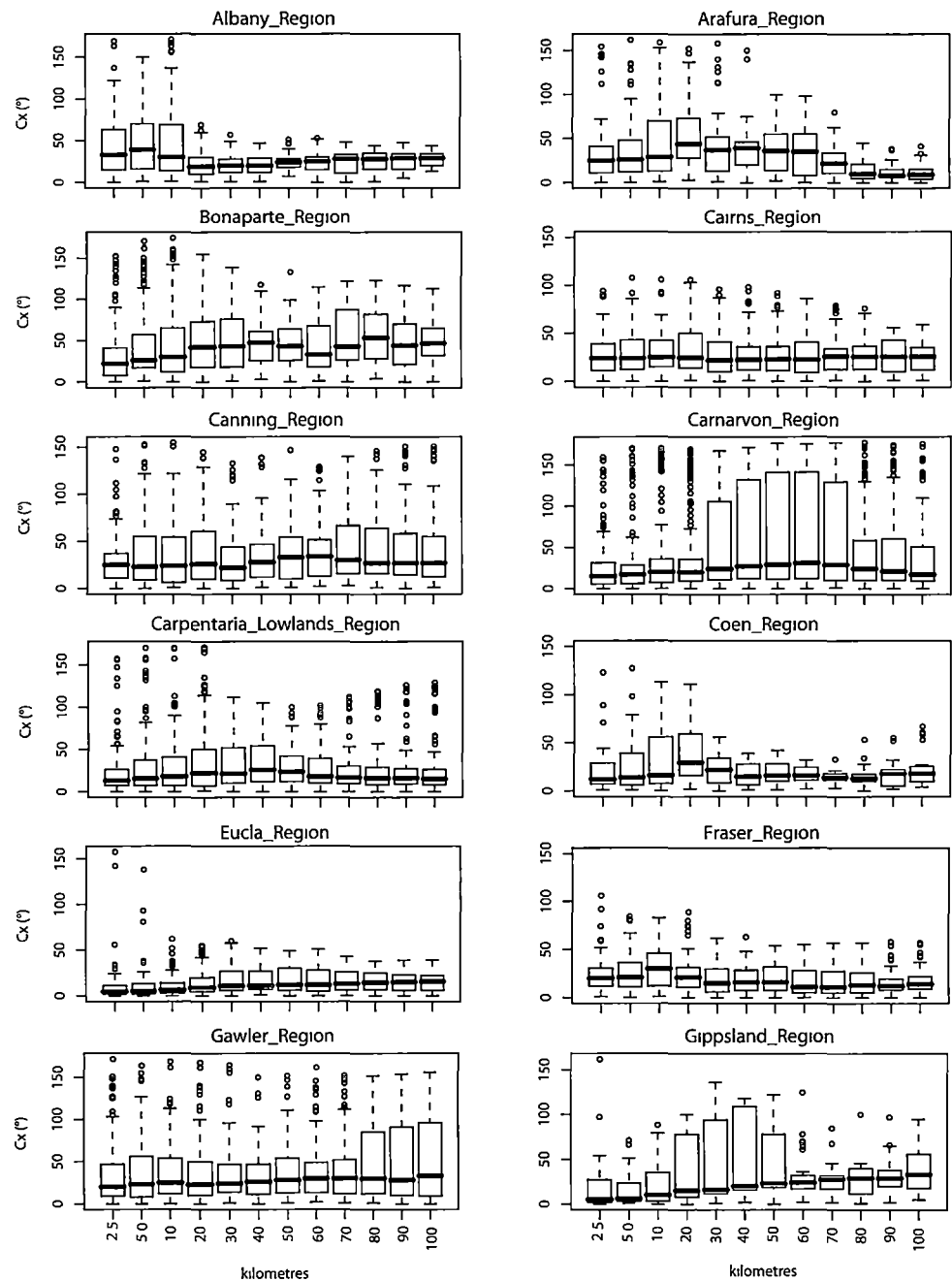


Fig 3.8a: Boxplots of  $C_x$  expressed in degrees ( $^{\circ}$ ), at varying length scales (2.5 – 100 km) for geological regions of Albany, Arafura, Bonaparte, Cairns, Canning, Carnarvon, Carpentaria Lowlands, Coen, Eucla, Fraser, Gawler and Gippsland geological regions. The horizontal bar in the middle of each boxplot indicates the median value of length scale, with the top and bottom of these boxes capturing the 75<sup>th</sup> and 25<sup>th</sup> percentile, also referred to as the interquartile range. The whiskers indicate the full range of data, while the circles represent the outliers. Outliers are values more than 1.5 times the interquartile range above the 75<sup>th</sup> or below the 25<sup>th</sup> percentile (Crawley, 2005). The y-axis represents the  $C_x$  measured in degrees and the x-axis represents the length scale ranging from 2.5 km - 100 km.

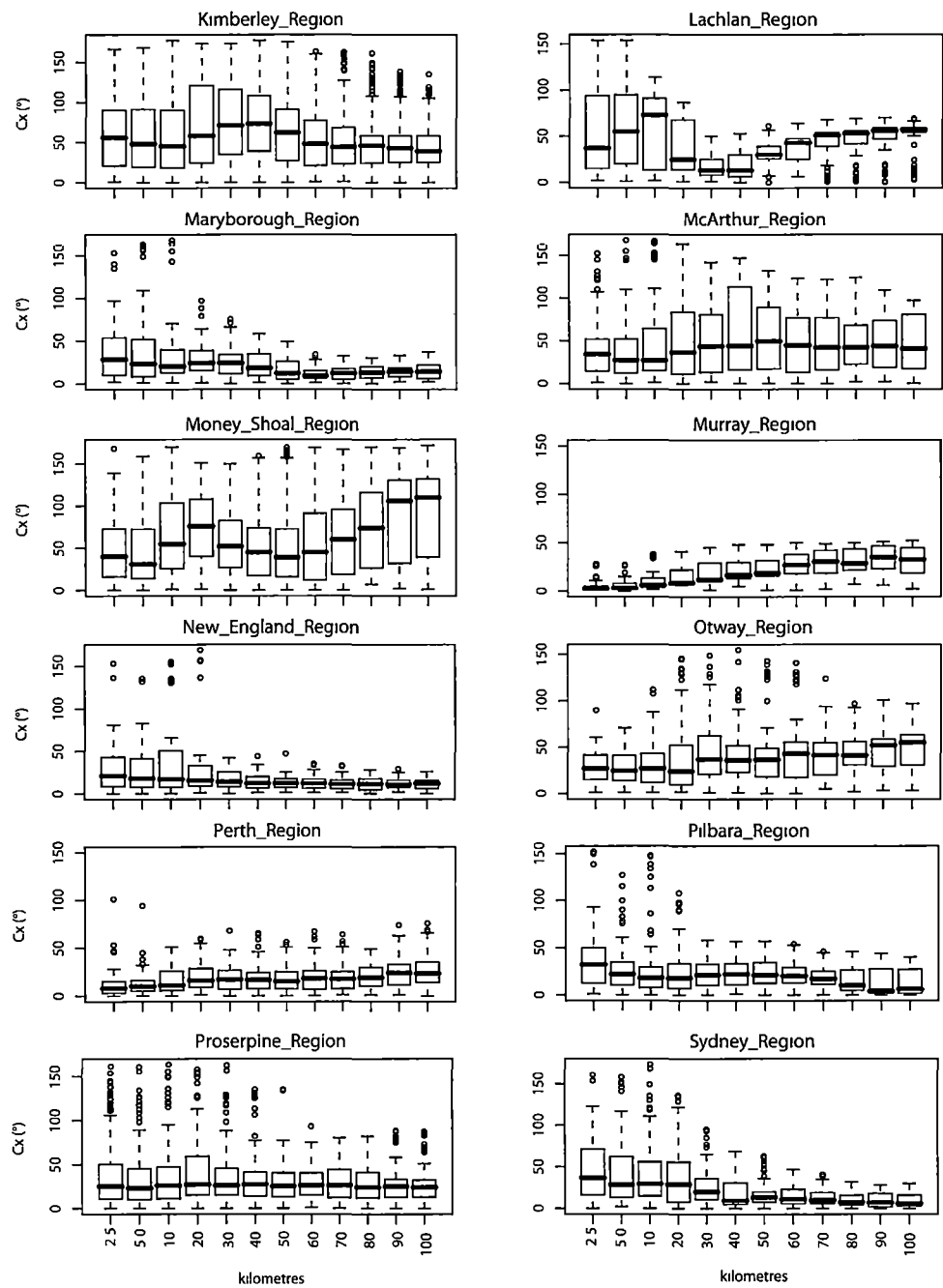


Fig. 3.8b: Boxplots of  $C_x$ , expressed in degrees ( $^{\circ}$ ), at varying length scales (2.5 – 100 km) for geological regions of Kimberley, Lachlan, Maryborough, McArthur, Money Shoal, Murray, New England, Otway, Perth, Pilbara, Proserpine and Sydney geological regions.

3.5.2 Geological regions and physical variables

The following maps represent metrics of physical variables derived within each geological region. They included  $R_g$  (Fig. 3.9), height (Fig. 3.10) age (Fig. 3.11) and the Shannon diversity index for lithology (Fig. 3.12). The variables representing marine processes are summarised in the variables  $W_{ef}$  (Fig. 3.13) and  $T_{ef}$  (Fig. 3.14).

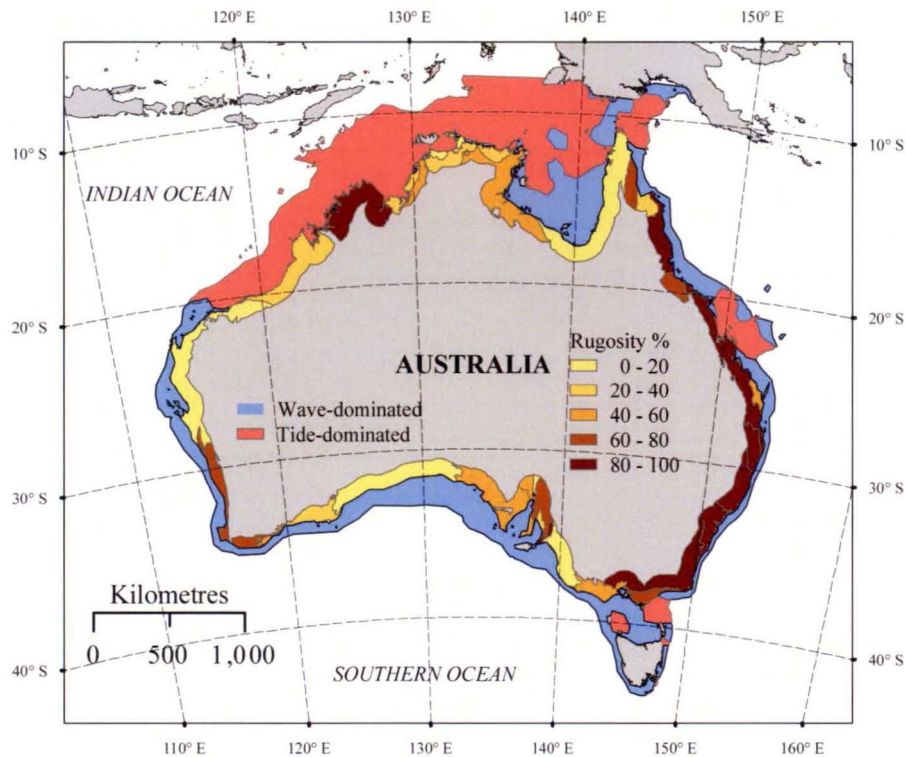


Fig. 3.9: Rugosity ( $R_g$ ) expressed in percentiles for each Geological Region.



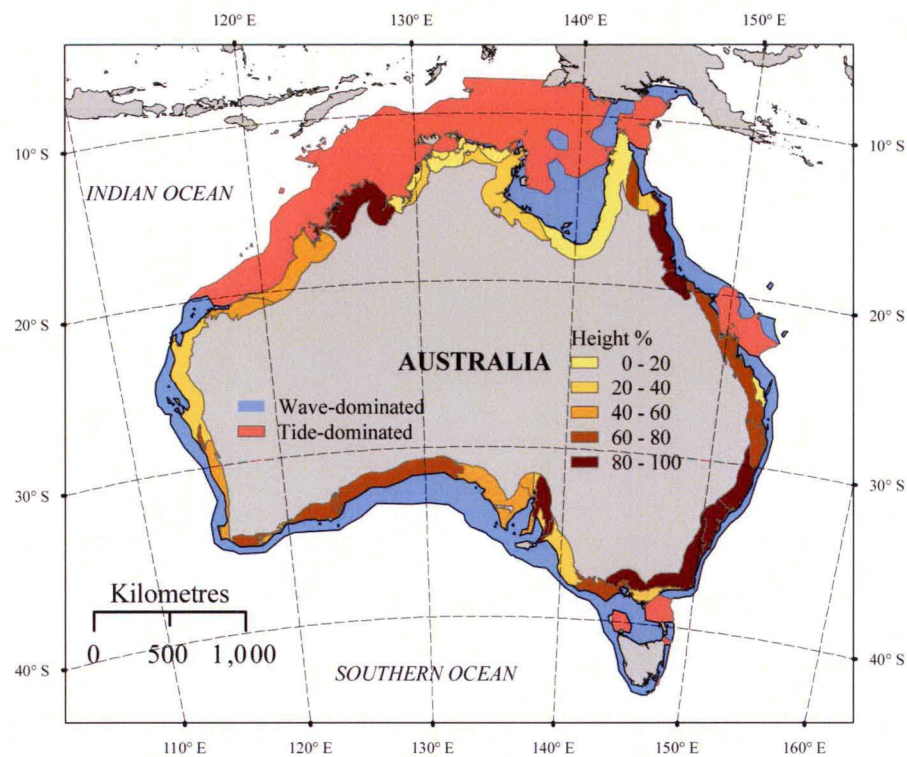


Fig. 3.10: Elevation expressed in percentiles for each Geological Region.

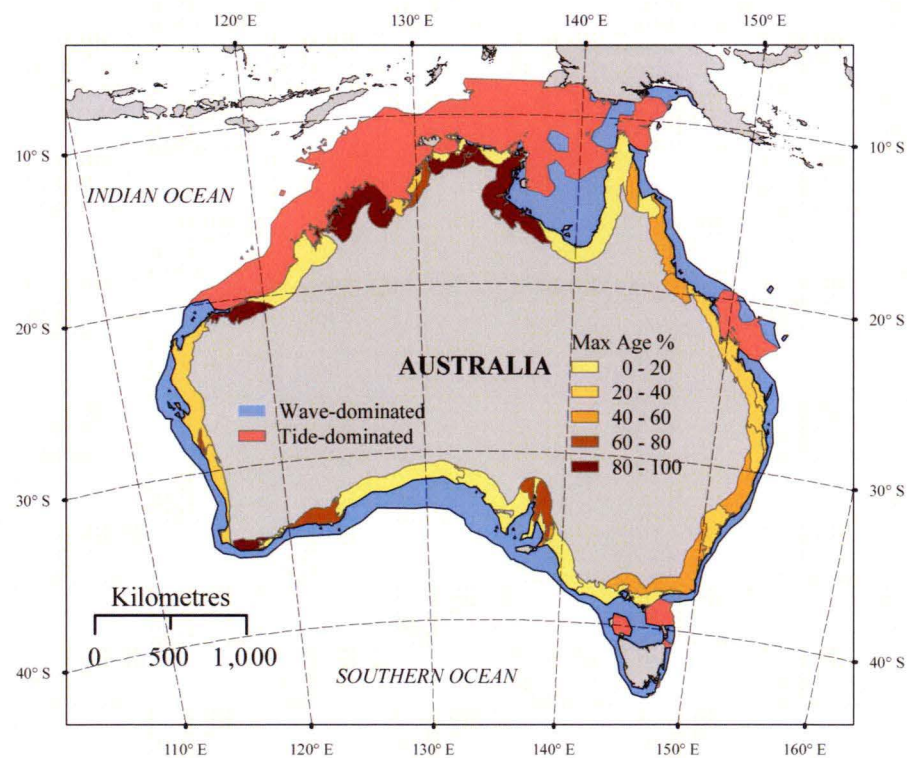


Fig. 3.11: Geological age expressed in percentiles for each Geological Region.



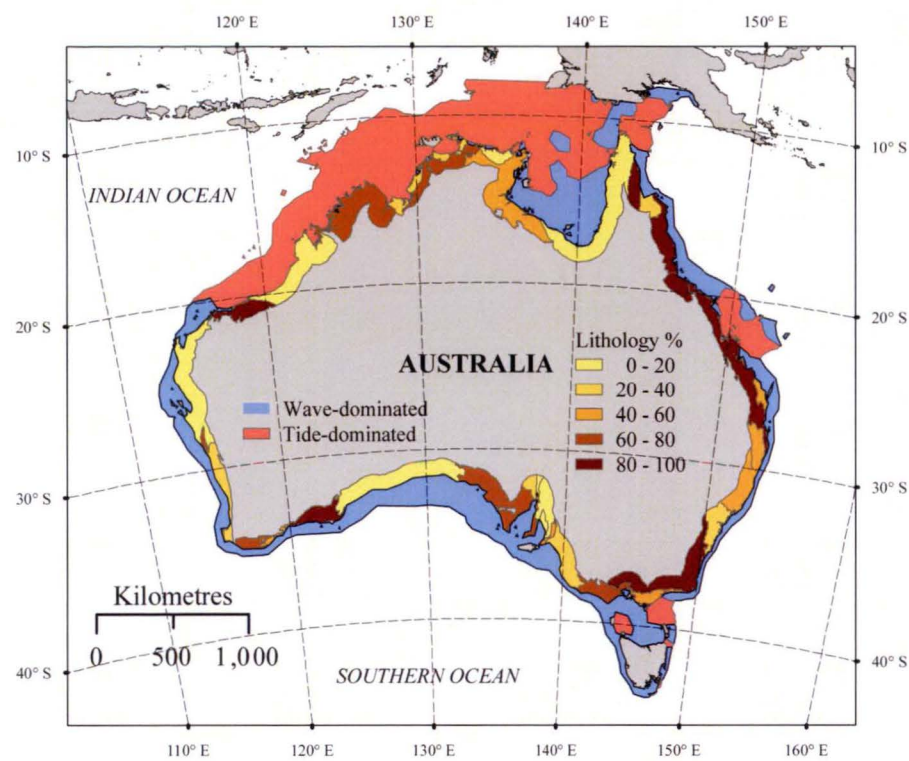


Fig. 3.12: Lithology expressed in percentiles for each Geological Region.

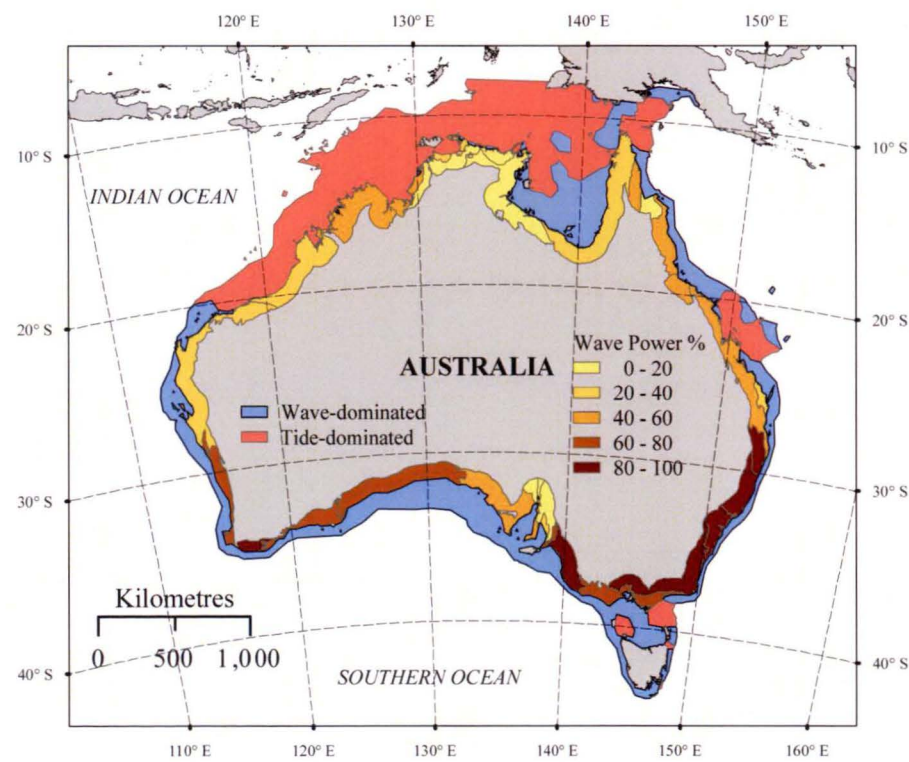


Fig. 3.13: Wave power ( $W_{erf}$ ) acting on the coastline expressed in percentiles for each Geological Region.

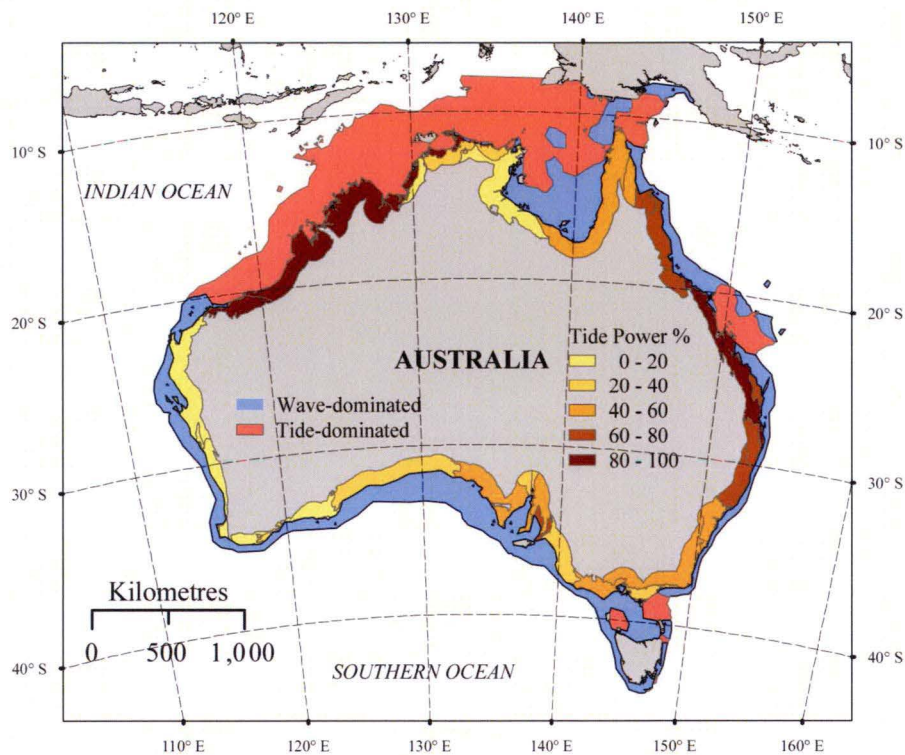


Fig. 3.14: Tide power ( $T_{er}$ ) acting on the coastline expressed in percentiles for each Geological Region.

### 3.5.3 Hierarchical cluster of $C_X$ values

The hierarchical structure of each geological region, based on the Euclidean distance, is given in Fig. 3.15, with each geological region listed on the right. It is acknowledged that a number of different classes or subclasses could be delineated depending on the Euclidean distance or ordination of interest. Here, eight main classes are identified; however, additional classes and subclasses are also highlighted and discussed.

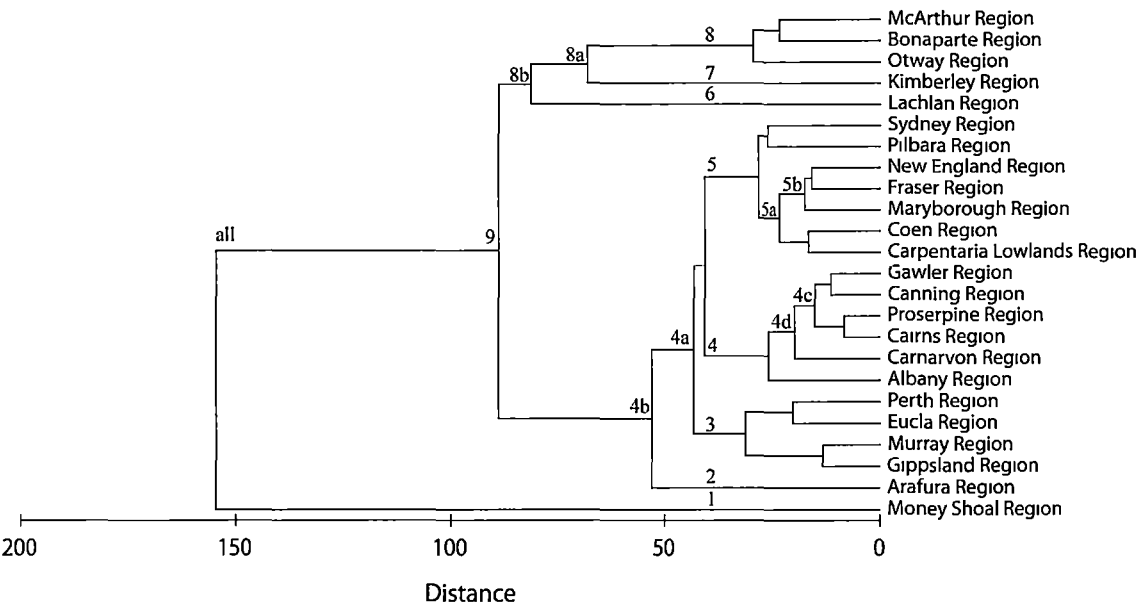


Fig. 3.15: Hierarchical structure of the cluster analysis for the geological regions based on Euclidian distance.

3.5.4 Correlation of hierarchical  $C_x$  table and physical variables

The Spearman rank correlation coefficient ( $\rho$ ) was calculated to explain the variance of the classes from Fig. 3.15. This was done by correlating the clustered  $C_x$  length scales with a similarity matrix of the predictor physical variables ( $W_{\phi}$ ,  $T_{\phi}$ ,  $R_{\phi}$ , height, age, and lithology). Results from this analysis are listed in Table 3.3 showing each class or subclass, the correlation coefficient and the dominant variables.

Table 3.3: Physical variables driving the structure of groupings

Class	Correlation ( $\rho$ )	Dominant Variables
All	0.27	$T_{\phi}$ Height, Age, Lithology
9	0.28	$T_{\phi}$ $R_x$ , Height, Age, Lithology
8	0.90	Lithology
8a	0.77	$R_x$
8b	0.55	$R_x$
5	0.20	$W_{\phi}$ $T_{\phi}$ Age
5a	0.30	Lithology
4	0.80	$W_{\phi}$ $T_{\phi}$ $R_x$ Height
4a	0.23	$W_{\phi}$ Height, Age
4b	0.30	$W_{\phi}$ Height, Age
4c	0.94	Age, Lithology
4d	0.45	$T_{\phi}$ $R_x$ Age
3	0.94	Height, Lithology

The overall results for the main classes and subclasses are discussed and summarised in more detail in the following paragraphs.

Class 1 comprises the Money Shoal Region, located in northern Australia. This is a stand-alone class (Fig. 3.15).  $C_x$  shows a high variability across the length scale range, but is typically  $\sim 60^\circ$  (Fig. 3.8b). The  $C_x$  peaks around 20 km, and then drops off slightly before increasing to larger value at longer length scales. The median age of this region is young (65 ma), and it lies adjacent to a high-energy tidal environment. A comparison of the dominant variables across all regions ( $T_{\phi}$  height, age and lithology ( $\rho = 0.27$ )) with those driving the ordination of class 9 ( $T_{\phi}$   $R_x$ , height, age and lithology ( $\rho = 0.28$ )) suggests that the ordination of class 1 (Money Shoal) is characterised by its very low  $R_x$ . This is evident in the low-lying morphology, with characteristic plains, coastal dunes and dissected plateaus (cut up by gully and stream incision) evident throughout this region.

In class 2, the Arafura Region is also a stand-alone class. The  $C_x$  peaks around 10 km, with the median value of  $44^\circ$  dropping off to  $\sim 10^\circ$  at longer length scales. The Arafura has a low mix of lithology types. It is also low-lying (median height of  $\sim 27$  m) with a similar age to Class 1 at  $\sim 65$  ma, and is adjacent to a tide-dominated shelf. Geographically this region has dissected plateaus as well as coastal and littoral plains.

Class 3 comprises the Perth, Eucla, Murray and Gippsland regions that are characterised by very low  $C_x$  values of  $\sim 10^\circ$ . These regions are all relatively low-lying and have low  $R_x$ . The Eucla region, in particular, maintains a low  $C_x$  and variability through the range of length scales, indicating that its coastline is generally very straight. Similarly, the Perth region has low  $C_x$  ( $\sim 15^\circ$ ) that remains constant throughout the range of length scales. Gippsland shows more variability around the 30 - 40 km length scale; however, the median value of  $C_x$  is still very low. The Murray region shows an increase in  $C_x$  as the length scale increases. It is worth noting that these regions are equally young at 65 ma. They have the straightest coastlines and all are situated adjacent to wave-dominated shelves. The class 3 regions have a low lithological mix, particularly the Eucla region. The dominant variables are height and lithological mix ( $\rho = 0.94$ ; Table 3.3). The Perth region has low dissected plateaus, dune fields and alluvial plains in the south, while the Eucla region is characterised by sand plains in the north and karst plains in the south. The Murray region has sand plains, dune fields, salt lakes and alluvial plains. The Gippsland region has dissected uplands and terraced coastal plains. The Murray and Gippsland regions are most similar, followed by the Perth and Eucla regions.

Class 4 includes the Gawler, Canning, Proserpine, Cairns, Carnarvon and Albany regions with an average  $C_x$  of  $\sim 27^\circ$ . The Carnarvon region shows a high variability for length scales of 30 – 70 km, and has complex features like Shark Bay and the area around Exmouth. The Proserpine and Cairns regions, which are close together, are the most similar, with both featuring mountain ranges, hills, ridges, dissected plateaus and coastal plains. These two regions lie adjacent to the Great Barrier Reef coast, which is protected by the outer reef. The reef lagoon areas are a low-moderate wave energy environment, although the Proserpine region (in the Whitsunday area), has a strong tidal environment. The Gawler and Canning regions are the next most similar, and both characterised by low hills, ridges, dissected plateaus and coastal dunes.

In class 5, encompassing the Sydney, Pilbara, New England, Fraser, Maryborough, Coen and Carpentaria Lowlands regions, values of  $C_x$  are consistently low, generally  $< 20^\circ$  across the length scale range. Coen and Carpentaria Lowlands show similar increases in complexity around the 20 km length scale, with both regions bordering the Great Barrier Reef coast. The southwestern half of the Carpentaria Lowlands is low and flat compared to the northeastern half, which is more rugged. The lagoonal areas are a low-moderate wave

energy environment. These two regions are characterised by low dissected plateaus and by alluvial sand and clay plains. The Maryborough, New England and Sydney regions are noticeably more complex at shorter length scales (up to  $\sim 30$  km), becoming less complex (and less variable) as the length scale increases. These three regions are close together on the New South Wales coast. The class 5 regions all have complex lithologies and, with the exception of the Pilbara, which is tidally dominated, all these regions are adjacent to wave-dominated shelves. Wave-dominated areas tend to have shorter characteristic length scales ( $\sim 2.5$ ); this is particularly evident in the NSW coast in the narrow shelf regions of Sydney and Maryborough. The shorter length scale of  $C_x$  could be due to terrestrial erosion given that the geological regions on the East Coast have steep adjacent morphologies and display catchment-driven processes.

Class 6 has one member, the Lachlan region, and shows a peak of  $C_x$  at around the 10 km length scale, with a high variability at lower length scales. The region is adjacent to a wave-dominated shelf, has a highly complex lithology mix, characterised by high elevation ( $\sim 535$  m) as well as dissected plateaus (tablelands), hills, ridges and plains.  $R_p$ , as suggested by the ordination of class 8b dominates it.

Class 7 consists of one geological region, the Kimberley. This region is tidally dominated, has a highly dissected coastline, with high elevation and  $R_x$  (this is further supported by examining the dominant variables of classes 8a and 8b, driven by  $R_y$ ). The Kimberley region has a highly variable  $C_x$  through most of the length scales, and is one of the oldest regions on the continent at ( $\sim 1,840$  ma).

Class 8 groups the McArthur, Bonaparte and Otway regions and is highly dominated by lithology ( $\rho = 0.99$ ). All regions share moderately complex lithology with mixed ages and moderate levels of  $R_x$ . The Bonaparte and McArthur regions have highly variable  $C_x$  in most of the middle length scales and are situated adjacent to tide dominated shelves. The Otway Region, to the south, is adjacent to a wave-dominated shelf, and displays moderate  $C_x$  with low variability throughout all length scales and is the youngest of the three regions at  $\sim 65$  ma. The Bonaparte region is  $\sim 306$  ma, while the Macarthur Regions is much older at  $\sim 1560$  ma.

### 3.6 Discussion

This research has investigated coastline form, as a function of  $C_x$ , in the context of both terrestrial and marine processes as well as considering geological inheritance. Previously, a number of hypotheses proposed to explain coastal complexity; with some relating  $C_x$  to geological inheritance, suggesting that coastlines become more complex through time (Langford-Smith and Thom, 1969; Bishop and Cowell, 1997) while others relating  $C_x$  to the influence of external processes, proposing that  $C_x$  is reduced over time (Scheidegger, 1983). Despite these opposing hypotheses, both agree that  $C_x$  is a function of structural evolution. This study found that age is certainly an important factor determining  $C_x$ ; however, it must be considered with respect to lithological type.

#### 3.6.1 Coastal complexity

Certainly there is a correlation of age with lithological diversity, when geological regions are ranked into quartiles according to age (Fig. 3.11), the lithological diversity (Fig. 3.12) similarly increases with age ( $R^2 = 0.45$ ). This implies that, over time, geological processes increase structural complexity juxtaposing diverse lithologies. Therefore, through time, geological regions evolve from a homogeneous lithological mix to one that is heterogeneous. This explains why younger geological regions, with a singular lithological typology, are less complex. The coastline, becoming more complex with age, is more susceptible to wave action that targets vulnerable margins. Third and fourth quartiles possess 3 times the lithological diversity and 2.5 times the average elevation than the first and second quartiles. This implies that more lithological types are exposed to differing erosion rates and further coastal complexity.

It has been proposed that  $C_x$  may relate to rough terrain,  $R_g$ , rather than to marine processes (Jiang and Plotnick, 1998; Zhu et al., 2004). In this study there was little discernable correlation between  $R_g$  (Fig. 3.9) and  $C_x$ . However, there was a noticeable change in  $C_x$  when ranking the  $R_g$  into high and low values. The  $C_x$  at  $> 40$  km length scales increased implying that  $R_g$  was evident at these longer length scales. In contrast, high

values of  $C_x$  along with high values of both  $W_g$  and  $T_g$  with low accompanying terrestrial  $R_g$  would indicate that the coastline might be responding to marine processes.

The results from this study suggest that geological inheritance controls the magnitude of these signals. For example, when considering two adjacent regions, such as the Kimberley (Fig. 3.8b) and Canning (Fig. 3.8a) regions, with strikingly different characteristic signatures, it becomes apparent that geological control is responsible, as similar marine processes are acting on them both. In this instance, the characteristic signatures show that, although the regions are proximate, different geological regions have unique length scale composition according to their geological makeup.

### 3.6.2 Wave and tide dominated coasts

Past research has examined the role of wave and tides as controls on the geomorphology of coastal depositional environments (Boyd et al., 1992; Dalrymple et al., 1992). Others have used this concept of wave-tide power ratio in the development of coastal depositional environments to examine regional morphologies of Australian estuaries (Harris et al., 2002). Other researchers have theorised that coastline morphology is a function of the hydraulic pressure from wave action and the structural strength of the rocks (Fairbridge, 2004). Many different erosive processes demonstrate rapid erosion through wave-quarrying and structural assault by wave action. The varying complexity of the Australian coastline was examined to determine if a correlation exists between wave and tide-dominated areas of the continental shelf.

The characteristic length scales in tide-dominated areas – particularly Kimberley (Fig. 3.8b), Arafura (Fig. 3.8a), Money Shoal (Fig. 3.8b), and the Proserpine (Fig. 3.8b) are generally more complex at longer length scales. In contrast, complex coastlines in the wave-dominated geological regions such as New England, Sydney and Lachlan geological regions (Fig. 3.8b) are complex at shorter length scales. This suggests that wave-dominated coastlines may respond to processes at a smaller length scale, although these processes may be operating at distances shorter than the minimum length scale of 2.5 km used in this study. Harris et al. (2002) demonstrated that areas of low wave and tide power are generally depositional environments. Therefore, it is likely that the longer length scales displayed in



areas such the Money Shoal region are characteristic of areas that are depositional in nature rather than erosional.

Of the world's coastlines, it is estimated that 75% consists of rocky coastlines with many morphological types where wave action is recognised as the main erosive force (Davis and FitzGerald, 2004). The actual length of the coastline of the Australian mainland 1:100,000-scale topographic map (as opposed to the Euclidean distance) is  $\sim 36,593$  km. The length of wave-dominated coastlines compared to tide-dominated coastlines is similar at 19,751 km and 16,842 km respectively. By taking a ratio ( $L_{Er}$ ) of a length of coastline between two points and the actual Euclidean distance, for wave- and tide-dominated coastlines these ratios are  $\sim 2.15$  and  $\sim 3.45$  respectively, implying that tidal coastlines are more crenulated. However, in contrast to accepted theory, this analysis shows that wave action actually straightens the coast rather than crenulating it over most length scales (Fig. 3.16).

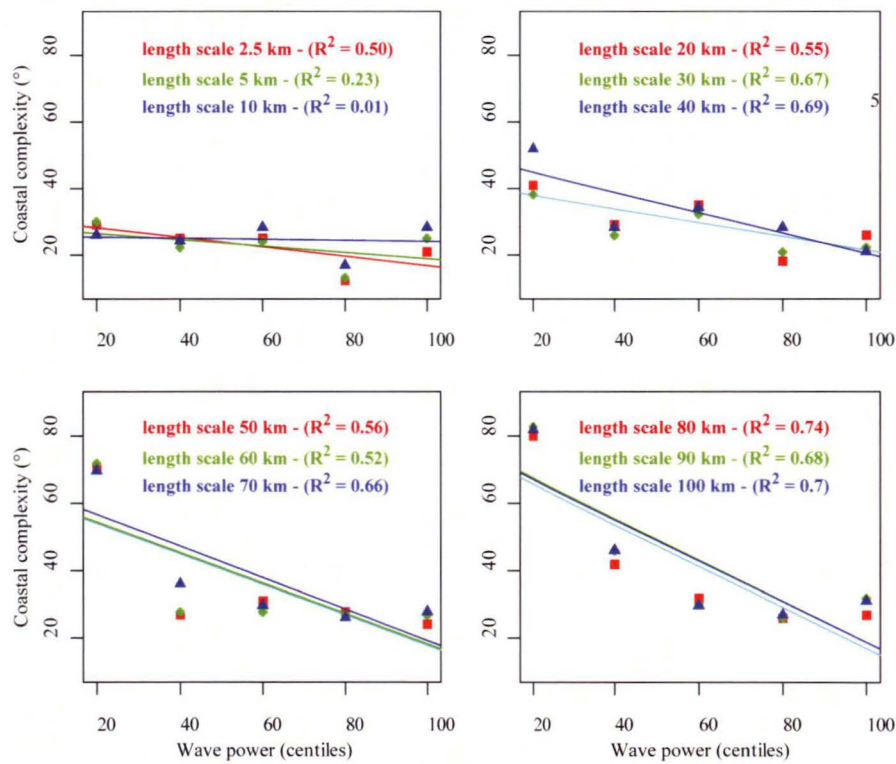


Fig. 3.16: Graph demonstrating inverse linear relationship of wave power ( $W_{ef}$ ) vs. coastal complexity ( $C_x$ ).

On an initial examination,  $C_x$  is  $\sim 50\%$  higher in tidally dominated shelves. In order to evaluate the effects of  $W_{ef}$  and  $T_{ef}$  on the coastline, the behaviour of  $C_x$  was examined for different ranges of  $W_{ef}$  (Fig. 3.16). Simply dividing the coastline into wave and tide dominated shelves (Porter-Smith et al., 2004) is not practical, as each region has varying

amounts of wave and tide influence on the coastlines. There was a proportional relationship (Fig. 3.16) showing that  $W_g$  was inversely proportion to  $C_x$ . Therefore the accepted view that wave action causes a coastline to become more complex over time is challenged by these results.

Of course, wave action is opportunistic in attacking and eroding sections of coastline but this could be the result of geological makeup. If a coastline is flat, straight with homogeneous lithology, and subjected to wave action then it is likely to remain straight. An example is the highly energetic southern coastline of the Eucla region in the Great Australian Bight, which is the straightest in the continent. However, if the adjacent terrestrial lithology is heterogeneous then waves will erode the weaker lithological sections. It is acknowledged that wave action can act on terrestrial forms like drainage networks (Bishop and Cowell, 1997). High sea levels can cause a crenulated coast with smaller embayments as the sea penetrates into the drainage network (Bishop and Cowell, 1997). Wave action will exploit weaknesses in the coastline, but these are ultimately geologically controlled. The  $C_x$  of the Australian coastline differs in wave and tide-dominated areas.

By ranking the geological regions according to tidal energy (Fig. 3.14), there is no noticeable increase of  $C_x$  throughout the length scale range. There is some evidence to suggest that tide energy affects  $C_x$  in the 2.5 – 40 km range ( $R^2 = \sim 0.3$ ). However, this could be because a higher tidal range associated with high tidal energy is delivering wave action to terrestrial features that promote further wave-quarrying erosion, the more area of shoreline exposed to attack due to higher intertidal zone. A direct relationship of tidal energy to  $C_x$  is harder to attribute, without taking explicit account of tidal current direction. The directions of tidal currents will differ spatially, whereas wave direction is generally more predictable (onshore). However, there is a detectable latitudinal trend in  $C_x$  at longer length scales particularly at the 20 – 40 km length scale ( $R^2 = 0.27$ ). This latitudinal trend may be due either to the weakening of wave power as the increase in latitude towards the equator (Young and Holland, 1996.), or because north Australia is older and therefore displays a more complex lithological signature, or it is a combination of both.

### 3.6.3 Lithological control

The four important variables responsible for  $C_x$  are lithological mixture (Fig. 3.12), age (Fig. 3.4), elevation (Fig. 3.10) and  $R_g$  (Fig. 3.9). Lithological composition appears to be a major control of complexity. Coastlines of a homogeneous lithology tend to be straight compared to coastlines of mixed lithology. Conversely, geological regions that have a complex coastline generally have heterogeneous lithology, consistent with the softer lithological material being eroded over time, as suggested by Davidson et al., (2002). Therefore,  $C_x$  is controlled by geological inheritance (Langford-Smith and Thom, 1969; Bishop and Cowell, 1997), but mediated by contemporary environmental processes. Therefore, at the length scales examined, the results of this study suggest that wave action promotes a straight coastline if the lithology is homogeneous and a complex one if the lithology is heterogeneous. Specific lithological types do not seem as important as the variation or mix of lithological types. Over time, the coastline will conform to the inherent geology.

## 3.7 Conclusion

The research in this study is particularly novel as it categorises a range of relevant variables at different scales. By applying various geocomputational techniques to quantify coastal complexity this work provides a valuable method which is repeatable at multiple length scales. This application of spatial analysis provides a methodical and quantitative estimation of the modal composition and length scales of some of the processes involved in the coastline's morphological evolution. The degree of  $C_x$  and amount of variation quantifies these processes. The  $C_x$  values for each geological region were examined and evaluated over a range of length scales. Each geological region is different in that each has a distinctive pattern of complexity that allows grouping of regions based on similar graphs. The modes vary in their correlations and relationship to geological inheritance,  $W_g$  and  $T_g$ . Derivation of the length scales associated with each geological region along with metrics of physical variables allowed regional comparison and classification.

This study has demonstrated that lithological composition is a major control of  $C_x$ . Furthermore, either  $C_x$  may increase or decrease with age, dependent on whether the lithology is homogeneous or heterogeneous in composition, respectively, which is effectively, measures of structural complexity. The Canning and Kimberley geological regions in the northwest lend a clue as to what extent geological inheritance plays a role. While they are spatially proximate, these coastlines have responded in terms of their complexity to their inherent geology in very different ways. Coastlines of a singular lithology type tend to be straighter than coastlines of mixed lithological typology. In heterogeneous regions, processes erode the softer material away leaving a crenulated edge over time. This evolution to comparable complexity across scales is in contrast to the usual hypothesis of coastlines becoming straighter over time. This indicates that lithological makeup is an important determining factor, and further demonstrates that geological inheritance provides the major influence in determining the control over variability represented by the characteristic length scales.

Ultimately, tectonics is the basic driver of  $C_x$ . Over time, terrestrial and oceanographic processes are opportunistic in exploiting the geological character determined by tectonics to modify the coastline. Age and/or geology are probably the best gauge and an important dimension in the likelihood of a coastline becoming increasingly complex, although this neglects specific processes that might cause the complexity. In tide-dominated areas, the characteristic length scales tend to be longer, while in wave-dominated shelves the characteristic length scales are shorter. However, a simple separation into wave- and tide-dominated areas does not take into account the spatial variations in  $W_g$  and  $T_g$ .

## **CHAPTER 4      CANYON CLASSIFICATION**

### **4.1 Abstract**

This chapter presents an approach to the classification of submarine canyons on the Australian continental slope and provides an opportunity to undertake a characterisation and inventory of these potentially important resources. By establishing a shelf break and foot of slope based on gradient, submarine catchments are defined based on a drainage network derived from across the continental shelf and slope. On completion of this classification, metrics are derived for both the drainage network representing submarine canyons and the catchment morphology.

The derived submarine catchments are further classified according to depth strata. In keeping with existing research, it was decided to adopt the bathomic classification adapted from classical definitions of neritic and bathyal zonation. This bathomic structure is attractive because a submarine canyon cuts across many depth bands and faunal distributions are more fundamentally correlated with depth strata than a singular geomorphic feature. These depth strata are described within a hierarchical classification scheme to address issues of consistency in the classification of geomorphic features such as submarine canyons. This hierarchical scheme allows further subdivisions, which accommodates lower-level characterisation. This approach will enable regional comparison and provide a framework for categorisation and further investigation into canyon processes and form.

### **4.2 Introduction**

#### **4.2.1 Background**

The Earth's crust is evolving over time, erosion and the subsequent channels that carry away the detritus are evident as rivers and streams, both past and present. Similarly,

submarine canyons have developed and evolved by erosive processes over time. Some, particularly those incised on the continental shelf, owe their genesis to terrestrial rivers and channels which flowed over the shelf at periods of low sea level, while others are caused by gravity-induced processes on the continental slope. Using modern elevation-bathymetric models, it is possible to infer and investigate the locations and routes of these drainage channels, revealing the links between modern terrestrial drainage systems and submarine channels. One of the advantages of knowing the routes and pattern of the submarine drainage systems is that it offers an insight into how processes may have evolved over time, for instance, the location of ancient water bodies that may have existed at a sea level lowstand. Without this methodology, it could be difficult to visualise any linkage between land and ocean river channels past and present (Meybeck et al., 2006).

The rationale for this research is to demonstrate the application of algorithms developed for drainage analysis. These algorithms have traditionally been applied in terrestrial environments for the automatic extraction of drainage networks and catchments from digital elevation models (O'Callaghan and Mark, 1984). This work is made possible by recent advances in deep-sea multibeam technology, so that the seafloor morphology can be mapped in higher definition of  $\sim 25$  m (Kloser et al., 2001; Hill et al., 2005; Green et al., 2007). With the recent advances in data quality, these algorithms can be applied to a integrated and combined model of both elevation and bathymetric datasets (Pratson et al., 1994; Pratson and Ryan, 1996) to provide better insight into geomorphological features, including the relationships between subaqueous sedimentary canyons, channels and drainage system morphology (Kloser et al., 2007). Drainage analysis provides a rapid automatic procedure to derive networks on the continental shelf and slope. This analytical procedure can locate drainage channels that are obscured to the naked eye in the gridded data (Pratson and Ryan, 1996). This methodology will undoubtedly overestimate numbers of channels as the algorithm will allocate channel networks in minor depressions. However the extracted network over the combined terrestrial elevation and bathymetry will possess a uniform overestimation, thereby still allowing a regional comparison (Pratson and Ryan, 1996).

By extracting a drainage network and the underlying catchments this methodology can be used to investigate the influence of geomorphological structures. For instance, a drainage network which is space-filling is deemed to be free of geological constraints (Cheng et al.,

2001). Conversely, the lengthening of canyon network and associated compression of width demonstrates control by geological inheritance. Past researchers have used these ratios to infer relationships between the channel composition and process. These include tectonics (Ollier, 1981; Cox, 1989; Burbank, 1992), geological structure (Abrahams and Flint, 1983) and erosion processes (Dunne, 1980). The process of calculating drainage area is critical to the correct delineation of underlying catchment structure.

Submarine canyons are situated on continental slopes the world over and are well-documented. They act as natural conduits, transporting sediment from the shelf edge through channels into the thalwegs of main canyons which pass the sediment to the abyssal environment ~ 2000 - 5000 m below sea level (Hill et al., 2005). Conversely, they deliver nutrient-rich waters up onto the shelf, therefore giving them significant biological importance (Pratson and Ryan, 1996; Gardner et al., 2003; Steffens et al., 2003; Huyghe et al., 2004; Mitchell et al., 2007b). Physically, they modify the continental slope and shelf and their genesis is still the subject of significant scientific debate (Andrews et al., 1970; Twichell and Roberts, 1982; Hagen et al., 1996; Lewis and Barnes, 1999; Kenyon et al., 2002; Mitchell et al., 2007a).

Submarine canyon walls can be as high as or higher than the Grand Canyon (~ 5 km) (Fairbridge, 1966). Resembling terrestrial canyons, the canyons generally have a V- or U-shaped morphology, with associated slope steepness of 35° and 10° respectively (Fairbridge, 1966). It is thought that U-shaped canyons evolve from V-shaped ones when shelf-derived sediment flows reduce and the canyon stabilises (Mitchell et al., 2007b). The canyon systems often develop dendritic canyon heads, similar to terrestrial systems (Mitchell et al., 2007b). Submarine canyons can also be grouped together to form amphitheatres, e.g. off Perth and Bass Strait, Australia. It is tempting to consider a common hypothesis for the formation and genesis of submarine canyons, but given their differing morphologies and spatial variability, it is important to consider these varying types separately, rather than to attempt to apply a single explanation (Fairbridge, 1966). Their genesis is likely to include multiple marine processes including tectonics and in some cases, fluvial incision (Shepard and Dill, 1966).

Early mappings of submarine canyons have been likened to terrestrial systems (Veatch and Smith, 1939). Many submarine canyon heads are relatively nearshore; reinforcing the hypothesis that there is a linkage between marine and terrestrial systems, and that

submarine canyons are part of drowned river valleys when sea level was lower. Many researchers have suggested a relationship between submarine canyons and modern valleys (Hopkins, 1966) and believe that canyons that breach the shelf edge could be associated with past and present rivers. The rationale is that during lowstand, the process of fluvial incision would initiate canyoning of the shelf and upper slope, or similarly canyons that intrude onto the shelf are typically associated with rivers during such lowstands (Ewing et al., 1963; Twichell et al., 1977; Twichell and Roberts, 1982; Goff, 2001). However, the character of submarine valleys is generally different from a river valley (Fairbridge, 1966), so a direct link may be unjustifiable. Many years of seafloor mapping have certainly revealed dendritic drainage networks on shelves and slopes (Puig et al., 2003; García et al., 2006) that are similar to terrestrial systems (Straub et al., 2007). These marine drainage networks, like terrestrial drainage networks, have regional variability (Hess and Normark, 1976; Schlee and Robb, 1991; Pratson and Ryan, 1996). The resultant morphology is strangely similar to drainage patterns of terrestrial slopes (Fairbridge, 1966) and subsequently, these networks have been termed submarine drainage systems (Hesse, 1989; Pratson and Ryan, 1996). During periods of lower sea-level, fluvial erosion by rivers flowing across the continental shelf may have initiated the genesis of some of these submarine drainage systems, therefore, depth of shelf break and width of continental shelf may be important variables in determining this origin.

Even though there are parallels with terrestrial drainage systems, submarine channels are formed differently (Fig. 4.1). In terrestrial systems, water discharge drives the flow through the network. Erosion produced by this water discharge is further controlled by drainage area (Howard, 1980) and is an important driver of channel development (Hack, 1957). Conversely, the erosive process in submarine systems is due to sediment flows, which are controlled by slope and substrate failure (Whitlow, 1984; Pratson and Ryan, 1996; Straub et al., 2007). Direct observation of these erosive sediment flows is difficult due to the great depths and their temporal infrequency (Xu et al., 2004). Many studies have confirmed that sediment gravity flows (or turbidity currents) move large quantities of material, promoting the formation and evolution of submarine canyons (Heezen and Ewing, 1952; Fairbridge, 1966; Conolly and Von der Borch, 1967; Keller and Shepard, 1978; Inman, 1994; Pratson et al., 1994; Kudrass et al., 1998; Michels et al., 1998; Khripounoff et al., 2003). For marine systems, it is also hypothesised that sediment delivery is a factor (O'Grady et al., 2000). This highlights the importance of submarine catchment definition, as this would exert



some control on how much sediment is flowing through the canyons. As likely or not, canyon evolution is due to multiple processes including erosion and deposition (Goff, 2001). Generally accepted examples include sediment accumulation and over-steepening, tidal or storm waves, and sea-level fluctuation. The sediment gravity flows are dependent on the prevailing forcing in a given system (Zühlsdorff et al., 2008). The periodic nature of gravity flows has implications for biological systems.

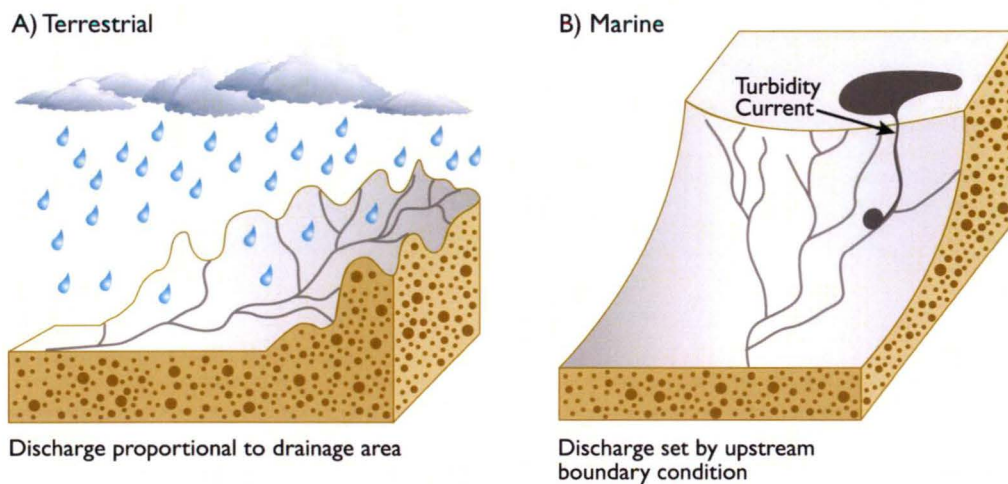


Fig. 4.1: Discharge in terrestrial systems based upon precipitation and catchment area. Marine systems are dependant upon slope gradient sediment reservoir on adjacent continental shelf edge.

Some studies of submarine canyons suggest that canyons are slope-confined, with the head of the canyon typically well below any lowstand limit that may implicate terrestrial river system linkage (Twichell and Roberts, 1982). Shelf-incised canyons and their catchments are geomorphic features that are physically adjacent to the shelf break. Canyons confined to the slope, but not incised onto the shelf are termed “headless canyons” (Twichell and Roberts, 1982) inferring that processes causing canyon formation are independent of terrestrial drainage influences and sediment from the continental shelf (Twichell and Roberts, 1982). This reinforces the idea that slope-confined canyons have an erosional genesis driven by sediment flow and supply (Green et al., 2007). Another hypothesis of canyon genesis is that the immature canyon phase begins with pre-canyon downslope rills developing from local failures on steep upper slopes. Sediment flows cause the canyon to evolve, their erosive power exploiting weaknesses on the middle to lower slopes, leading to further upslope headward-erosion (Pratson et al., 1994; Pratson and Coakley, 1996).

Similarly, there are external influences such as climate and onshore morphology which can contribute towards canyon formation (Hill et al., 2005). This may be related to sediment transport processes on wave- and tide-dominated shelves around the continental shelf (Porter-Smith et al., 2004). The sediment flow and supply is dependent on the morphology of the shelf and its capacity to hold sediment. Pre-canyon downslope rills can be identified by their elongated catchment areas and indicate young canyon systems. Mappings of catchments shape as well as combining variables such gradient and shelf width and shelf dominance will provide context and aid the prediction of canyon evolution.

#### **4.2.2 Canyon systems**

Submarine canyon systems are abundant around the Australian continental slope, as demonstrated in the 'Geomorphic map of Australia's EEZ' (Heap and Harris, 2008). Various researchers have studied canyon systems, particularly on Australia's southern margin (Fig. 4.2), including the Albany Canyons (Exon et al., 2005), Bass Canyon (Mitchell et al., 2007b) and the Murray Canyons - one of the steepest and most rugged sections of the Australian continental margin (Sprigg, 1947; Hill et al., 2005). The Bass Canyon system is amongst the largest temperate canyon systems in the world, consisting of several shelf-incised and slope-confined tributary canyons that converge into the massive Bass Canyon 3000 m below sea level (Mitchell et al., 2007b). Many canyons that incise the shelf are thought to have fluvial connections. Anemone Canyon was a strong contender for such a fluvial nature, however, this was disproved by further investigation (Holdgate et al., 2003; Mitchell et al., 2007a; Mitchell et al., 2007b) and the canyon structure was subsequently linked to a depression that diverted lowstand river systems towards the canyon head (Mitchell et al., 2007b).

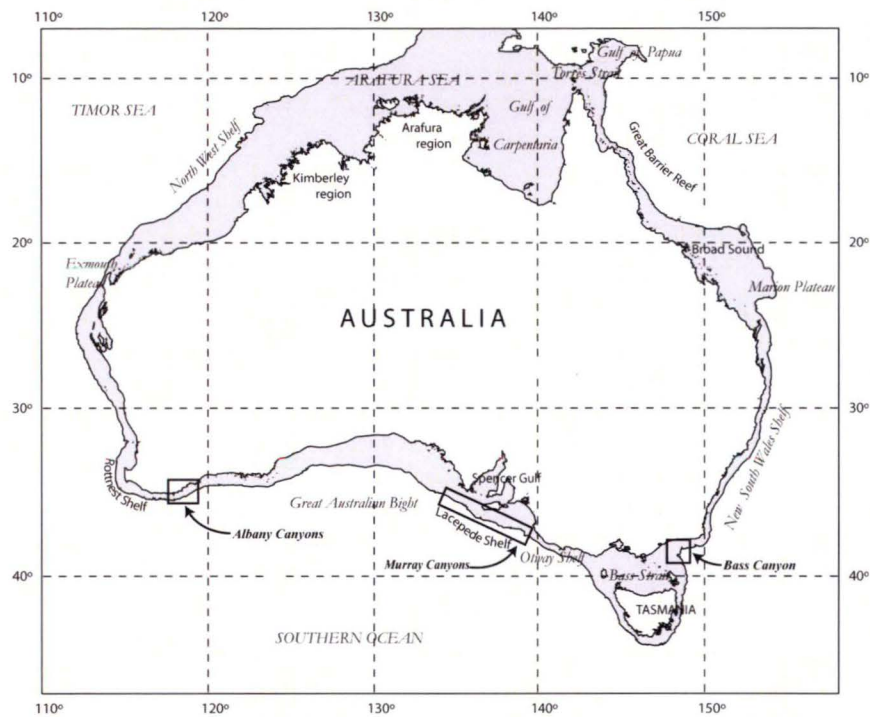


Fig. 4.2: Location diagram showing the extent of the continental shelf (coloured grey).

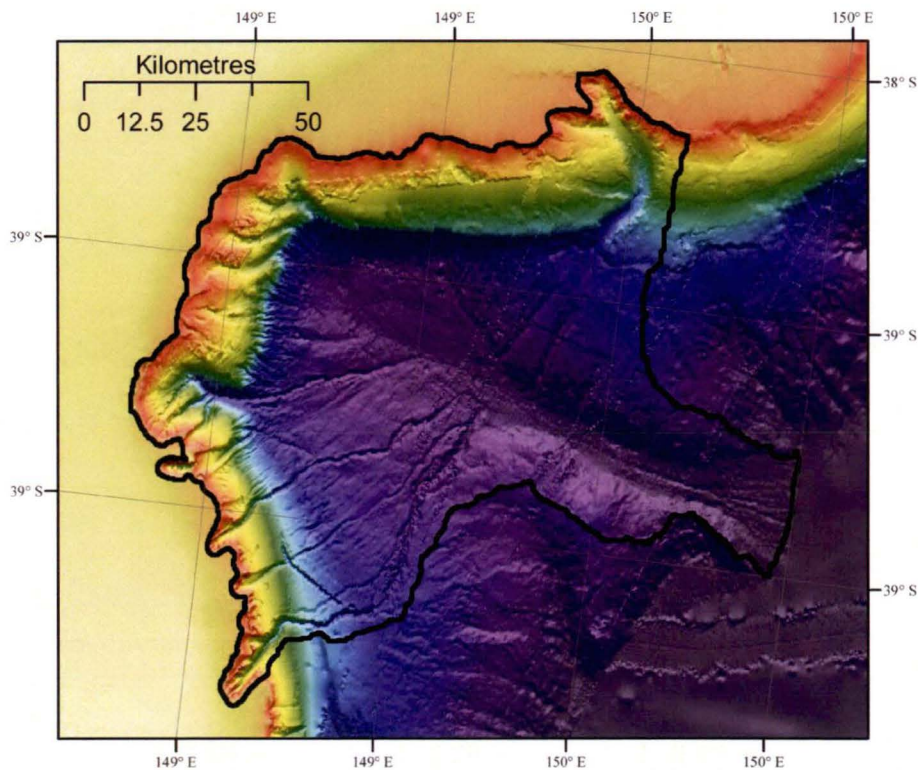


Fig. 4.3: The Bass Canyon amphitheatre is the largest canyon amphitheatre in Australia and consists of several shelf-incised and slope confined canyons that converge into the main tributary of Bass Canyon. The ridgeline defining the Bass Canyon catchment is outlined in black.

### 4.2.3 Past classification of canyons

In trying to answer questions about canyon genesis, evolution and underlying geology, some researchers have concentrated on treating canyons as systems or ensembles (Goff, 2001; Green et al., 2007) rather than discrete morphological features, classifying the canyon systems by cross-slope profiles and the downslope progression of statistical parameters. Analysis of American canyon systems have revealed three basic types of canyons (linear, exponential and Gaussian) based on their slope profiles (Adams and Schlager, 2000). Adams and Schlager (2000) hypothesised that the differences were due to the interplay of marine and sediment processes (e.g. wave-dominated transport and gravity-driven transport at the shelf break), noting that mud slopes tend to have a lower slope angle. These parameters included slope gradient and root mean square (RMS) relief, the latter being a measure of departure from the mean depth of the profile. On linear slopes the RMS relief decreases with depth; on exponential slopes the RMS relief increases; and on Gaussian slopes the RMS relief remains constant (Goff, 2001). Other ensemble approaches have found a strong relationship between canyon incision and continental slope morphology (O'Grady et al., 2000), and by classifying canyons this way, a methodology was provided to quantify depositional and erosional processes in canyons (Adams et al., 1998; Adams and Schlager, 2000; O'Grady et al., 2000; Goff, 2001). However, rather than treating submarine canyons as singular features or examining the profiles of groups of submarine canyon, a catchment-based approach will group the submarine canyons into discrete networks.

### 4.2.4 Catchment-based approach

It has been recognised that submarine canyons are similar to terrestrial systems in that the connection between gradient and area influences the frequency and magnitude of erosive sedimentary flows (Mitchell, 2005). Rather than individual, profile types or cross-profile ensemble, this study adopts a catchment-based approach that is an extension of work proposed by Pratson and Ryan (1996). Frequently used in terrestrial research, this type of automated approach has merit in defining submarine drainage by identifying possible submarine pathways, as well as delineating the areas that contribute towards them in the form of catchments. Additionally, this technique can be used to investigate terrestrial-

marine connectivity. This work not only derives a holistic drainage network but also identifies each contributing catchment area on the slope. An advantage of this is that it could be used to isolate areas of the shelf break that may be contributing sediment down through the slope. This approach will facilitate the identification and natural groupings of these canyon systems.

#### **4.2.5 Depth structure**

Although catchment delineation perpendicular to the shelf break is important, another consideration is depth. Depth delineation is useful because of biological implications and because of its relevance to hierarchical structure in classifying marine biodiversity in marine resource planning. The continental shelf and slope (or neritic and bathyal zones) occupy 7.6% and 8.5% of the ocean floor respectively (Whitlow, 1984). The 200 m isobath is generally taken as the arbitrary boundary between the neritic (coastal) and bathyal (oceanic) zones (Marshall, 1979) and is an approximation of where the continental shelf break is located. Additionally, the continental shelf break generally demarks the boundary between shelf and deep water masses (Longhurst, 1998) although this is a fuzzy boundary. As temperature, light and pressure vary enormously on the continental slope (Gage and Tyler, 1991), it is necessary to subdivide the submarine canyons on the slope into meaningful depth strata. The ecological significance is unique, with each of the depth strata displaying discrete biological assemblages (Williams et al., 2008). The calculated slope can be further classified by describing canyons according to depth strata. This addresses issues of classification of geomorphic features that include submarine canyons in a regional marine planning process.

## 4.3 Methods

### 4.3.1 Drainage analysis

The GIS used to manipulate and extract the data was Arc/Info (ESRI, 1996). This software allows the assimilation of large complex datasets to be efficiently handled and has many vector and raster functions embedded in its software. In particular, Arc/Info GRID is well suited to the manipulation and analysis of grids of rows and columns representing the various data levels. Using GIS and spatial analysis techniques made it possible to extract and analyse the drainage catchments and associated drainage network. The scripts for processing the large datasets were written in Arc Macro Language (AML), giving a consistent methodology and procedure when trying to optimise the processing.

The improved vertical and horizontal accuracy of this dataset relied on up-to-date swath bathymetry collected by CSIRO Marine National Facility combined with the latest bathymetric model from Geoscience Australia (Geoscience Australia, 2008) which was based on available multibeam swath data at 250 m resolution. This model includes the most up to date data available for the Australian continental margin. There are some issues with bathymetric datasets. Merging high-resolution multibeam swath with national coverage has problems, as the chosen resolution of the national bathymetry dataset is 250 m, while multibeam swath can be accurate up to 10 m. There are a number of options available to combine bathymetric datasets, these include merging and mosaicing (ESRI, 1996). Merging allows the first dataset to be given preference over a succeeding one, whereas mosaicing interpolates between the two. These issues can have implications as although merging is preferable as far as maintaining the integrity of the more accurate swath, the result can mean that there are some artefacts (such as stepping) in the final product. Of the two, merging seemed to be the best method of combining these datasets, introducing least errors. The implications of spatial variability are that uncertainties in the input data generally affect the outcome geomorphic features.

Many methods are available to calculate drainage from elevation-bathymetric models and delineate drainage networks and catchments (Mark, 1983; Band, 1986; Jenson and Domingue, 1988; Martz and Garbrecht, 1998). For elevation-bathymetric models to



become hydrologically valid they require ‘filling’ to remove any sink errors (Martz and Garbrecht, 1998). These sinks are data errors rather than natural depression features. The filling procedure ensures a down-slope path is available in the elevation-bathymetric grid to the lowest outlet (Martz and Garbrecht, 1998) to avoid calculated flow directions opposing each other either side of a depression (therefore failing to comply with the natural flow of fluids). Artefact depressions often represent real morphological features. However, with this methodology it is impossible to distinguish between a lake or flat area even though drainage is apparent (Turcotte et al., 2001). In many cases, such flat areas can be the result of lack of accurate data and interpolation errors (Mark, 1983; Jenson and Domingue, 1988; Mark, 1988; Martz and Garbrecht, 1992; Tribe, 1992; Zhang and Montgomery, 1994; Martz and Garbrecht, 1998).

On completion of the filling procedure, the drainage pattern information was extracted (Jenson and Domingue, 1988; Tarboton et al., 1991) from the elevation-bathymetric model (Hutchinson and Dowling, 1991; Petkovic and Buchanan, 2002). The stream location was derived, as well as a stream order according to the Strahler system (Strahler, 1952). Strahler’s classification ordering system defines streams with no tributaries as first-order streams. Two of these streams form a second-order stream. The order is increased (or incremented) to the next order when two streams of the same order meet (Strahler, 1952). The streams were outputted as vector coverage with the tributaries labelled according to the aforementioned system (ranging from 1 - 7). This labelling could be useful in ranking canyons. For example, a major canyon may have a label of seven, which would give an indication of the number and size of contributing tributaries. The submarine canyon networks on the slope were assigned stream orders according to this criterion from the edge of the shelf break to the foot of slope.

### **4.3.2 Continental shelf break and foot of slope**

An important part of deriving slope catchments was to clearly define the location of the continental shelf break boundary and the foot of the continental slope based on gradient, as the establishment accuracy of delineating catchments along the slope. Identifying catchments and the delineation process depends upon the location of features where the

gradient exceeds  $1^\circ$  (Fairbridge, 1966; Whitlow, 1984). The justification is that the breaks that delineate the shelf from the slope and similarly the foot of slope from the continental rise are defined by a change in gradient  $> 1^\circ$ . A slope grid was generated from the bathymetry using the algorithm:

$$Slope = \arctan \sqrt{\left(\frac{dz}{dx}\right)^2 + \left(\frac{dz}{dy}\right)^2} \quad \text{units are degrees}^\circ \quad (1)$$

To highlight this demarcation in gradient, the bathymetric model was first smoothed using a low-pass filter to eliminate potential gradient noise, and a gradient grid was produced by identifying the maximum change in height from each cell to its neighbours (Burrough, 1986); each grid cell potentially had a value of  $0 - 90^\circ$ . A gradient of  $> 1^\circ$  was defined to demark the upper and lower boundaries of the continental slope. To highlight this boundary, the slope grid was squared and then contoured, to target the shelf break and foot of slope at  $1^\circ$ . Derived contours above and below  $1^\circ$  from this squared grid were removed, thereby isolating the continental slope from the shelf and continental rise. The shelf break was derived and used as an input to enable the accurate extraction of catchments on the continental slope.

### 4.3.3 Catchment zonation

The topographic boundaries separating the individual catchments consisted of ridge lines that could potentially delineate fluid flow (Straub et al., 2007). To calculate the area drained by each grid cell into natural groupings of grid cells and delineate network drainage areas, work was done to isolate bathymetric ridges that separate these catchments into discrete areas on the shelf and slope. Catchments were generated from the elevation-bathymetric model to identify catchment features based on the morphology of the continent, enabling comparisons between catchments and provide some context for processes (Meybeck et al., 2006). The catchments generated on the continental slope grouped into submarine canyon networks demonstrating where shelf sediments may converge onto specific catchment areas. These catchment areas are defined as the total area that drains to a common outlet;



each area being bounded by a ridge or divide. The outlet of these areas is the lowest point along the boundary of the contributing area.

#### 4.3.4 Geomorphic measures of drainage network

Three classical measures of terrestrial drainage measures are used to characterise the submarine drainage networks: the bifurcation ratio ( $R_b$ ), the length ratio ( $R_l$ ) and the slope ratio ( $R_s$ ) (Horton, 1945). The Horton's ratios are indicators of geomorphological characteristics of a catchment. They can be used to characterise a drainage network, have been widely recognised as fundamental descriptors of drainage network composition and are often used to compare characteristic drainage (Strahler, 1952; Schumm, 1956; Chorley, 1957; Morisawa, 1962; Press and Siever, 1986; Ritter, 1986; Summerfield, 1991a). The bifurcation ratio is derived from the number of different stream orders when they converge from one order to the next in a drainage catchment (i.e. number of streams of one order divided by the number of streams of the next highest order, Equation 2). An average of these ratios is taken to represent the whole drainage network. (Horton, 1945; Whitlow, 1984).

Within each slope catchment boundary, the bifurcation, length and slope ratios were derived.

The bifurcation ratio  $R_b$  is defined by,

$$R_b = N_i / N_{i+1}, \quad (2)$$

where  $N_i$  is the number of channels in network of order  $i$ .

The length ratio  $R_l$  is defined by,

$$R_l = L_i / L_{i+1}, \quad (3)$$

where  $L_i$  is the length of channels in network of order  $i$ .

The slope ratio  $R_s$  is defined by,

$$R_s = S_i / S_{i+1}, \quad (4)$$

where  $S_i$  is the mean slope of channels in network of order  $i$ .

In addition, the drainage density ( $D_d$ ) was calculated as the averaged length of channels per drainage area,

$$D_d = \sum L / A, \quad (5)$$

where  $L$  is the total length in a channel network, and  $A$  is the area drained by the channel network (Ritter, 1986; Silverman, 1986).

Attributes for each submarine catchment were tabulated (Table 4.1), these attributes included basic information about catchment morphology, such as area, perimeter and length as well as aforementioned  $D_d$ .  $Lr1 - Lr6$ ,  $Rb1 - Rb6$  and  $Sr1 - Sr6$  represented values that enabled the calculations of length ratio ( $R_l$ ), bifurcation ratio ( $R_b$ ) and slope ratio ( $R_s$ ) respectively for each catchment. Additionally, geometric information about the catchment shape was collated. Information about a catchment was derived by plotting the values of  $R_b$ ,  $R_s$  and  $R_l$  of the channels respectively versus channel order. The Horton ratio plots of terrestrial drainage networks are generally linear over the range of stream orders (Horton, 1945; Pratson and Ryan, 1996; Turcotte, 2007).

Table 4.1: Attributes defined for each submarine catchment

Num	Attributes	Definitions	Methods
1	Area	Area of drainage catchment (m <sup>2</sup> )	ArcInfo ARC
2	Perimeter	Perimeter of drainage catchment (m)	ArcInfo ARC
3	Len_km	Total length in a channel network (m)	ArcInfo TABLES
4	<i>Dd</i>	Drainage density	ArcInfo GRID
5	<i>L1</i>	Length of stream order 1	ArcInfo GRID
6	<i>L2</i>	Length of stream order 2	ArcInfo GRID
7	<i>L3</i>	Length of stream order 3	ArcInfo GRID
8	<i>L4</i>	Length of stream order 4	ArcInfo GRID
9	<i>L5</i>	Length of stream order 5	ArcInfo GRID
10	<i>L6</i>	Length of stream order 6	ArcInfo GRID
11	<i>Lr1</i>	Length ratio of L2 over L1	ArcInfo TABLES
12	<i>Lr2</i>	Length ratio of L3 over L2	ArcInfo TABLES
13	<i>Lr3</i>	Length ratio of L4 over L3	ArcInfo TABLES
14	<i>Lr4</i>	Length ratio of L5 over L4	ArcInfo TABLES
15	<i>Lr5</i>	Length ratio of L6 over L5	ArcInfo TABLES
16	<i>N1</i>	Number of stream order 1	ArcInfo GRID
17	<i>N2</i>	Number of stream order 2	ArcInfo GRID
18	<i>N3</i>	Number of stream order 3	ArcInfo GRID
29	<i>N4</i>	Number of stream order 4	ArcInfo GRID
20	<i>N5</i>	Number of stream order 5	ArcInfo GRID
21	<i>N6</i>	Number of stream order 6	ArcInfo GRID
22	<i>Rb1</i>	Bifurcation ratio N2 over N1	ArcInfo TABLES
23	<i>Rb2</i>	Bifurcation ratio N3 over N2	ArcInfo TABLES
24	<i>Rb3</i>	Bifurcation ratio N4 over N3	ArcInfo TABLES
25	<i>Rb4</i>	Bifurcation ratio N5 over N4	ArcInfo TABLES
26	<i>Rb5</i>	Bifurcation ratio N6 over N5	ArcInfo TABLES
27	<i>S1</i>	Mean slope of stream order 1	ArcInfo GRID
28	<i>S2</i>	Mean slope of stream order 2	ArcInfo GRID
39	<i>S3</i>	Mean slope of stream order 3	ArcInfo GRID
30	<i>S4</i>	Mean slope of stream order 4	ArcInfo GRID
31	<i>S5</i>	Mean slope of stream order 5	ArcInfo GRID
32	<i>S6</i>	Mean slope of stream order 6	ArcInfo GRID
33	<i>Sr1</i>	Slope ratio of S2 over S1	ArcInfo TABLES
34	<i>Sr2</i>	Slope ratio of S3 over S2	ArcInfo TABLES
35	<i>Sr3</i>	Slope ratio of S4 over S3	ArcInfo TABLES
36	<i>Sr4</i>	Slope ratio of S5 over S4	ArcInfo TABLES
37	<i>Sr5</i>	Slope ratio of S6 over S5	ArcInfo TABLES
38	Min	Minimum slope (°)	ArcInfo GRID
39	Max	Maximum slope (°)	ArcInfo GRID
40	Range	Range of slope (°)	ArcInfo GRID
41	Std	Standard deviation of slope (°)	ArcInfo GRID
42	Mean	Mean slope (°)	ArcInfo GRID
43	Median	Median slope (°)	ArcInfo GRID
44	Major-axis	Majoraxis of catchment (km)	ArcInfo GRID
45	Minor-axis	Minoraxis of catchment (km)	ArcInfo GRID
46	<i>M<sub>Mr</sub></i>	ratio of Major-axis and Minor-axis	ArcInfo GRID

## 4.4 Results

### 4.4.1 Continental shelf and slope boundaries

The Australian continental shelf and slope is highly variable in character, both varying in width, depth, gradient and profile. For instance, the shelf width can vary between 10 and 500 km (Fig. 4.4). The slope analysis provides locations at the shelf break and foot of slope, the former is quite different from the conventional 200 m isobath. For this slope-defined shelf break, the median depth can vary between  $\sim 20 - 1000$  m. Nonetheless, there is reasonable agreement in many areas between the gradient contour and the 200 m isobath. An important part of the analysis, this departure from the traditional measure of 200 m may indicate processes and underlying structures that are different from the norm. For instance, there are marked differences between the continental slope and shelf break in the northwest and southeast. The northwest continental shelf break is difficult to define. In contrast, the southeast continental slope is steep, with signs of slumping exposing further areas of slope that are precipitous.

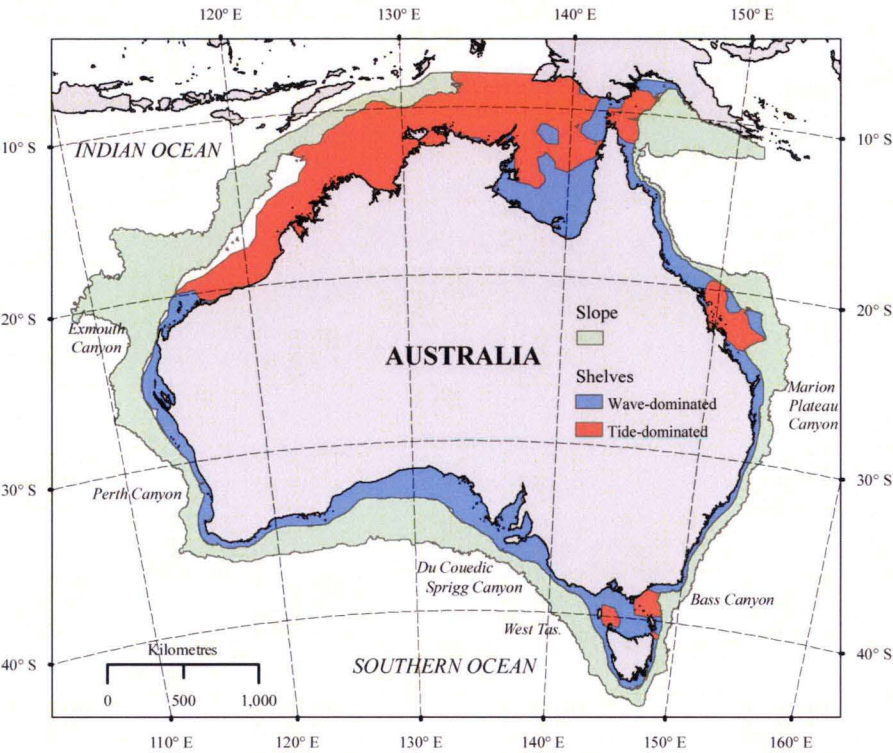


Fig. 4.4: The continental slope is shown in green and adjacent to areas of wave and tide-dominated shelves. The continental slope is characterised by having numerous dendritic canyon networks that transfer sediment to the abyssal plain and nutrients onto the continental shelf.

The continental margin was divided up into four areas of northeast, northwest, southeast and southwest. Metrics were derived for the gradient shelf break against depth, the distance of shelf break to 200 m, the foot of slope against depth and distance of foot of slope to the gradient shelf break (Fig. 4.5). Similarly, histograms were constructed (Fig. 4.6).

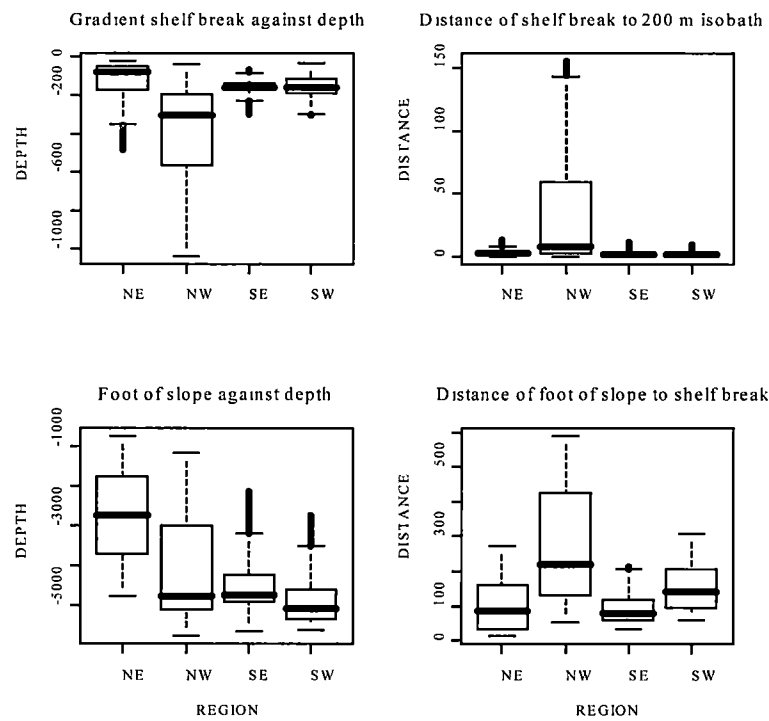


Fig. 4.5. Boxplots of northeast, northwest, southeast and southwest differences of gradient shelf break and foot of slope. The horizontal bar in the middle of the boxplot indicates the median value of length scale. The top and bottom of the box indicate the 75<sup>th</sup> and 25<sup>th</sup> percentile respectively, marking the interquartile range inside which 50% of the data lie. The whiskers indicate the range of data. The circles represent the outliers, which are values more than 1.5 times the interquartile range above the 75<sup>th</sup> or below the 25<sup>th</sup> percentiles (Crawley, 2005).

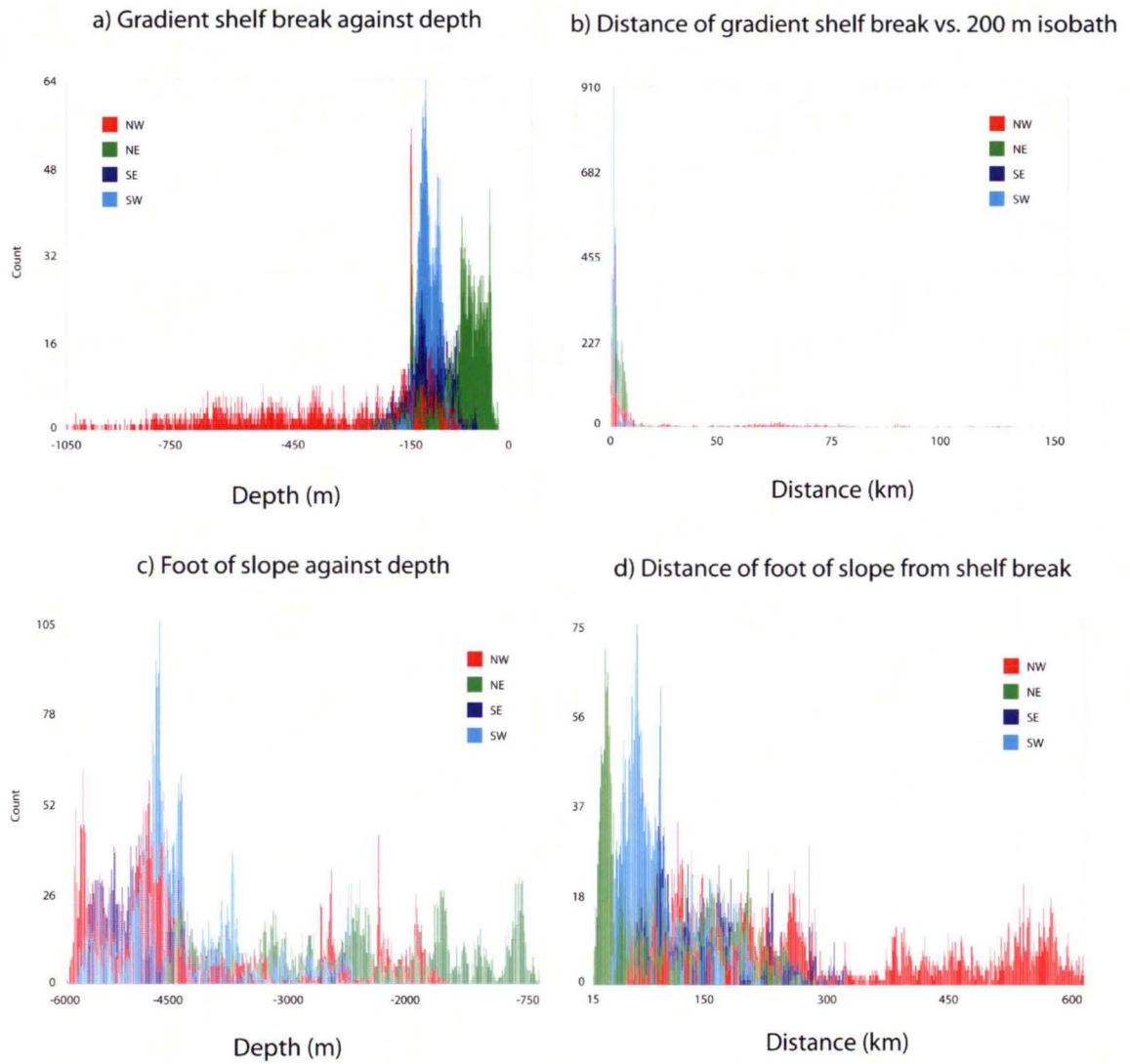


Fig. 4.6: Histograms of northeast, northwest, southeast and southwest differences showing a) the gradient shelf break against depth, b) the distance of gradient shelf break to the 200 m isobath, c) the foot of slope against depth and d) the distance of foot of slope from the gradient shelf break.

The median depth of the gradient-derived shelf break is 162 m. There is a noticeable departure from this median depth in the northwest shelf, where the gradient-based shelf break tends to be much deeper water than the conventional 200-m isobath. The gradient shelf break also shows most variation in the northwest (Fig. 4.5; Fig. 4.6) with a median of 306 m for the depth and a median of 8.2 km for the distance from the 200 m isobath. The northwest also has the greatest variation of depth along the foot of slope and the greatest distance and variation from the foot of slope to the shelf break. However, it is worth noting that the northwest does not have a classic definitive shelf break.

Overall, the mean depth of the foot of slope is  $\sim 4600$  m, unlike the shelf break there is much more variation, particularly in the northwest and northeast. The foot of slope values in the southwest and southeast tend to be consistently deeper. The areas with the least amount of variation of depth or distance to the shelf break are the southwest and southeast. In both these quadrants, the depths are clustered near a similar median depth of  $\sim 160$  m. The shallowest shelf break is in the northeast at a median depth of  $\sim 80$  m. The foot of slope is the shallowest at a median depth of  $\sim 2740$  m, but the continental slope terminates in the Coral Sea Basin.

#### **4.4.2 Continental slope catchments**

The number of shelf-incised catchments using the methodology is ( $n = 257$ ), not counting the catchments that are situated within the slope (Fig. 4.7). The area of these shelf-incised catchments totals  $\sim 1,365,660$  km<sup>2</sup>. The size of the catchments varies regionally. The mean area of these Australian submarine catchments is 5314 km<sup>2</sup>, with standard deviation ( $std = 12486$ ) demonstrates a huge variation in catchment area. There is a strong tendency for the catchments on the eastern seaboard to be smaller and steeper than the rest of the continent (Fig. 4.7). The median values are 1120 km<sup>2</sup>/3.7° in the east, compared with 5085 km<sup>2</sup>/1.7° for the remainder. Within each slope catchment, the number of sub-catchments were delineated (Fig. 4.8 presents an example for Bass Canyon) Not surprisingly, the number of sub-catchments is strongly correlated with the size of the catchment ( $R^2 = 0.99$ ). Within each slope catchment area, the drainage analysis revealed the characteristic dendritic quantities.



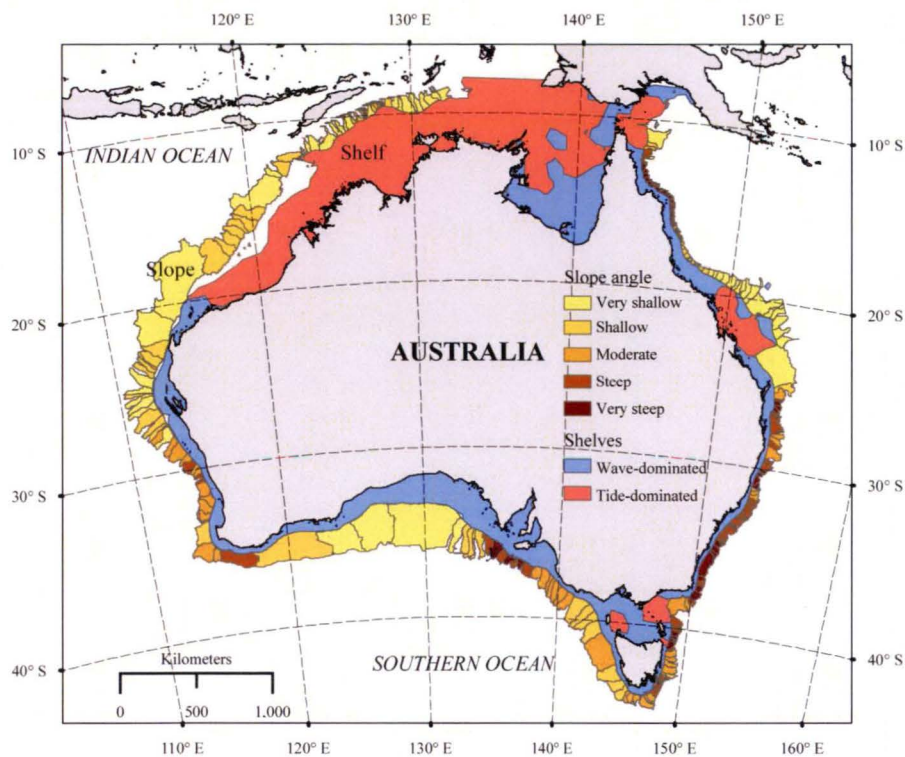


Fig. 4.7: Approximately 257 catchments are derived on the continental slope from the current available bathymetric data. The catchments slope angles are percentile ranked and in 20% bins ranging from 'very shallow' to 'very deep'. The slope angles are 0° - 1.1°, 1.1° - 2.0°, 2.0° - 3.2°, 3.2° - 4.8° and 4.8° - 10.6°. The area of wave- and tide-dominated shelves around Australia is ~ 1.1 million km<sup>2</sup> and ~ 1.3 million km<sup>2</sup> respectively.

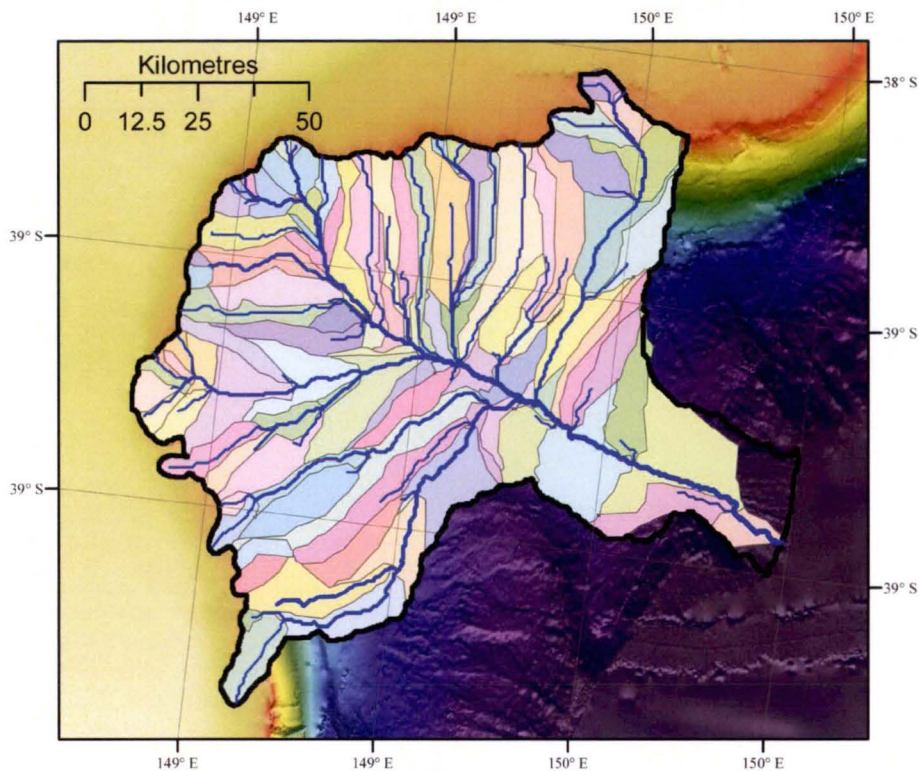


Fig. 4.8: Derived sub-catchments within for the Bass Canyon catchment. These sub-catchments are typically elongated demonstrating the steepness of slope.

The median slope angle of catchments on the slope that incise onto the continental shelf is  $\sim 2.5^\circ$ , and larger catchments have a tendency to be less steep. For instance, the catchments in the Great Australian Bight (GAB) are gently sloping, typically just over  $1^\circ$ , whereas those catchments in the NSW shelf are much steeper at  $\sim 6^\circ$ . The catchments south and east of Spencer Gulf are typically  $\sim 5^\circ$  and the catchments between Spencer Gulf and southern Tasmania  $\sim 2.5^\circ$ . The northern Great Barrier Reef (GBR) has a narrow continental shelf and steep drop-off, while the southern GBR up to and including Marion Plateau has broad shelf and gently sloping catchments. The northeast continental slope catchments are generally very small and steep, particularly in the northern half of the Great Barrier Reef. Generally, the continent's southwestern-facing catchments tend to have a median steepness of  $\sim 2.5^\circ$ , whereas the southeastern catchments are smaller in area, with a more severe angle of slope  $\sim 3.6^\circ$ . The southeast shelf and slope are extremely narrow ( $\sim 35$  km and  $\sim 60$  km respectively). The shape of slope catchments varies considerably inferring that there are morphological implications in the evolution and development of submarine canyon networks.

### 4.4.3 Drainage networks

The drainage analysis reveals a myriad of drainage channels that connect terrestrial systems, and many shelf water bodies that drain internally to areas on the shelf (endorheism). The larger such water bodies include Lake Carpentaria, Bass Lake (Fig. 4.9) and the anomalous lagoon of Bonaparte Gulf which used to drain into the regional Timor Sea. For comparison, the canyon classification as part of the ‘Geomorphology of the Australian margin and adjacent seafloor’ (Heap and Harris, 2008) is shown (Fig. 4.10). The drainage pattern shows reasonable agreement with the canyons west of Tasmania. An examination of catchments reveals that  $D_d$  was highest in the southeast (Fig. 4.11). The drainage network shows good visual agreement between obvious channelling in the interpolated bathymetric model and the extent of canyons and rills evident in the analysis. The severity of incision varies around the slope. For instance, there are extensive parallel channels west of Bass Strait and Tasmania indicating possible pre-canyon rills in the early stages of canyon evolution. These features run parallel down the slope, in some cases extending for nearly 100 km off northwest Tasmania (Fig. 4.9). These features were not evident in ‘Geomorphology of the Australian margin and adjacent seafloor’ (Heap and Harris, 2008).



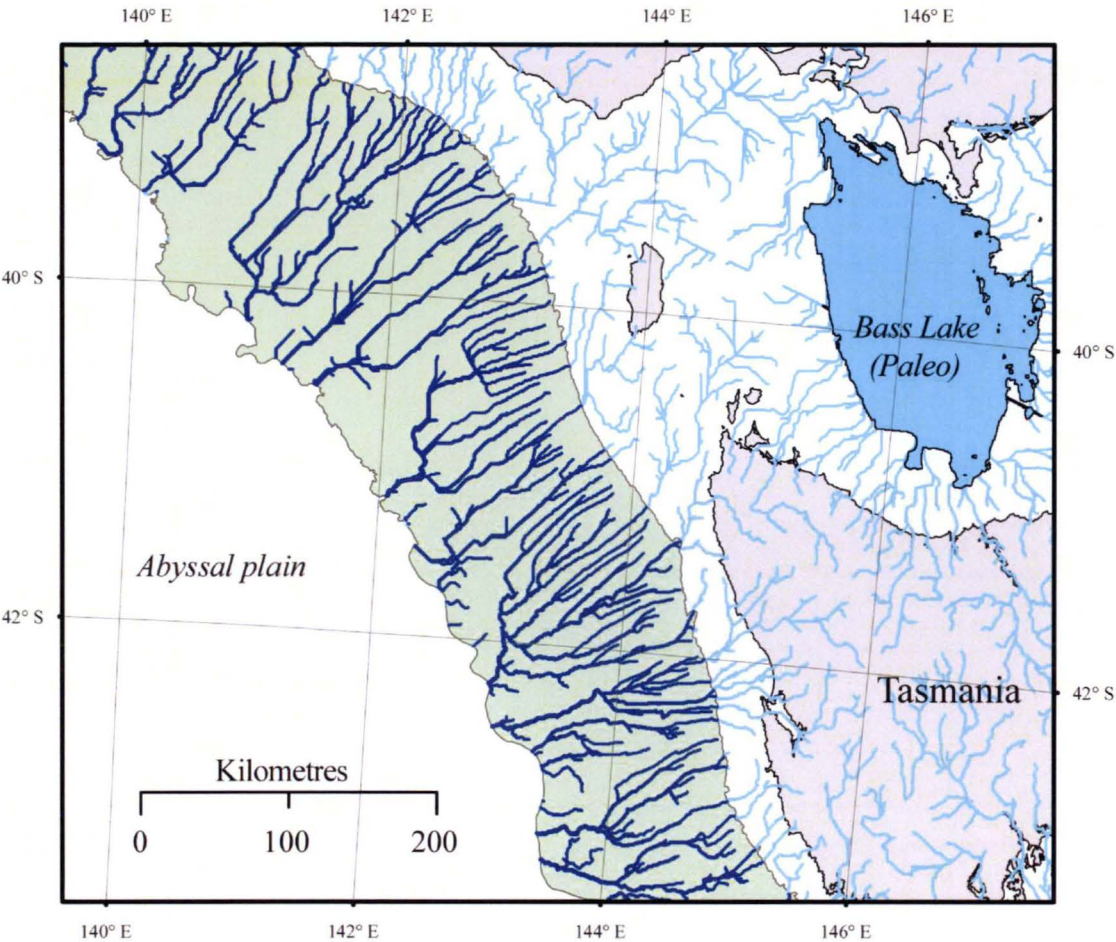


Fig. 4.9: Drainage off Bass Strait and western Tasmania showing parallel channels (possibly pre-canyon rills) particularly on the upper slope. The resultant drainage analysis of the elevation-bathymetric grid has revealed paleo Bass Lake that was flooded by rising sea level ~ 15,000 years ago. The drainage pattern indicates possible terrestrial – shelf – slope relationships.

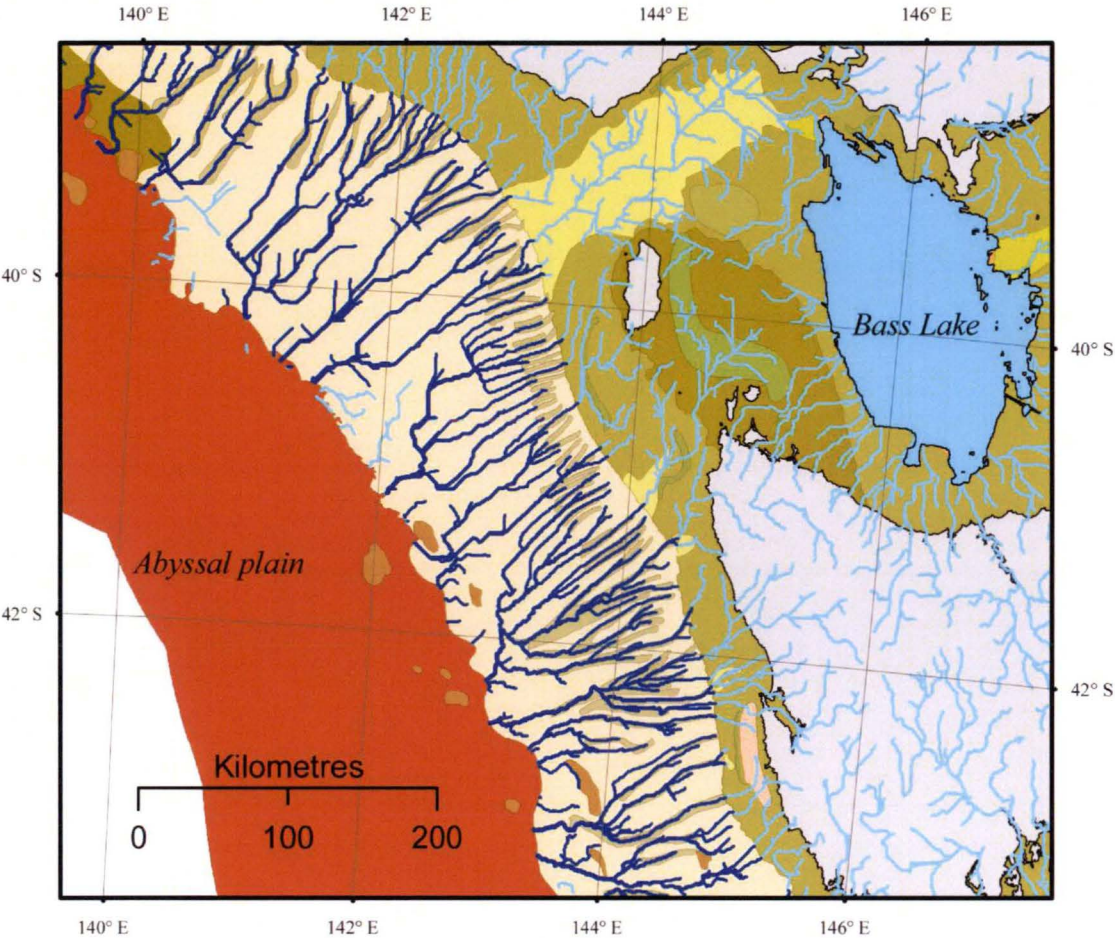


Fig. 4.10: The canyons west of Tasmania according to the the 'Geomorphic map of Australia's EEZ' (Heap and Harris, 2008) drafted in green with the derived drainage analysis (in blue) superimposed.



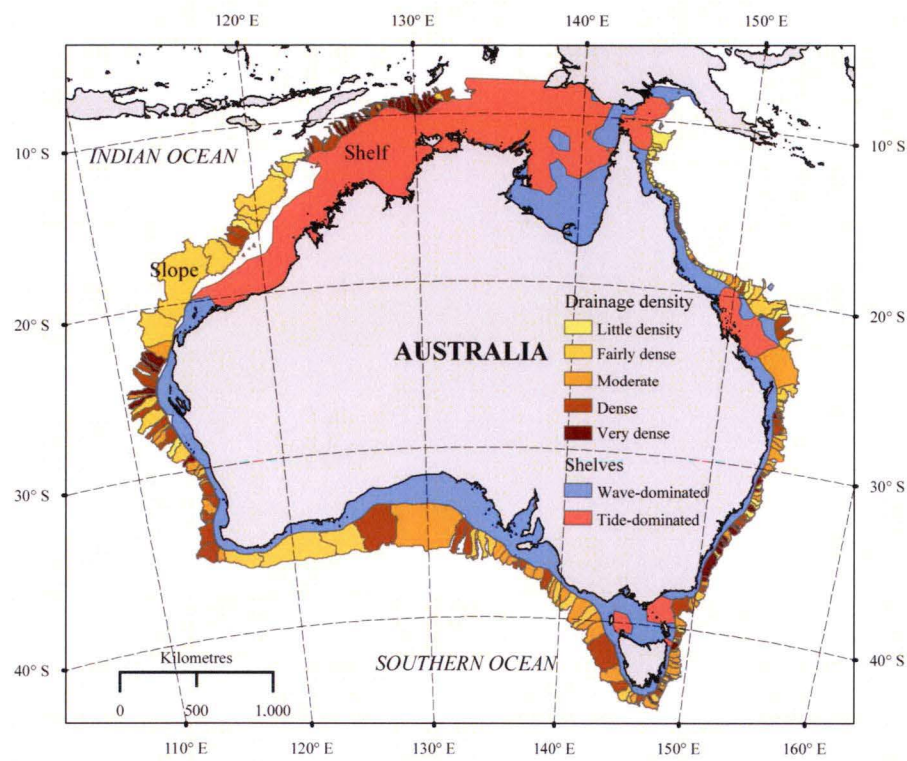


Fig. 4.11: Drainage density on continental margin. The catchments are percentile ranked in 20% bins ranging from “Little density” to “Very dense”.

Six example catchments of Exmouth, NSW, Du Couedic, Sprigg, Bass and West Tasmania canyon systems were chosen to demonstrate differences of the drainage networks (Fig. 4.12). The catchments were selected on the basis that they offered enough stream order variability for accurate analysis. Of the six selected catchments, the drainage density vs. slope diagram shows that the NSW catchment has the highest drainage density and slope, while the Exmouth catchment has the lowest density and slope values (Fig. 4.13). Each of the sample catchments demonstrated a linear relationship between stream order and bifurcation ( $R^2 = 0.79 - 0.98$ ), length ( $R^2 = 0.87 - 0.99$ ) and slope ( $R^2 = 0.7 - 0.98$ ) ratios (Fig. 4.13). The West Tasmanian catchment shows a lower drainage density, suggesting that this catchment has less contributing channel orders and has a steeper gradient. The highest drainage density occurs in the catchments on the slopes of the narrow shelves of the southwest and the southeast.

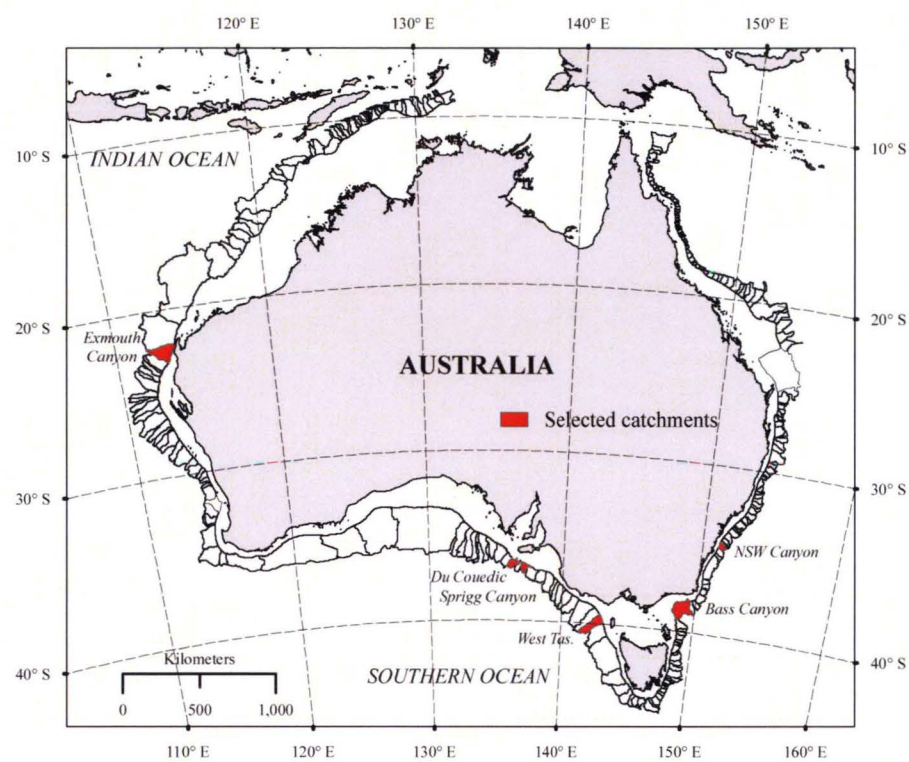


Fig. 4.12: Location diagram of selected catchments to compare statistical characteristics.

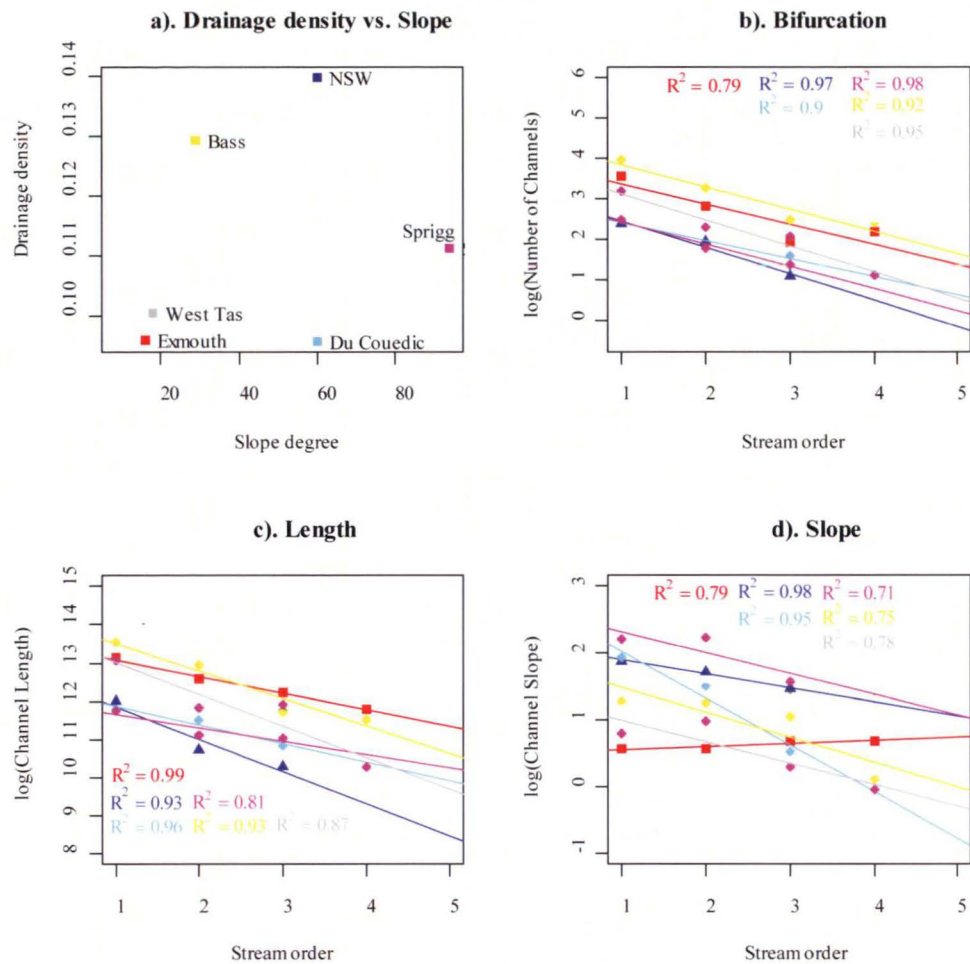


Fig. 4.13: a). Drainage density vs. slope and semi-log plots of the Horton ratios for b) bifurcation ( $R_b$ ), c) length ( $R_l$ ) and d) slope ( $R_s$ ) for the six catchments.  $R^2$  is the correlation coefficient for best-line fit (derived from Table 4.1). Figures b), c) and d) for bifurcation, length and slope show a linear regression indicating that there is a relationship between stream orders.

Table 4.2 contains metrics from six example catchments demonstrating some morphological differences. The variables major-axis and minor-axis are metrics derived from an ellipsoidal approximation of the catchment's shape. These parameters reflect the lengths of the ellipse's axis that represent the basic shape and size of the catchment. The metric  $M_{Mf}$  is a ratio of variables 'major-axis' and 'minor-axis' and gives information on catchment type. The  $M_{Mf}$  for West Tasmania indicates that it is a narrow catchment area and is likely to contain long straight canyons extending down the continental slope. The bifurcation length and slope ratios indicate that the slope can be characterised on these metrics alone (Fig. 4.13). The NSW catchment has the highest drainage density together with a steep slope. In contrast, West Tasmania and Exmouth catchments are characterised



by low drainage density and shallow gradient. A more rounded catchment area would result in sediment supply from other parts of the catchment to be diffused.

Table 4.2: Metrics from six catchments demonstrating morphological differences.

Name	Exmouth	NSW	Du-Couedic	Sprigg	Bass	West-Tas
Area (km <sup>2</sup> )	11822	1709	2956	2292	10753	7897
Perimeter (km)	661	255	345	353	734	631
Drain Len (km)	1134	239	283	255	1389	793
Drain density	0.1	0.14	0.1	0.11	0.13	0.1
Mean slope (°)	2.2	7.1	7.8	11.3	4.2	2.7
Std slope (°)	1.8	4.5	6.3	9	3.5	2.3
Median slope (°)	1.6	6	6	9.4	2.9	1.8
Major-axis (km)	75	28	39	30	65	93
Minor-axis (km)	50	19	24	25	52	27
$M_{Mr}$	1.5	1.4	1.6	1.2	1.25	3.4

4.4.4 Bathomic structure

Table 4.3 below demonstrates differences in the four areas of northwest, northeast, southwest and southeast using the standardised depth ranges for the bathomic structure of Last et al. (2005). These depth limits were determined by using fish datasets to delineate them into unique classes called bathomes. The bathomes intersect the submarine catchment area and the relevant areas calculated over each of these regions. These bathomes demonstrate that a canyon system can be further subdivided to take into account the likely faunal diversity described by Last et al. (2005) and Williams et al. (2008).

Table 4.3: Standardised bioregions/bathomic structure (Last et al., 2005; Williams et al., 2008). Showing area (km<sup>2</sup>), median angle (°) and variability (std (°))

Depth (m)	Bathome	NW			NE			SW			SE		
		Area	Std	Med.	Area	Std	Med.	Area	Std	Med.	Area	Std	Med.
110-220	Outer shelf	8123	2.2	0.5	8109	2.5	1.1	3172	1.8	1.9	5932	1.3	1.8
220-275	transition	9472	1.3	0.3	9226	1.9	0.5	2744	2.3	2	4149	2.0	2.8
275-500	Upper slope	34033	1.1	0.4	62888	1.6	0.2	13787	2.6	1.6	14675	2.6	3.1
500-630	transition	16275	1.2	0.8	10411	2.6	0.8	9698	2.4	1.4	6788	3.2	4
630-775	Mid-upper slope	17408	1.2	1	7892	2.9	1.2	14060	2.2	1.1	7608	3.7	3.9
775-870	transition	11868	1.2	1	4163	3.0	1.5	9848	2.1	1.1	5473	3.9	3.4
870-1100	Mid-slope	41621	1.1	0.7	8825	3.2	1.6	22090	2.6	1.2	14876	3.9	2.9
1100-1500	transition	83407	1.1	0.6	14462	3.4	1.5	33753	3.3	1.3	29252	4.0	2.6
>1500	Lower slope	222628	2.6	1.4	46484	3.7	2.1	289981	3.8	1.3	247923	3.8	2.5

4.5 Discussion

4.5.1 Classifying catchments

Drainage pattern analysis seeks to identify some empirical explanation for dendritic structures, and to what extent, forms are dependent upon controlling variables. If a drainage network and catchment has a particular shape then it can be concluded that there is a control acting on the morphology and development of the drainage network thereby demonstrating control by geological inheritance (Cheng et al., 2001). The chosen catchments varied not only in area but also in shape, the  $M_{Mr}$  for West Tasmania indicates that it is a narrow catchment area and is likely to contain long straight canyons extending down the continental slope. Catchments on steeper slopes tended to be long and narrow; this characteristic was particularly prevalent in the southeast. The northwest has a prograding shelf, which has made it more difficult to define submarine catchments.

The characters of submarine catchments vary spatially. However, the graphs Fig. 4.13b, Fig. 4.13c and Fig. 4.13d for  $R_b$ ,  $R_i$ , and  $R_s$  respectively demonstrate that for the six sample catchments there exists a geometric relationship between the streams of a given order ( $i$ ) and the adjacent orders ( $i + 1$  and  $i - 1$ ). All the values lie on a straight line, demonstrating an exponential relationship that is independent of drainage network pattern. These

exponential relationships expressed by the drainage network patterns are in turn responding to the morphology of the elevation-bathymetric grid. One of the drawbacks of using Horton ratios was that many of the slope catchments did not offer several orders for analysis, therefore, only a few catchments were suitable for comparison. However, the catchment approach proved the most useful for holistically analysing all slope catchments.

Generally, catchments with the smallest value of  $D_d$  tend to be adjacent to tidally dominated shelves. A possible explanation for this is that that maximum tidal currents tend to travel parallel to the isobaths, in contrast to wave energy, which is most pronounced on and directly towards shore. Some of the longest canyons are situated in the Great Australian Bight, south of Spencer Gulf and west of Tasmania. Catchments in the southeast have greatest drainage density, being small in area, and steep. In addition to gradient, causing slope failure, continental shelf width may be a contributing factor in the evolution of submarine canyons. Continental shelves adjacent to these slopes may overload the reservoir of sediment, destabilising the shelf break and causing further slope failure. Canyons that incise the shelf break, sediment flows are probably initiated by storm activity and sediment transport dynamics at the shelf break is a likely catalyst for large sediment flows (Straub et al., 2007). Therefore, the mobilisation of sediment on the shelf in wave- or tide-dominated shelves (Porter-Smith et al., 2004) adjacent to the slopes could have implications for submarine canyon development and evolution (Fig. 4.7). Continual mobilisation of sediment in the wave-dominated southeast could destabilise sediment deposits at the shelf break, leading to sediment flows and subsequent canyon evolution. The significance of canyons on slope areas that do not receive any sediment input would be that the canyon evolution is more likely to be slope-derived. Similarly, the variability of sediment gravity flows would have temporal implications for a biological regime within canyons. For instance, biological regimes would be completely different to ones that experience more frequent sediment gravity flows.

The northern Australian shelf is generally broad and can be as much as 500 km wide including the Arafura Sea (Church and Craig, 1998). The width of the northwest shelf in contrast to the southeast shelf is 150 km and 20 km respectively. It is probable that the narrower the shelf, the more likely there has been a terrestrial-marine relationship in the form of paleochannels that have since been obscured by sediment infilling by rising sea level and marine processes, such as waves and tides. In addition, due to historic sea level

rise since the last glacial maximum, this morphological categorisation would have previously extended beyond the coast to  $\sim 120$  m isobath. In much of the shelf, this is a significant distance. It is likely that some of the present submarine channels would have been terrestrial rivers and streams as most recently as the pre-Holocene ( $\sim 12,000$  years ago). This type of research can investigate the existence of systematic patterns in drainage networks that could have implications for biology for instance, the relationship of biota to paleo-fluvial systems.

#### **4.5.2 Bathomic classification**

Another important consideration of this approach is that it not only recognised the catchment delineation of drainage network on the continental slope, but also considered depth structure as being important because of biological implications and because of its relevance to classifying marine biodiversity in marine resource planning. The bathomic structure (Last et al., 2005; Williams et al., 2008) is relevant because a submarine canyon can cut across many depth bands. Therefore, faunal distributions are more fundamentally correlated with depth strata than with a singular geomorphic feature such as a canyon (Williams et al., 2008). Each of these bathomes could potentially represent a unique faunal assemblage. This particular characteristic has implications for environmental management. The catchments are characterised on the depth-based bathomic classification (Butler et al., 2001; Last et al., 2005; Williams et al., 2008; Last et al., 2010) that are based on neritic and bathyal zones (Fairbridge, 1966). This approach highlights spatial differences in the depth strata (Table 4.3). Delineating the submarine catchments and quantifying the area in each of these bathomes highlights regional differences.

#### **4.5.3 Other issues**

It is acknowledged with the catchment-based approach that the drainage is calculated globally and is a summary technique. It does not take into account the volume of individual canyons. However, the advantage is that it is rapid and applies a consistent methodology to

all areas. A natural extension of this work would be to calculate volumes of canyons and construct a feature inventory, particularly in the 200 – 700 m isobath range, as well as including a geomorphic description of canyons. There are also implications for biology in the morphological shape of canyons – whether the morphology is compressive or decompressive in the depth range of the deep scattering layer that cyclically migrates up and down submarine canyons. It is acknowledged that the holistically-derived drainage is unrealistic for calculating the volume of channelling. For terrestrial systems, digital elevation models generally require a horizontal resolution of around 10 m (Montgomery and Dietrich, 1988), however this level of resolution is unavailable for most undersea areas (Pratson and Ryan, 1996) particularly in areas on the continental slope, as data-rich areas are usually confined to near-shore and shelf regions. For this research to be extended to consider canyon volume and the internal geomorphology of submarine canyons, a much higher resolution elevation-bathymetric grid will be required.

Similarly, other possible geomorphological controls were not investigated for instance, in many submarine channel systems, a sharp anisotropic trend is apparent. Examples include submarine channels of the west coast of North America where 80% hook sharply to the left. These were attributed to the Coriolis effect (Menard, 1955) forcing the current flow to the right, building up the right bank higher, in turn gradually forcing the flow to swing left (Fairbridge, 1966).

Although there are some advantages of mapping single canyons (e.g. enables research to be site specific) conversely, by adopting this catchment-based approach is being able to produce holistic characterisation, comparison and extraction of metrics. Additionally, this methodology also provides a high-level structure from which lower scale characterisations and regionalisations can be implemented.

## **4.6 Conclusion**

This study demonstrates an approach to automatically and rapidly derive a catchment-based characterisation of canyons using current bathymetric data. The process is efficient and with the advent and availability of new survey data the submarine catchments and

canyon systems can quickly be redefined incrementally, value-adding to the accuracy and relevancy. Past research has mostly concentrated on either individual canyons, or profiles of groups of canyons. This research has analysed the submarine canyons within discrete catchment networks. This approach has the advantage of being process-based, with clear relevance to submarine canyon genesis and evolution.

By establishing a shelf break and foot of slope based on gradient, submarine catchments can be derived on the continental slope based on the drainage analysis. The Australian continental slope contains 257 shelf-incised catchments based on analysis of a bathymetric model mapped at a resolution of 250 m. The drainage analysis demonstrates the capabilities of correctly predicting the layout of dendritic patterns leading to a better geological understanding.

This catchment-based approach provides morphological metrics for analysis. In a broader sense, this methodology provides a high-level structure from which lower scale characterisations and regionalisations can be implemented. Several metrics can be derived from both the drainage network and catchment morphology. Using Horton's ratios, we were able to classify drainage within catchments on the slope. The results show that the derived drainage networks did conform to Horton's laws and demonstrated a geometric relationship between the streams of a given order ( $i$ ) and the adjacent orders. ( $i + 1$  and  $i - 1$ ). However, one of the drawbacks of using Horton ratios was that many of the slope catchments did not offer enough orders for an accurate analysis, therefore, only a few catchments were suitable for comparison. In contrast, using basic geometric and calculations based on slope proved the most useful.

Adopting this catchment-based approach highlights possible contributions of sediment sources from the continental shelf that is so important in submarine canyon evolution. This enables a holistic insight into geomorphic processes and form when viewing the Australian continent both regionally and as a whole. Future challenges are to investigate individual canyons, and also the implications of morphology and volume. Eventually this technique could produce a geomorphic description of canyons, including a feature inventory particularly in the bathymetric depth ranges and the synergies with associated biology.

Considering depth structure is important because of biological implications and because of its relevance to classifying marine biodiversity in marine resource planning. The bathymetric

structure (Last et al., 2005; Williams et al., 2008) is relevant because a submarine canyon can cut across many depth bands. Therefore, faunal distributions are more fundamentally correlated with depth strata than with a singular geomorphic feature such as a canyon (Williams et al., 2008). Each of these bathomes could potentially represent a unique faunal assemblage. Delineating the submarine catchments and quantifying the area in each of these bathomes, enables comparison.

## CHAPTER 5 CONCLUSION

### 5.1 Key findings

This thesis used a holistic approach to quantify and analyse how both terrestrial and marine processes influence form of the Australian continental margin as well as examining how coast, continental shelf and slope vary regionally. The analysis relied on estimates of modelled waves and tides along with other physical variables to define and investigate these marine areas. It is expected that these quantitative process-based delineations can provide a relevant techniques for other classifications and create a platform for the integration of marine and terrestrial regionalisation.

The aim of this research was to produce a series of robust and quantifiable process-based delineations of the Australian continental margin from coastline to the foot of the slope and examine some geomorphic forms resulting from erosive processes in order to quantify characteristics of the Australian margin's evolution. The intention was to develop a framework from which other processes and biological inferences can be derived in order to contribute towards current regional marine planning efforts. The advantage of these methodologies is that they are quantitative, process-based supervised classifications rather than qualitative or unsupervised ones that might rely upon potentially arbitrary variables or ordinations. Main outcomes of this thesis include:

- A delineation of wave- and tide-dominated shelves based on quantitative measures of modelled wave climate and tidal cycles;
- A comprehensive analysis of coastal complexity ( $C_x$ ) and attributed to main causative driver variables at a mesoscale;
- A delineation of submarine catchments on the continental slope that ultimately determines extent of submarine canyon evolution through sediment gravity flows.



## 5.2 Detailed assessment of objectives

**Objective (1)** was to delineate continental shelves based on the relative dominance of marine processes such as swell waves and tides and to define the physical relationship between mobilising processes and shelf sediments.

This work was done to gain an understanding of the relationships between relative domination of waves and tides on the continental shelf. It was also calculated as an input to define the relationship to coastline complexity and submarine catchments around the continental margin. Using modelled estimates of tidal current speed and significant wave height and period, the Australian continental shelf was categorised into wave- and tide-dominated shelf environments. The relative distribution of these regions is similar to previous conceptually based regionalisations; however, with the advantage that it is for the first time quantitative. The results suggest that the Australian continental shelf is mostly dominated by tides rather than by waves. Examination of the distribution of dominance indicates that there are areas on the continental shelf which are either wave-dominated or tide-dominated, some areas where waves and tides are of relatively equal importance and still other areas where neither is significant.

The first step was to examine sediment entrainment thresholds to delineate the wave- and tidally-dominated shelves. These delineations were based upon quantitatively estimating the wave and tidal erosive capacity and the spatial extent across which they can mobilise shelf sediment. An examination of these sediment-entraining processes independently quantified their relative importance on the continental shelf and established percentages of the Australian shelf subject to different processes. The results from this analysis confirmed that the Australian shelf is dominated by waves over ~ 31% of its area and by tidal currents over ~ 41% its area. The result contrasts with other estimations that about ~ 80% of the world's shelves are dominated by storm-waves, ~ 17% by tidal currents and the remaining ~ 3% by intruding ocean currents (Walker, 1984; Swift et al., 1986).

Results from this analysis indicate that the region of zero mobility accounts for ~ 27% of the shelf. This could have many implications e.g. sediment reservoirs that accumulate off shelf breaks and contribute to periodic sediment gravity flows. The zero mobility regions are generally located in deep water (mean depth > 189 m) away from mobilising processes

such as swell waves. These areas are characterised by coarse-grained sediments with low mud content. This contradicts the conventional, graded shelf model (Swift and Thorne, 1991) and Aigner's 'proximality' diagram (Aigner, 1985), which suggest that mud content and the rate of bioturbation increase in an offshore direction with lower energy and increasing depth. This thesis also confirms that these coarse-grained sediments are not in hydraulic equilibrium with the prevailing tide and wave current regime. This is demonstrated by the existence of a weak positive correlation between tidal current speed and grain size ( $R^2 = 0.38$ ; Fig. 2.10A), while there is no evident correlation between mean grain size and wave power (Fig. 2.10B). This can be explained by the fact that wave-dominated regions are more efficient at winnowing and dispersing mud and finer-grained sediment, leaving a coarse, sorted lag deposit.

In contrast, some tide-only regions appear to trap fine sediment particles, as supported by previous observations of tidal turbidity maxima at several locations around Australia, including Gulf of St. Vincent (Phillips and Scholz, 1982), King Sound (Semeniuk, 1982) and Torres Strait (Harris and Baker, 1991). An explanation might be that, as the Australian shelf is more tidally dominated, the maximum tidal direction is likely to be parallel to the isobaths, and the process of breaking down sediment is likely to occur along this pathway. The analysis demonstrates that tidal currents and bottom sediments in tide-dominated regions of high mud content are associated with peak tidal current vectors directed along the coastline. In contrast, areas of low mud content are associated with seaward-directed maximum tidal current vectors. Therefore, in regions where tidal processes control sediment transport, mud appears to be trapped on flood-dominated shelves but not on ebb-dominated shelves. It is known that calcareous detrital silt is generated in tidal shelf environments by the disintegration of soft carbonate grains during bedload transport (Harris, 1994). This explains the high mud content (41%) in tide-dominated regions and the trapping of mud on the shelf associated with landward and along-shelf oriented maximum tidal current vectors, whereas off-shelf directed current vectors are associated with low mud content deposits. The delineation of the shelf based upon modelled wave, tide and sediment entrainment demonstrated that the results contradict the conventional, graded shelf model of Swift and Thorne (1991). In conclusion, Australia's deep-water; outer-shelf sediments are not in equilibrium with modern tide and wave hydrodynamic processes.

Although results presented in the study do not provide a provincial type distribution, they do quantify the processes on the shelf that have significant effects on the Australian coast and slope. The results demonstrate a predictive, process-based understanding of the shelf sedimentary system that has applications to regionalisation and other research where shelf sediment mobilisation is a factor. Sediment eroded from the land by terrestrial processes modifies the coastline structure. Marine processes transport the sediment across the continental shelf, and this transport depends on whether an area of the shelf is wave- or tide-dominated.

**Objective (2)** was to quantify coastline complexity and establish the relationship between the varying length scales, geological structure and influence from various marine shelf processes.

This was achieved by producing models that quantified the relationship between  $C_x$ , the structure of the land and the forcing from processes such as waves and tides. This was done to establish whether  $C_x$  increases with age increases or decreases with age. Very distinctive signatures of some geological regions indicate there is or has been dominant physical processes or characteristics at work driving the varying  $C_x$ . Patterns of  $C_x$  are likely to be a product of the prevailing wave climate and tidal conditions. Current hypotheses suggest that waves provide the greatest influence on  $C_x$  (Sapoval et al., 2004). Therefore, the patterns of erosion are likely to respond to the varying wave climate.

However, the main outcome of this chapter demonstrates that terrestrial processes primarily drive  $C_x$  and that various geological regions respond differently to marine processes. Previous approaches have largely ignored the land-ocean interface, and the novelty of this study is through a holistic treatment of this margin in order to correlate coastline variation with distinct terrestrial and marine form, taking account of the complex interaction between terrestrial and marine influences.

Terrestrial erosion is dependent on climatic differences, contrasting rock hardness and different tectonic histories (Whitlow, 1984). There is little accurate data on various past climates or rock hardness. Tectonic history can be evident from areas of orogeny, with the rate of erosion being proportional to height (Wright, 1985). Therefore, age is one of the best proxies for  $C_x$ , as over time the coastline will respond to its inherent geology. There is a positive correlation between age and lithological diversity. In other words, when

geological regions are percentile ranked according to age, the lithological diversity increases with age. This implies that through time, tectonic processes cause a mix of lithological types through orogenic processes. Through time and erosion, diverse lithological types are exposed, leading to differing terrestrial erosion rates and opportunistic wave-induced erosion leading to increased  $C_x$ . Thereby, geological regions may develop from a homogeneous lithology to one that is heterogeneous through tectonic processes. As a result of this increase in lithological diversity, coastlines tend to become more complex with age. In heterogeneous regions, processes erode the softer material away to leave a crenulated coastline. This indicates that geological inheritance is an important determinant. A specific lithological type does not seem as important as the variation or mix of lithological types. Coastlines of a singular lithology type tend to be straighter than coastlines of mixed lithological typology and over time, a coastline will respond to its inherent geology.

The generally accepted view that wave action causes a coastline to become more complex over time (Sapoval et al., 2004) is challenged by this study which found that wave power is inversely proportional to  $C_x$ . However, this may be a reflection of the homogenous lithology in wave-dominated waters around much of Australia. Wave action is opportunistic in attacking and eroding sections of coastline and the nature of its effect is dependent on the geology. This in turn exerts influence on how wave action may target more vulnerable and easier erodible margins. Therefore, a straight coastline with homogenous lithology that is subjected to wave action is likely to remain straight regardless, due to the uniform degree of resistance of the lithology to marine erosion by wave attack. Wave action will exploit existing weaknesses in the coastline of mixed lithology thereby creating irregular coasts. Additionally, a beach can change form over time through (processes of) wave erosion, diffraction and accretion, forming characteristic patterns, suggesting that autonomous feedback processes can promote structure where none existed.

There is some evidence to suggest that tide energy is responsible for increased  $C_x$ . However, this could be because a higher tidal range is delivering wave action into terrestrial features that can promote further erosion. There is a length-scale difference in wave- and tide-dominated coasts. In tide-dominated areas, the characteristic length scales tend to be longer than those for wave-dominated coasts. This is evidenced by areas such as the

Kimberley and Proserpine regions, compared to wave-dominated geological regions like Sydney and Bremer, where the  $C_x$  peaks at a shorter length scale.

A considerable amount of past research has gone into understanding the geomorphological processes responsible for the genesis and evolution of the present day form of the coastline. The research presented in this thesis is particularly novel as it categorises the coastline at characteristic length scales. The results have shown that geological inheritance, namely the lithological mix, has the primary influence in determining the control over variability in  $C_x$ . Additional research is needed to determine spatial metric values obtained for coastal segments and their specific correlations to tectonic and geological and ocean processes.

**Objective (3)** was to classify the continental slope into discrete submarine catchments and to derive metrics from both the drainage analysis and associated catchments.

A framework was developed to examine and classify submarine canyons on the Australian continental slope. This involved the derivation of catchments around the Australian slope, where independent drainage networks were categorised. As canyon formation is mainly due to sediment movement and flow under gravity, the catchment approach seemed the most appropriate.

Oceanographers know that the shelf-break region is one of enhanced physical mixing and turbulence, particularly on those shelves, which have a classic definitive shelf-break front. An important part of this classification was to correctly define the continental shelf break and bottom of the continental slope, based on change of gradient, as opposed to the more conventional 200-m isobath shelf break. Using the gradient shelf break and foot of slope enabled the continental slope catchments to be derived. Canyons are small ecological systems in their own right. Therefore, considering a submarine canyon as an ecological system requires further delineation of their structure, taking into account how a canyon intersects/interacts with the overlying water column. Canyons with similar structures in different locations will contain different suites of flora/fauna. In other words, the characteristics of a canyon are not determined by their geological or morphometric constructs alone.

A total of 257 slope catchments were identified around the Australian continental slope. It was possible to differentiate slope catchments adjacent to wave- and tide- dominated shelves. The southeast catchments had greatest drainage density, were small in area, and steep. Steepness was identified as a causative factor in slope failure and the development of submarine canyons, and continental shelf width may be a relevant factor. The steepest continental slopes, found in the northern Great Barrier Reef and in the southeast, have very narrow continental shelves.

Within each of these submarine catchments, the derived drainage networks representing the dendritic canyon systems display to a greater or lesser degree characteristics associated with geological constraints, as opposed to networks displaying space-filling properties (Cheng et al., 2001). The use of metrics demonstrating network constraint is useful, and the derivation of Horton ratios (of bifurcation length and slope ratios) indicate that regional differences can be highlighted and demonstrates a capacity to automatically and rapidly define the continental slope using this catchment-based approach.

The evolution of a stream is governed by geological constraints (Cheng et al., 2001) and submarine canyons are similar in their evolution to terrestrial systems, although the obvious differences on the continental slope are the flow medium and influences from water-borne currents. The controlling variables in this erosive process for submarine canyons are gravity and the relationship to morphology and topography. It is unlikely that random processes cause the drainage patterns that are observed. Lengthening of canyon path and compression of canyon width indicates that the drainage morphology in that particular catchment is being impeded or affected, therefore demonstrating control by geological inheritance (Cheng et al., 2001). A high drainage density, together with a steep slope, indicates the likelihood of active processes in submarine canyon formation and evolution. Slope and sediment supply are important factors in their evolution.

### **5.3 Summary**

This study has developed a holistic model which clarifies that the evolution of the Australian continental margin is largely governed by erosive processes. The study has used

erosion as the basic framework, and the modelled boundaries and distribution are based on quantitative processes. There are different erosive processes acting on the Australian margin – one area is exposed to the air and other one is exposed to the water. There are also different rates and types of erosion from coastline to slope. Although differential erosion has been recognised, this is the first national evaluation using quantitative statistics. Terrestrial erosion on the land is dictated by geological inheritance and modified by marine processes affecting  $C_x$ . The continental shelf was delineated on modelled estimates of wave and tidal energy; this delineation became a key metric in evaluating the adjacent  $C_x$ . On the shelf, marine processes tend to distribute sediment around the shelf. Although the shelf width varies enormously, it is generally flat, as the marine processes tend to smooth it out. However, the continental slope is more varied and there are systematic differences between the continental slope in the northwest and southeast. The northwest continental shelf break has all been but obliterated (possibly due to internal tides acting on the morphology). In contrast, the southeast continental slope is steep, and erosional processes cause the edge of the shelf to slump, exposing gradients that are more precipitous (very likely due to geological makeup). The cyclic nature of all the processes on the continental margin is the balance between structure being created and structure being destroyed. Given the synergy of these erosive processes acting on the margin from source to sink, it is hard to ignore their relevance and implications for regional marine planning and management. Only by quantifying these regional differences can accurate planning objectives be achieved for this important national resource.

## 5.4 Implications

In recent years there has been much effort invested into understanding and quantifying geological, oceanographic and biological factors that may determine how the Australian shelf and slope could be regionalised for marine planning purposes (CSIRO, 1996; IMCRA, 1998; Lyne et al., 1998; Butler et al., 2001; Commonwealth of Australia, 2005; Last et al., 2010). Previous studies of continental platforms have had difficulty in defining the relative importance of geological, oceanographic and biological processes. Using Australian examples, the province level of shelf regionalisation is a high-level perpendicular

zonation of boundaries around the continental margin (CSIRO, 1996; IMCRA, 1998; Lyne et al., 1998; Butler et al., 2001; Commonwealth of Australia, 2005). The current higher-level structure (CSIRO, 1996) reflects paleo-historic evolutionary processes from a biological (fish) perspective that define contemporary marine and coastal ecological systems. These delineate discrete zones around the shelf and slope.

Benthic regionalisations for the Australian continental shelf have been developed using a hierarchical framework and quantitative estimates of geological features, geomorphic features, oceanographic processes and biological data. Methodologies have progressed from a Delphic approach to one that is more quantitatively driven and therefore statistically robust. Shortages of available or relevant data have very often constrained the regionalisation process, leading to a complex hierarchical structure being represented by a regional or mesoscale perspective. These regional data sets are then pieced together to produce a continent-wide picture. From the marine planning perspective, it all depends on the purpose of the classification: like all classifications, it may work well for some purposes and not for others. However, a regionalisation that is based on quantitative metrics will define important boundaries of the Australia margin and the processes involved. For instance, the  $C_x$  of Australia's coastline may reflect underlying processes that determine its tortuosity. Although it is obvious that each section of coastline is a result of many past and ongoing processes, the challenge is to identify some of the dominant formative conditions that apply to regional areas of coastline.

The delineated shelf-based wave and tidal process covers the entire shelf and affects provinces, bathomes (neritic zones consisting of estuarine, coastal marine and demersal areas) and geomorphic units. One of the additional advantages of defining wave- and tide-dominated areas of the shelf is that it has been demonstrated to be important not only for physical processes, but also that the biodiversity and abundance of benthic species is inversely related to the mobility of the substrate (Shepherd, 1983; Poiner and Kennedy, 1984). The lowest abundance and diversity is associated with bedforms. This has practical implications for marine planning purposes in these delineated zones on the continental shelf, but measurements of sediment mobility can provide the basis for predicting the spatial extent of benthic habitats.

$C_x$  affects provinces in the neritic zone, which covers the continental shelf and consists of estuarine, coastal marine and demersal bathomes. The inner bathome includes the coastline



and in the past researchers have had a tendency to ignore this important littoral zone when regionalising the character of the inner shelf. The implication for regional marine planning is that this extra detail and information can be used as an additional surrogate in predictive modelling of biodiversity to investigate regional environment relationships. By incorporating  $C_{\infty}$  with its important relationship to geological inheritance, marine regionalisation is given a terrestrial context, providing a holistic view of the Australian margin.

The catchment-based submarine canyon work affects provinces, bathomes, and geomorphic units. Although submarine canyons are strictly a geomorphic unit, they do cross several depth zones that have different biotic assemblages. The submarine canyon work has not only provided a regional comparative framework, but it has also defined the difference in bathomic structure by correctly defining major geophysical boundaries (e.g. neritic and oceanic zones at the shelf break). This will have implications for the classification and evolution of biota. By mapping these important submarine canyons on the continental shelf, the technique provides a framework to further classify and map distinctive biological assemblages responding to ecological niches provided by the canyon as it descends towards the abyssal plain.

Instinctively level 3 'Geomorphic Units' should be smaller than level 2 'Bathomes'; however, this does not necessarily hold for submarine canyons that can traverse across several depth-dependant bathomes. This bathomic structuring (Last et al., 2005; Williams et al., 2008; Last et al., 2010) is attractive because a submarine canyon may cut across many depth bands, and faunal distributions are more fundamentally correlated with these bands than a singular geomorphic feature (Williams et al., 2008). This work addresses the issue of consistent geomorphological analysis of canyons enabling regional comparison. Similarly, it has implications and relevance for the accurate depiction of these geomorphic units (Heap and Harris, 2008). It will provide a framework for categorisation and further investigation into canyon process and form that can be fed back into the regional marine planning process and the current hierarchical classification scheme.

## 5.5 Future work

This study has demonstrated that the shelves can be sensibly delineated into wave-/tide dominated areas. This process is a first step but future work might include taking pre-existing independently derived sedimentological and biological-ecological classifications and comparing them directly. However, more work is needed on wave and tide maximum currents and their directional patterns. The directionality of marine processes could be investigated to examine pathways and areas of sediment deposition. This would also benefit work with  $C_x$  as well as submarine catchments and the evolution of submarine canyons that are dependant on sediment movement and deposition on the shelf. As further step would be to carry out an examination of the capacity of the continental shelf to hold the transported sediment regionally around the Australian margin.

A natural progression of this study is to extend the research on  $C_x$  to a more detailed analysis of lithological types and their associated mechanical strength, as this can vary regionally. Additionally, terrestrial erosion may also be controlled by catchment area acting in synergy with the underlying geology. Catchment area has a fundamental influence on the development of drainage networks and river evolution, directly influencing embayment size or coastal character (Bishop and Cowell, 1997). Further studies might use a quantification of geological makeup as a more relevant measure in determining how  $C_x$  might evolve, for instance, using mechanical strengths or an index of vulnerability to weathering.

Canyon work could be advanced by carrying out a morphological study of shelf width. This could be carried out by examining profiles from the coastline to bottom of slope. The profiles could take the direct route to foot of slope. These profiles could later be clustered into discrete classes. Other variables might incorporate using estimates of wave and tide energy. Another approach would be to use the same aggregating and clustering technique of coastline segmentation on shelf width and slope steepness again to identify unique classes. To examine estimates of canyon sediment load, estimates of sediment entrainment and direction would be useful. Additionally, further study could be done on internal tides and their relationship to the continental shelf break and slope to determine how they interact with the morphology particularly on the northwest shelf. This catchment-based analysis of submarine canyons does not account for individual submarine canyon volume. This study could be extended to include this feature.

## REFERENCES

- Abercrombie, M., Hickman, C.J. and Johnson, M.L., 1951. A dictionary of biology. Hunt Barnard, Aylesbury.
- Abrahams, A.D. and Flint, J.J., 1983. Geological Controls on the Topological Properties of Some Trellis Channel Networks. *Geological Society of America Bulletin*, 94(1): 80-91.
- Adams, E.W. and Schlager, W., 2000. Basic types of submarine slope curvature. *Journal of Sedimentary Research*, 70(4): 814-828.
- Adams, E.W., Schlager, W. and Wattel, E., 1998. Submarine slopes with an exponential curvature. *Sedimentary Geology*, 117(3-4): 135-141.
- AGSO, 1998. Geology (1:2,500,000) (National Geoscience Dataset). Geoscience Australia (formally AGSO), Canberra, Australia, pp. <http://www.ga.gov.au/meta/ANZCW0703002305.html>.
- AGSO, 1999. Bathymetric 30' grid. Australian Geological Survey Organisation, Canberra Australia.
- Aigner, T., 1985. Storm depositional systems: Lecture Notes in Earth Sciences No. 3. Springer-Verlag, Berlin, pp. 174.
- Andersen, O.B., Woodworth, P.L. and Flather, R.A., 1995. Intercomparison of recent ocean tide models. *Journal of Geophysical Research-Oceans*, 100(C12).
- Andrews, J.E., Shepard, F.P. and Hurley, R.J., 1970. Great Bahama Canyon. *Bulletin of the Geological Society of America*, 81(4): 1061-1078.
- Andrle, R., 1994. The Angle Measure Technique - a New Method for Characterizing the Complexity of Geomorphic Lines. *Mathematical Geology*, 26(1): 83-97.
- Andrle, R., 1996. Complexity and scale in geomorphology: Statistical self-similarity vs characteristic scales. *Mathematical Geology*, 28(3): 275-293.
- Baker, E.K. and Harris, P.T., 1991. Copper, Lead, and Zinc Distribution in the Sediments of the Fly River Delta and Torres Strait. *Marine Pollution Bulletin MPNBAZ*, 22(12).
- Band, L.E., 1986. Topographic partition of watersheds with digital elevation models. *Water Resources Research*, 22: 15-24.
- Bartley, J.D., Buddemeier, R.W. and Bennett, D.A., 2001. Coastline complexity: a parameter for functional classification of coastal environments. *Journal of Sea Research*, 46(2): 87-97.
- Biro, P., 1970. *Les Régions Naturelles du Globe*. Masson et Cie, Paris, 380 pp.
- Bishop, P. and Cowell, P., 1997. Lithological and drainage network determinants of the character of drowned, embayed coastlines. *Journal of Geology*, 105(6): 685.
- Black, K.P. and Oldman, J.W., 1999. Wave mechanisms responsible for grain sorting and non-uniform ripple distribution across two moderate-energy, sandy continental shelves. *Marine Geology*, 162(1): 121-132.

- Blake, D.H. and Kilgour, B., 1998. Geological Regions (National Geoscience Dataset). 1:5 million scale digital map dataset, Geoscience Australia, Canberra, Australia.
- Blaszczyński, J.S., 1997. Landform characterization with Geographic Information Systems. *Photogrammetric Engineering and Remote Sensing*, 63(2): 183-191.
- BoM, 2007.  
[http://www.bom.gov.au/climate/averages/climatology/tropical\\_cyclones/tropical\\_cycl.shtml](http://www.bom.gov.au/climate/averages/climatology/tropical_cyclones/tropical_cycl.shtml).
- Booij, N., Ris, R.C. and Holthuijsen, L.H., 1999. A third-generation wave model for coastal regions, Part I, Model description and validation. *Journal of Geophysical Research*, 104(C4): 7649-7666.
- Bourg, A.C.M., 1987. Trace metal adsorption modelling and particle-water interactions in estuarine environments. *Continental Shelf Research*, 7: 1319-1332.
- Boyd, R., Dalrymple, R. and Zaitlin, B.A., 1992. Classification of clastic coastal depositional environments. *Sedimentary Geology*, 80(3-4): 139-150.
- Buchanan, C., 1998. 30 arc second gridded bathymetry [CDROM]. Geoscience Australia (formerly AGSO), Canberra, Australia.
- Burbank, D.W., 1992. Causes of Recent Himalayan Uplift Deduced from Deposited Patterns in the Ganges Basin. *Nature*, 357(6380): 680-683.
- Burrough, P.A., 1986. Principles of Geographical Information Systems for Land Resources Assessment. Oxford University Press, New York.
- Butler, A., Harris, P.T., Lyne, V., Heap, A., Passlow, V. and Porter-Smith, R., 2001. An Interim Bioregionalisation for the continental slope and deeper waters of the South-East Marine Region of Australia.
- Cheng, Q.M., Russell, H., Sharpe, D., Kenny, F. and Qin, P., 2001. GIS-based statistical and fractal/multifractal analysis of surface stream patterns in the Oak Ridges Moraine. *Computers & Geosciences*, 27(5): 513-526.
- Chivas, A.R., Garcia, A., van der Kaars, S., Couapel, M.J.J., Holt, S., Reeves, J.M., Wheeler, D.J., Switzer, A.D., Murray-Wallace, C.V., Banerjee, D., Price, D.M., Wang, S.X., Pearson, G., Edgar, N.T., Beaufort, L., De Deckker, P., Lawson, E. and Cecil, C.B., 2001. Sea-level and environmental changes since the last interglacial in the Gulf of Carpentaria, Australia: an overview. *Quaternary International*, 83-5: 19-46.
- Chorley, R.J., 1957. Illustrating the laws of morphometry. *Geological Magazine*, 94(2): 140-150.
- Church, J.A. and Craig, P.D., 1998. Australia's Shelf Seas: Diversity and Complexity. The Sea, 11. John Wiley and Sons, Inc.
- Church, J.A. and Forbes, A.M.G., 1983. Circulation in the Gulf of Carpentaria. I. Direct observations of currents in the south-east corner of the Gulf of Carpentaria. *Australian Journal of Marine and Freshwater Research*, 34: 1-10.
- Church, J.A., Hunter, J.R., McInnes, K.L. and White, N.J., 2006. Sea-level rise around the Australian coastline and the changing frequency of extreme sea-level events. *Australian Meteorological Magazine*, 55(4): 253-260.
- Clarke, K.R. and Ainsworth, M., 1993. A method of linking multivariate community structure to environmental variables. *Marine Ecology-Progress Series*, 92: 205-205.



- Clarke, K.R., Gorley, R.N. and Plymouth Marine, L., 2001. PRIMER V5: User Manual/tutorial. PRIMER-E Ltd.
- Clarke, K.R. and Warwick, R.M., 1994. Change in Marine Communities: an approach to statistical analysis and interpretation, 2nd edition Plymouth.
- Clifton, H.E. and Dingler, J.R., 1984. Wave-formed structures and paleoenvironmental reconstruction. *Marine Geology*, 60(1-4): 165-198.
- Collins, L.B., 1988. Sediments and history of the Rottneest Shelf, southwest Australia: a swell-dominated, non-tropical carbonate margin. *Sedimentary geology*, 60(1-4): 15-49.
- Commonwealth of Australia, 2005. National Marine Bioregionalisation of Australia. Summary, Department of Environment and Heritage, Canberra, Australia.
- Condie, S.A. and Harris, P.T., 2005. Interactions between Physical, Chemical, Biological and Sedimentological Processes in Australia's Shelf Seas. *The Sea*, 14. President and Fellows of Harvard College, Harvard.
- Conolly, J.R. and Von der Borch, C.C., 1967. Sedimentation and physiography of the sea floor south of Australia. *Sedimentary Geology*, 1: 181-220.
- Cook, P.J. and Mayo, W., 1978. Sedimentology and Holocene history of a tropical estuary, Broad Sound, Queensland: Australian Bureau of Mineral Resources. *Bulletin*, 170: 206.
- Cox, K.G., 1989. The Role of Mantle Plumes in the Development of Continental Drainage Patterns. *Nature*, 342(6252): 873-877.
- Crawley, M.J., 2005. *Statistics: An Introduction using R*. John Wiley & Sons, Chichester, West Sussex, England.
- CSIRO, 1996. Interim marine bioregionalisation for Australia: Towards a national system of marine protected areas. Lyne, V. and Last, P. (eds.). CSIRO Division of Fisheries and CSIRO Division of Oceanography. Report to ERIN as part of the Ocean Rescue 2000 Program. CSIRO Marine Laboratories, Hobart.
- D'Alessandro, L., De Pippo, T., Donadio, C., Mazzarella, A. and Miccadei, E., 2006. Fractal dimension in Italy: a geomorphological key to interpretation. *Zeitschrift Fur Geomorphologie*, 50(4): 479-499.
- Dalrymple, R.W., Zaitlin, B.A. and Boyd, R., 1992. Estuarine facies models; conceptual basis and stratigraphic implications. *Journal of Sedimentary Research*, 62(6): 1130.
- Davidson, J.P., Reed, W.E. and Davis, P.M., 2002. *Exploring Earth: An Introduction to Physical Geology*. Prentice-Hall Inc, Upper Saddle River, NJ.
- Davies, P.J., 1979. Marine geology of the continental shelf off southeast Australia. *Bureau of Mineral Resources Bulletin*, 195: 51.
- Davis, R.A. and FitzGerald, D., 2004. *Beaches and Coasts*. Blackwell Publishing, Malden (MA)/Oxford/Victoria (Australia).
- Dean, R.G. and Dalrymple, R.A., 1990. *Water Wave Mechanics for Engineers and Scientists*. Singapore: World Scientific Publishing Co., Englewood Cliffs.

- Dickson, M.E. and Woodroffe, C.D., 2005. Rock coast morphology in relation to lithology and wave exposure, Lord Howe Island, southwest Pacific. *Zeitschrift Fur Geomorphologie*, 49(2): 239-251.
- Duckham, M. and Drummond, J., 2000. Assessment of error in digital vector data using fractal geometry. *International Journal of Geographical Information Science*, 14(1): 67-84.
- Dunne, T., 1980. Formation and controls of channel networks. *Progress in Physical Geography*, 4(2): 211 - 239.
- Durr, H.H., Meybeck, M. and Durr, S.H., 2005. Lithologic composition of the Earth's continental surfaces derived from a new digital map emphasizing riverine material transfer. *Global Biogeochemical Cycles*, 19(4).
- Easton, A.K., 1970. The tides of the continent of Australia. Research Report., Horace Lamb Centre for Oceanographic Research, Flinders University, South Australia, South Australia.
- Egbert, G.D., Bennett, A.F. and Foreman, M.G.G., 1994. TOPEX/POSEIDON tides estimated using a global inverse model. *J. Geophys. Res.*, 99(24): 821–24.
- ESRI, 1996. ARC/INFO Unix Version 7. Esri Inc, Redlands, California.
- Ewing, J., Le Pichon, X. and Ewing, M., 1963. Upper stratification of Hudson Apron region. *Journal of Geophysical Research*, 68: 6303–6316.
- Exon, N.F., Hill, P.J., Mitchell, C. and Post, A., 2005. Nature and origin of the submarine Albany canyons off southwest Australia. *Australian Journal of Earth Sciences*, 52(1): 101-115.
- Fairbridge, R.W., 1966. The Encyclopedia of Oceanography. Encyclopedia of earth sciences series.
- Fairbridge, R.W., 2004. Classification of coasts. *Journal of Coastal Research*, 20(1): 155-165.
- Finkl, C.W., 2004. Coastal classification: Systematic approaches to consider in the development of a comprehensive scheme. *Journal of Coastal Research*, 20(1): 166-213.
- Freeland, H.J., Boland, F.M., Church, J.A., Clarke, A.J., Forbes, A.M.G., Huyer, A., Smith, R.L., Thompson, R. and White, N.J., 1986. The Australian Coastal Experiment: A Search for Coastal-Trapped Waves. *Journal of Physical Oceanography*, 16(7): 1230-1249.
- Gagan, M.K., Chivas, A.R. and Herczeg, A.L., 1990. Shelf-wide erosion, deposition, and suspended sediment transport during Cyclone Winifred, central Great Barrier Reef, Australia. *Journal of Sedimentary Research*, 60(3): 456-470.
- Gage, J.D. and Tyler, P.A., 1991. *Deep-Sea Biology: A Natural History of Organisms at the Deep-Sea Floor*. Cambridge University Press.
- Gao, J. and Xia, Z.G., 1996. Fractals in physical geography. *Progress in Physical Geography*, 20(2): 178-191.
- García, M., Alonso, B., Ercilla, G. and Gràcia, E., 2006. The tributary valley systems of the Almeria Canyon (Alboran Sea, SW Mediterranean): Sedimentary architecture. *Marine Geology*, 226(3-4): 207-223.

- Gardner, J.V., Dartnell, P., Mayer, L.A. and Clarke, J.E.H., 2003. Geomorphology, acoustic backscatter, and processes in Santa Monica Bay from multibeam mapping. *Marine Environmental Research*, 56(1-2): 15-46.
- Geoscience Australia, 2004. GEODATA Coast 100k. Geoscience Australia, Canberra, ACT.
- Geoscience Australia, 2008. GEODATA 9 Second DEM and D8 Digital Elevation Model Version 3 and Flow Direction Grid. User Guide, Fenner school of Environment an Society, ANU and Geoscience Australia, Canberra, Australia.
- Goff, J.A., 2001. Quantitative classification of canyon systems on continental slopes and a possible relationship to slope curvature. *Geophysical Research Letters*, 28(23): 4359-4362.
- Goodchild, M., 1980. Fractals and the accuracy of geographical measures. *Mathematical Geology*, 12(2): 85-98.
- Goodchild, M.F. and Mark, D.M., 1987. The fractal nature of geographic phenomena. *Annals of the Association of American Geographers*, 77(265).
- Gordon, A.D. and Hoffman, J.G., 1986. Sediment features and processes of the Sydney continental shelf. *Recent Sediments in Eastern Australia: Marine Through Terrestrial*. Geological Society of Australia (NSW Division), Sydney: 29–51.
- Grant, W.D. and Madsen, O.S., 1979. Combined wave and current interaction with a rough bottom. *Journal of Geophysical Research*, 84(C4): 1797-1808.
- Grant, W.D. and Madsen, O.S., 1986. The Continental-Shelf Bottom Boundary Layer. *Annual Reviews in Fluid Mechanics*, 18(1): 265-305.
- Gray, J.S., 1981. The ecology of marine sediments. *Cambridge studies in modern biology* 2. Cambridge University Press, Cambridge, pp. 185.
- Green, A.N., Goff, J.A. and Uken, R., 2007. Geomorphological evidence for upslope canyon-forming processes on the northern KwaZulu-Natal shelf, SW Indian Ocean, South Africa. *Geo-Marine Letters*, 27: 399-409.
- Greenslade, D.J.M., 2001. The assimilation of ERS-2 significant wave height data in the Australian region. *Journal of Marine Systems*, 28(1-2): 141-160.
- Griffin, J.D., Hemer, M.A. and Jones, B.G., 2008. Mobility of sediment grain size distributions on a wave dominated continental shelf, southeastern Australia. *Marine Geology*, 252(1-2): 13-23.
- Gross, G.M., 1972. *Oceanography: A View of the Earth*. Prentice-Hall, Inc, Englewood Cliffs.
- Hack, J.T., 1957. Studies of longitudinal stream profiles in Virginia and Maryland. U.S. Geol. Survey Prof. Paper, 294-B: 45–97.
- Hagen, R.A., Vergara, H. and Naar, D.F., 1996. Morphology of San Antonio submarine canyon on the central Chile forearc. *Marine Geology*, 129(3-4): 197-205.
- Hammond, T.M. and Collins, M.B., 1979. On the threshold of transport of sand-sized sediment under the combined influence of unidirectional and oscillatory flow. *Sedimentology*, 26(6): 795-812.

- Harbison, P., 1984. Regional Variation in the Distribution of Trace Metals in Modern Intertidal Sediments of Northern Spencer Gulf, South Australia. *Marine Geology*, 61(2/4).
- Hardisty, J., 1994. Beach and nearshore sediment transport. *Sediment Transport and Depositional Processes*. Oxford: Blackwell Scientific Publications: 219–255.
- Harris, P.T., 1994. Comparison of tropical, carbonate and temperate, siliciclastic tidally dominated sedimentary deposits: Examples from the Australian continental shelf. *Australian Journal of Earth Sciences*, 41(3): 241–254.
- Harris, P.T., 1995. Marine geology and sedimentology of the Australian continental shelf. *The State of the Marine Environment Report for Australia, Technical Annex*, 1: 11–23.
- Harris, P.T. and Baker, E.K., 1991. The nature of sediments forming the Torres Strait turbidity maximum. *Australian Journal of Earth Sciences*, 38(1): 65–78.
- Harris, P.T., Baker, E.K., Cole, A.R. and Short, S.A., 1993. A preliminary study of sedimentation in the tidally dominated Fly River Delta. *Gulf of Papua: Continental Shelf Research*, 13: 441–472.
- Harris, P.T. and Coleman, R., 1998. Estimating global shelf sediment mobility due to swell waves. *Marine Geology*, 150(1–4): 171–177.
- Harris, P.T., Heap, A.D., Bryce, S.M., Porter-Smith, R., Ryan, D.A. and Heggie, D.T., 2002. Classification of Australian clastic coastal depositional environments based upon a quantitative analysis of wave, tidal, and river power. *Journal of Sedimentary Research*, 72(6): 858–870.
- Harris, P.T., Pattiaratchi, C.B., Collins, M.B. and Dalrymple, R.W., 1995. What is bedload parting? In: B.W. Flemming and A. Bartholoma (Editors), *Tidal Signatures in Modern and Ancient Environments*. International Association of Sedimentologists Special Publication, pp. 1–16.
- Harris, P.T., Porter-Smith, R., Heggie, D., A.D., H., Bryce, S. and Ryan, D., 2000. Classification of Australian estuaries based on wave, tide and river energy regime, *Third International River Management Symposium*, Brisbane, Queensland, Australia, pp. 33.
- Harris, P.T., Tsuji, Y., Marshall, J.F., Davies, P.J., Honda, N. and Matsuda, H., 1996. Sand and rhodolith-gravel entrainment on the mid-to outer-shelf under a western boundary current: Fraser Island continental shelf, eastern Australia. *Marine Geology*, 129(3): 313–330.
- Hasselmann, S., Hasselmann, K., Bauer, E., Janssen, P., Komen, G.J., Bertotti, L., Lionello, P., Guillaume, A., Cardone, V.C. and Greenwood, J.A., 1988. The WAM model—A third generation ocean wave prediction model. *Journal of Physical Oceanography*, 18(12): 1775–1810.
- Heap, A.D., 2000. Composition and Dynamics of Holocene Sediment next to the Whitsunday Islands on the Middle Shelf of the Great Barrier Reef Platform, Australia. Unpublished PhD Thesis, James Cook University of North Queensland, 158.
- Heap, A.D. and Harris, P.T., 2008. Geomorphology of the Australian margin and adjacent seafloor. *Australian Journal of Earth Sciences* 55: 555–585.



- Hearn, C.J. and Holloway, P.E., 1990. A Three-Dimensional Barotropic Model of the Response of the Australian North West Shelf to Tropical Cyclones. *Journal of Physical Oceanography*, 20(1): 60-80.
- Hedgepeth, J.W. (Editor), 1957. *Treatise on marine ecology and paleoecology*. Ecology, vol 1. Geological Society of America, New York.
- Heezen, B.C. and Ewing, W.M., 1952. Turbidity currents and submarine slumps, and the 1929 Grand Banks [Newfoundland] earthquake. *American Journal of Science*, 250(12): 849.
- Hemer, M.A., 2006. The magnitude and frequency of combined flow bed shear stress as a measure of exposure on the Australian continental shelf. *Continental Shelf Research*, 26(11): 1258-1280.
- Hemer, M.A., Hunter, J.R. and Coleman, R., 2006. Barotropic tides beneath the Amery Ice Shelf. *Journal of Geophysical Research-Oceans*, 111(C11).
- Herzfeld, U.C., 2008. Master of the obscure - Automated geostatistical classification in presence of complex geophysical processes. *Mathematical Geosciences*, 40(5): 587-618.
- Hess, G.R. and Normark, W.R., 1976. Holocene Sedimentation History of Major Fan Valleys of Monterey Fan. *Marine Geology*, 22(4): 233-251.
- Hesse, R., 1989. Drainage Systems Associated with Mid-Ocean Channels and Submarine Yazoos - Alternative to Submarine Fan Depositional Systems. *Geology*, 17(12): 1148-1151.
- Hill, P.J., De Deckker, P. and Exon, N.F., 2005. Geomorphology and evolution of the gigantic Murray canyons on the Australian southern margin. *Australian Journal of Earth Sciences*, 52(1): 117-136.
- Hillis, R.R. and Müller, R.D., 2003. *Evolution and Dynamics of the Australian Plate*. Geological Society of America.
- Holdgate, G.R., Wallace, M.W., Gallagher, S.J., Smith, A.J., Keene, J.B., Moore, D. and Shafik, S., 2003. Plio-Pleistocene tectonics and eustasy in the Gippsland Basin, southeast Australia: evidence from magnetic imagery and marine geological data. *Australian Journal of Earth Sciences*, 50(3): 403-426.
- Holthuijsen, L.H., 2007. *Waves in oceanic and coastal waters*. Cambridge University Press, Cambridge, UK, 387 pp.
- Hopkins, B.M., 1966. Submarine canyons. *BHP tech. Bull*, 26: 39-43.
- Horton, R.E., 1945. Erosional Development of Streams and Their Drainage Basins - Hydrophysical Approach to Quantitative Morphology. *Geological Society of America Bulletin*, 56(3): 275-370.
- Howard, A.D., 1980. Thresholds in river regimes. In: D.R. Coates and J.D. Vitek (Editors), *Thresholds in Geomorphology*. Allen and Unwin, Boston, pp. 227-258.
- Hughes, M.G. and Heap, A.D., 2010. National-scale wave energy resource assessment for Australia. *Renewable Energy*, 35(8): 1783-1791.
- Hutchinson, M.F. and Dowling, T.I., 1991. A Continental Hydrological Assessment of a New Grid-Based Digital Elevation Model of Australia. *Hydrological Processes*, 5(1): 45.

- Huyghe, P., Foata, M., Deville, E. and Mascle, G., 2004. Channel profiles through the active thrust front of the southern Barbados prism. *Geology*, 32(5): 429-432.
- Ihaka, R. and Gentleman, R., 1996. R: A Language for Data Analysis and Graphics. *Journal of Computational and Graphical Statistics*, 5(3): 299-314.
- IMCRA, 1998. Interim Marine and Coastal Regionalisation for Australia: an ecosystem-based classification for marine and coastal environments. Interim Marine and Coastal Regionalisation for Australia., Version 3.3.
- Inman, D.L., 1994. Turbidity currents in submarine canyons and the littoral drift of sand; the effect of changing wave climate. *EOS*, 75: 203.
- James, N.P., Bone, Y., Borch, C.C. and Gostin, V.A., 1992. Modern carbonate and terrigenous clastic sediments on a cool water, high energy, mid-latitude shelf: Lacepede, southern Australia. *Sedimentology*, 39(5): 877-903.
- Jenkins, C.J., 2000. Generation of seafloor sediment griddings for the UTAS-AGSO shelf sediment mobility project. University of Sydney Ocean Science Institute, Report, 89: 1-12.
- Jenson, S.K. and Domingue, J.O., 1988. Extracting Topographic Structure from Digital Elevation Data for Geographic Information System Analysis. *Photogrammetric Engineering and Remote Sensing*, 54(11): 1593-1600.
- Jiang, J.W. and Plotnick, R.E., 1998. Fractal analysis of the complexity of United States coastlines. *Mathematical Geology*, 30(5): 535-546.
- Johnson, D.P., Searle, D.E. and Hopley, D., 1982. Positive relief over buried post-glacial channels, Great Barrier Reef Province, Australia. *Marine Geology*, 46: 149-159.
- Jones, H.A., 1973. Marine Geology of the Northwest Australian Continental Shelf. Bulletin 136, Bureau of Mineral Resources, Canberra.
- Jones, H.A. and Davies, P.J., 1983. Superficial sediments of the Tasmanian continental shelf and part of Bass Strait. *Bureau of Mineral Resources Bulletin*, 218: 1-25.
- Jones, H.A. and Kudrass, H.R., 1982. Sonne cruise (SO-15 1980) off the east coast of Australia bathymetry and seafloor morphology. *Geologisches Jahrbuch, Reihe D, Mineralogie, Petrologie, Geochemie, Lagerstättenkunde*, 56: 55-68.
- Kailola, P.J., Williams, M.J., Stewart, P.C., Reichelt, R.E., McNee, A. and Grieve, C., 1993. Australian Fisheries Resources. Bureau of Resource Sciences, Department of Primary Industries and Energy. Fisheries Research and Development Corporation, Canberra, Australia, 422.
- Kantha, L.H., 1995. Barotropic tides in the global oceans from a nonlinear tidal model assimilating altimetric tides. 1. Model description and results. *J. Geophys. Res.*, 100(25): 283-25.
- Keller, G.H. and Shepard, F.P. (Editors), 1978. Currents and sedimentary processes in submarine canyons off the northeast United States. *Sedimentation in Submarine Canyons, Fans, and Trenches*. Dowden, Hutchinson & Ross Inc., Stroudsburg, PA, 15-31 pp.
- Kendall, M.G., 1970. Rank correlation methods. Griffin, London.

- Kenyon, N.H., Klaucke, I., Millington, J. and Ivanov, M.K., 2002. Sandy submarine canyon-mouth lobes on the western margin of Corsica and Sardinia, Mediterranean Sea. *Marine Geology*, 184(1-2): 69-84.
- Khripounoff, A., Vangriesheim, A., Babonneau, N., Crassous, P., Dennielou, B. and Savoye, B., 2003. Direct observation of intense turbidity current activity in the Zaire submarine valley at 4000 m water depth. *Marine Geology*, 194(3-4): 151-158.
- Klinkenberg, B. and Goodchild, M.F., 1992. The Fractal Properties of Topography - a Comparison of Methods. *Earth Surface Processes and Landforms*, 17(3): 217-234.
- Kloser, R.J., Bax, N.J., Ryan, T., Williams, A. and Barker, B.A., 2001. Remote sensing of seabed types in the Australian South East Fishery-development and application of normal incident acoustic techniques and associated 'ground truthing'. *Marine and Freshwater Research*, 52(4): 475-89.
- Kloser, R.J., Williams, A. and Butler, A.J., 2007. Exploratory Surveys of Seabed Habitats in Australia's Deep Ocean using Remote Sensing – Needs and Realities. In: B.J. Todd and H.G. Greene (Editors), *Mapping the Seafloor for Habitat Characterization*. Geological Association of Canada, pp. 93-110.
- Komar, P.D. and Miller, M.C., 1973. The threshold of sediment movement under oscillatory water waves. *Journal of Sedimentary Research*, 43(4): 1101-1110.
- Komen, G.J., Cavaleri, L., Donelan, M., Hasselmann, K., Hasselmann, S. and Janssen, P., 1996. *Dynamics and Modelling of Ocean Waves*. Dynamics. Cambridge University Press, Cambridge.
- Kostylev, V.E., Todd, B.J., Fader, G.B.J., Courtney, R.C., Cameron, G.D.M. and Pickrill, R.A., 2001. Benthic habitat mapping on the Scotian Shelf based on multibeam bathymetry, surficial geology and sea floor photographs. *Marine Ecology-Progress Series*, 219: 121-137.
- Kudrass, H.R., Michels, K.H., Wiedicke, M. and Suckow, A., 1998. Cyclones and tides as feeders of a submarine canyon off Bangladesh. *Geology*, 26(8): 715-718.
- Lam, N.S. and Quattrochi, A.A., 1992. On the issue of scale, resolution, and fractal analysis in the mapping sciences. *The Professional Geographer*, 44: 88-98.
- Langford-Smith, T. and Thom, B.G., 1969. New South Wales coastal morphology. *Jour. Geol. Soc*, 16: 572-580.
- Last, P.R., Lyne, V.D., Williams, A., Davies, C.R., Butler, A.J. and Yearsley, G.K., 2010. A hierarchical framework for classifying seabed biodiversity with application to planning and managing Australia's marine biological resources. *Biological Conservation*, 143.
- Last, P.R., Lyne, V.D., Yearsley, G., Gledhill, D., Gomon, M., Rees, T. and White, W., 2005. Validation of national demersal fish datasets for the regionalisation of the Australian continental slope and outer shelf (> 40 m depth), National Oceans Office, Hobart, Tasmania.
- Lewis, K.B. and Barnes, P.L., 1999. Kaikoura Canyon, New Zealand: active conduit from near-shore sediment zones to trench-axis channel. *Marine Geology*, 162(1): 39-69.
- Long, B.G., Poiner, I.R. and Wassenberg, T.J., 1995. Distribution, biomass and community structure of megabenthos of the Gulf of Carpentaria, Australia. *Marine Ecology Progress Series*, 129(1): 127-139.

- Longhurst, A., 1998. Ecological geography of the sea. Academic Press, San Diego, CA, USA.
- Louis, J.P. and Radok, J.R.M., 1975. Propagation of tidal waves in the Joseph Bonaparte Gulf. *Journal of Geophysical Research*, 80(C12): 1689-1690.
- Lourensz, R.S., 1981. Tropical Cyclones in the Australian Region July 1909 to June 1980. Australian Government Printing Service, Canberra, 94.
- Ludwig, W., Probst, J.L. and Kempe, S., 1996. Predicting the oceanic input of organic carbon by continental erosion. *Global Biogeochemical Cycles*, 10(1): 23–41.
- Lyne, V.D., Butman, B. and Grant, W.D., 1990. Sediment Movement Along the United-States East Coast Continental-Shelf .1. Estimates of Bottom Stress Using the Grant-Madsen Model and near-Bottom Wave and Current Measurements. *Continental Shelf Research*, 10(5): 397-428.
- Lyne, V.D., Last, P.R., Scott, R., Dunn, J.R., Peters, D. and Ward, T., 1998. Large Marine Domains of Australia's EEZ: Report commission by Environment Australia, CSIRO Marine Research and Department of Environment & Land Management, Hobart, Tasmania.
- Lyne, V.D., White, W.T., Gledhill, D., Last, P.R., Rees, T. and Porter-Smith, R., 2009. Analysis of Australian continental shelf provinces and biomes based on fish data, CSIRO Marine & Atmospheric Research, Hobart.
- Madsen, O.S., 1994. Spectral wave-current bottom boundary layer flows, Proceedings of the 24th International Conference on Coastal Engineering. Coastal Engineering Research Council/ASCE, Kobe, Japan, pp. 384-398.
- Mandelbrot, B., 1967. How long is the coast of Britain? Statistical self-similarity and fractional dimension. *Science*, 156: 636-638.
- Mark, D.M., 1983. Automatic detection of drainage networks from digital elevation models. *Cartographica*, 21: 168 - 178.
- Mark, D.M., 1988. Network models in geomorphology. In: M.G. Anderson (Editor), *Modeling Geomorphological Systems*. John Wiley & Sons, New York, pp. 73-96.
- Mark, D.M. and Aronson, P.B., 1984. Scale-dependent fractal dimensions of topographic surfaces: an empirical investigation with applications in geomorphology and computer mapping. *Mathematical Geology*, 16: 671-83.
- Marshall, W.B., 1979. *Developments in Deep-Sea Biology*. Blanford Press, Dorset, U.K.
- Martz, L.W. and Garbrecht, J., 1992. Numerical definition of drainage network and subcatchment areas from digital elevation models. *Computers & Geosciences*, 18: 747-761.
- Martz, L.W. and Garbrecht, J., 1998. The treatment of flat areas and depressions in automated drainage analysis of raster digital elevation models. *Hydrological Processes*, 12(6): 843.
- McDonald, J.H., 2009. *Handbook of Biological Statistics*. Sparky House Publishing, Delaware.
- McMillan, J.D., 1981. Global Atlas of GEOS-3 Significant Waveheight and Comparison of the Data With National Buoy Data. *Dissertation Abstracts International Part B: Science and Engineering*[DISS. ABST. INT. PT. B- SCI. & ENG.], 42(3): 1981.

- Menard, H.W., 1955. Deep-sea channels, topography, and sedimentation. *AAPG Bulletin*, 39(2): 236-255.
- Meybeck, M., Durr, H.H. and Vorosmarty, C.J., 2006. Global coastal segmentation and its river catchment contributors: A new look at land-ocean linkage. *Global Biogeochemical Cycles*, 20(1).
- Michels, K.H., Kudrass, H.R., Hubscher, C., Suckow, A. and Wiedicke, M., 1998. The submarine delta of the Ganges-Brahmaputra: cyclone-dominated sedimentation patterns. *Marine Geology*, 149(1-4): 133-154.
- Miller, M.C., McCave, I.N. and Komar, P.D., 1977. Threshold of sediment motion under unidirectional currents. *Sedimentology*, 24(4): 507-527.
- Mitchell, J.K., Holdgate, G.R. and Wallace, M.W., 2007a. Pliocene-Pleistocene history of the Gippsland Basin outer shelf and canyon heads, southeast Australia. *Australian Journal of Earth Sciences*, 54(1): 49-64.
- Mitchell, J.K., Holdgate, G.R., Wallace, M.W. and Gallagher, S.J., 2007b. Marine geology of the quaternary bass canyon system, southeast Australia: a cool-water carbonate system. *Marine Geology*, 237(1-2): 71-96.
- Mitchell, N.C., 2005. Interpreting long-profiles of canyons in the USA Atlantic continental slope. *Marine Geology*, 214(1-3): 75-99.
- Montgomery, D.R. and Dietrich, W.E., 1988. Where do channels begin? *Nature*, 336(6196): 232-234.
- Morisawa, M.E., 1962. Quantitative Geomorphology of Some Watersheds in the Appalachian Plateau. *Geological Society of America Bulletin*, 73(9): 1025-1046.
- O'Callaghan, J.F. and Mark, D.M., 1984. The Extraction of Drainage Networks from Digital Elevation Data. *Computer Vision Graphics and Image Processing*, 28(3): 323-344.
- O'Grady, D.B., Syvitski, J.P.M., Pratson, L.F. and Sarg, J.F., 2000. Categorizing the morphologic variability of siliciclastic passive continental margins. *Geology*, 28(3): 207-210.
- Ollier, C.D., 1981. *Tectonics and Landforms*. Longman, Reading, 324 pp.
- Passlow, V., Rogis, J., Hancock, A., Hemer, M., Glenn, K.C. and Habib, A., 2005. Final Report, National Marine Sediments Database and Seafloor Characteristics Project: Record 2005/08, Geoscience Australia, Canberra.
- Pattiaratchi, C.B. and Collins, M.B., 1985. Sand transport under the combined influence of waves and tidal currents: an assessment of available formulae. *Marine Geology*, 67(1-2): 83-100.
- Pearce, A.F. and Pattiaratchi, C.B., 1997. Applications of satellite remote sensing to the marine environment in Western Australia. *Journal of the Royal Society of Western Australia*, 80: 1-14.
- Pentland, A., 1984. Fractal-based description of natural scenes. *IEEE Transactions on Pattern Analysis and Machine Intelligence*, PAMI-6: 661-674.
- Petkovic, P. and Buchanan, C., 2002. Australian bathymetry and topography grid. [CDROM], Geoscience Australia, Canberra, Australia.

- Phillips, D.M. and Scholz, M.L., 1982. Measured distribution of water turbidity in Gulf St Vincent. *Australian Journal of Marine and Freshwater Research*, 33(5): 723-727.
- Phillips, J.D., 1986. Spatial-Analysis of Shoreline Erosion, Delaware Bay, New-Jersey. *Annals of the Association of American Geographers*, 76(1): 50-62.
- Pinet, P.R., 1996. *Invitation to Oceanography*. West Publishing Co, St. Paul, MN.
- Pingree, R.D. and Griffiths, D.K., 1979. Sand transport paths around the British Isles resulting from M 2 and M 4 tidal interactions. *Journal of the Marine Biological Association UK*, 59: 497-514.
- Plumb, K.A., 1979. Tectonic Evolution of Australia. *Earth-Science Reviews*, 14(3): 205-249.
- Poiner, I.R. and Kennedy, R., 1984. Complex patterns of change in the macrobenthos of a large sandbank following dredging. *Marine Biology*, 78(3): 335-352.
- Porter-Smith, R., Harris, P.T., Andersen, O.B., Coleman, R., Greenslade, D. and Jenkins, C.J., 2004. Classification of the Australian continental shelf based on predicted sediment threshold exceedance from tidal currents and swell waves. *Marine Geology*, 211(1-2): 1-20.
- Pratson, L.F. and Coakley, B.J., 1996. A model for the headward erosion of submarine canyons induced by downslope-eroding sediment flows. *Bulletin of the Geological Society of America*, 108(2): 225-234.
- Pratson, L.F. and Ryan, W.B.F., 1996. Automated drainage extraction in mapping the Monterey submarine drainage system, California margin. *Marine Geophysical Researches*, 18(6): 757-777.
- Pratson, L.F., Ryan, W.B.F., Mountain, G.S. and Twichell, D.C., 1994. Submarine canyon initiation by downslope-eroding sediment flows; evidence in late Cenozoic strata on the New Jersey continental slope. *Bulletin of the Geological Society of America*, 106(3): 395-412.
- Press, F. and Siever, R., 1986. *Earth* (4th edn). WH Freeman and Co., New York.
- Puig, P., Ogston, A.S., Mullenbach, B.L., Nittrouer, C.A. and Sternberg, R.W., 2003. Shelf-to-canyon sediment-transport processes on the Eel continental margin(northern California). *Marine Geology*, 193(1): 129-149.
- R Development Core Team, 2004. *R: A language and environment for statistical computing* R Foundation for Statistical Computing, Vienna, Austria.
- Riley, S.J., DeGloria, S.D. and Elliot, R., 1999. A terrain ruggedness index that quantifies topographic heterogeneity. *Intermountain Journal of Sciences*, 5(1-4): 23-27.
- Ringrose, P.S., 1994. Structural and Lithological Controls on Coastline Profiles in Fife, Eastern Britain. *Terra Nova*, 6(3): 251-254.
- Ritter, D.F., 1986. *Process Geomorphology* Wm. C. Brown, Dubuque, Iowa.
- Sapoval, B., Baldassarri, A. and Gabrielli, A., 2004. Self-stabilized fractality of seacoasts through damped erosion. *Physical Review Letters*, 93(9).
- Scheibner, E., 1976. *Explanatory Notes on the Tectonic Map of New South Wales*. Geological Survey of New South Wales.

- Scheidegger, A.E., 1983. Instability principle in geomorphic equilibrium. *Zeitschrift Fur Geomorphologie*, 27: 1-19.
- Schlee, J.S. and Robb, J.M., 1991. Submarine Processes of the Middle Atlantic Continental Rise Based on Gloria Imagery. *Geological Society of America Bulletin*, 103(8): 1090-1103.
- Schumm, S.A., 1956. Evolution of Drainage Systems and Slopes in Badlands at Perth-Amboy, New-Jersey. *Geological Society of America Bulletin*, 67(5): 597-&.
- Semeniuk, V., 1982. Geomorphology and Holocene history of the tidal flats, King Sound, north-western Australia. *Journal of the Royal Society of Western Australia*, 65(2): 47-68.
- Shannon, C.E., 1948. A Mathematical Theory of Communication. *Bell System Technical Journal*, 27(3): 379-423.
- Shannon, C.E. and Weaver, W., 1949. *The Mathematical Theory of Communication*. University of Illinois Press, Urbana.
- Shaw, R.D., Yeates, A.N., Palfreyman, D. and Douth, H.F., 1999. *Geology of Australia*. Australian Geological Survey Organisation, Canberra.
- Shepard, F.P. and Dill, R.F., 1966. *Submarine canyons and other sea valleys*. Rand McNally & Company, Chicago.
- Shepherd, S.A., 1983. Benthic communities of upper Spencer Gulf, South Australia. *Transactions of the Royal Society of South Australia*, 107(1): 69-85.
- Short, A.D. and Woodroffe, C.D., 2009. *The Coast of Australia*. Cambridge University Press, Melbourne, Australia.
- Shum, C.K., Woodworth, P.L., Andersen, O.B., Egbert, G.D., Francis, O., King, C., Klosko, S.M., Le Provost, C., Li, X. and Molines, J.M., 1997. Accuracy assessment of recent ocean tide models. *Journal of Geophysical Research*, 102(C 11): 25173-25194.
- Silverman, B.W., 1986. *Density Estimation for Statistics and Data Analysis*. Chapman and Hall, New York.
- Smith, W.H.F. and Sandwell, D.T., 1997. Global Sea Floor Topography from Satellite Altimetry and Ship Depth Soundings. *Science*, 277(5334): 1956.
- Somers, I.F., 1987. Sediment type as a factor in the distribution of commercial prawn species in the western Gulf of Carpentaria, Australia. *AUST. J. MAR. FRESHWAT. RES.*, 38(1): 133-149.
- Sprigg, R.C., 1947. Submarine canyons of the New Guinea and South Australian coasts. *Transactions of the Royal Society of South Australia*, 71: 296-310.
- Steffens, G.S., Biegert, E.K., Sumner, H.S. and Bird, D., 2003. Quantitative bathymetric analyses of selected deepwater siliciclastic margins: receiving basin configurations for deepwater fan systems. *Marine and Petroleum Geology*, 20(6-8): 547-561.
- Strahler, A.N., 1952. Hypsometric (Area-Altitude) Analysis of Erosional Topography. *Geological Society of America Bulletin*, 63(11): 1117-&.
- Straub, K.M., Jerolmack, D.J., Mohrig, D. and Rothman, D.H., 2007. Channel network scaling laws in submarine basins. *Geophysical Research Letters*, 34(12).

- Summerfield, M.A., 1991a. *Global Geomorphology: An Introduction to the Study of Landforms*. Longman Scientific & Technical; Wiley, New York.
- Summerfield, M.A., 1991b. *Global Geomorphology: An Introduction to the Study of Landforms*. Longman, New York, 515 pp.
- Summerfield, M.A., 2000. *Geomorphology and Global Tectonics*. John Wiley, Hoboken, New Jersey.
- Sunamura, T., 1992. *Geomorphology of Rocky Coasts*. John Wiley & Sons, Chichester.
- Swift, D.J.P., Han, G. and Vincent, C.E., 1986. Fluid processes and sea-floor response on a modern storm-dominated shelf: middle Atlantic Shelf of North America. Part 1: The storm-current regime. *Shelf Sands and Sandstones: Canadian Society of Petroleum Geologists, Memoir*, 11: 99–119.
- Swift, D.J.P., Stanley, D.J. and Curray, J.R., 1971. Relict sediments on continental shelves: a reconsideration. *J. Geol.*, 79: 322–346.
- Swift, D.J.P. and Thorne, J.A., 1991. Sedimentation on continental margins, I: a general model for shelf sedimentation. *Shelf Sand and Sandstone Bodies: International Association of Sedimentologists, Special Publication*, 14: 3–31.
- Tarboton, D.G., Bras, R.L. and Rodrigueziturbe, I., 1991. On the Extraction of Channel Networks from Digital Elevation Data. *Hydrological Processes*, 5(1): 81–100.
- Todd, B.J., Kostylev, V.E., Fader, G.B.J., Courtney, R.C. and Pickrill, R.A., 2000. New approaches to benthic habitat mapping integrating multibeam bathymetry and backscatter, surficial geology and seafloor photographs: a case study from the Scotian Shelf, Atlantic Canada, ICES 2000 Annual Science Conference, Bruges, Belgium.
- Tribe, A., 1992. Automated recognition of valley lines and drainage networks from digital elevation models: a review and a new method. *Journal of Hydrology*, 139: 263–293.
- Turcotte, D.L., 2007. Self-organized complexity in geomorphology: Observations and models. *Geomorphology*, 91(3–4): 302–310.
- Turcotte, R., Fortin, J.P., Rousseau, A.N., Massicotte, S. and Villeneuve, J.P., 2001. Determination of the drainage structure of a watershed using a digital elevation model and a digital river and lake network. *Journal of Hydrology*, 240(3–4): 225–242.
- Twichell, D.C., Knebel, H.J. and Folger, D.W., 1977. Delaware River: Evidence for Its Former Extension to Wilmington Submarine Canyon. *Science*, 195(4277): 483–485.
- Twichell, D.C. and Roberts, D.G., 1982. Morphology, Distribution, and Development of Submarine Canyons on the United-States Atlantic Continental-Slope between Hudson and Baltimore Canyons. *Geology*, 10(8): 408–412.
- Veatch, A.C. and Smith, P.A., 1939. Atlantic submarine valleys of the United States and the Congo submarine valley: *Geol. Soc. America Spec. Paper*, 7: 101.
- Vincent, C.E., 1986. Processes affecting sand transport on a storm-dominated shelf. *Shelf sands and sandstones: Canadian Society of Petroleum Geologists Memoir II*: 121–132.
- Walker, R.G., 1984. Shelf and shallow marine sands. In: R.G. Walker (Editor), *Facies Models*. Geological Association of Canada, Toronto, pp. 141–170.



- Whitlow, J., 1984. Dictionary of Physical Geography. Penguin Books, London.
- Williams, A. and Bax, N.J., 2001. Delineating fish-habitat associations for spatially based management: an example from the south-eastern Australian continental shelf. *Marine and Freshwater Research*, 52(4): 513-536.
- Williams, A., Bax, N.J., Kloser, R.J., Althaus, F., Barker, B. and Keith, G., 2008. Australia's deep-water reserve network: implications of false homogeneity for classifying abiotic surrogates of biodiversity. *ICES Journal of Marine Science*.
- Wolanski, E.J., 1985. Some Properties of Waves at the Queensland Shelf Break, 7th Aust. Conf. Coastal and Ocean Eng.. Inst. Eng. Aust, Christchurch, N.Z., pp. 61-70.
- Wright, J.B., 1985. Geology and mineral resources of West Africa. Unwin Hyman.
- Xu, J.P., Noble, M.A. and Rosenfeld, L.K., 2004. In-situ measurements of velocity structure within turbidity currents. *Geophysical Research Letters*, 31(9).
- Xu, T.B., Moore, I.D. and Gallant, J.C., 1993. Fractals, Fractal Dimensions and Landscapes - a Review. *Geomorphology*, 8(4): 245-262.
- Young, I.R. and Holland, G.J., 1996. An atlas of the oceans' wind and wave climate, 1st edition. Pergamon, New York.
- Zhang, W. and Montgomery, D., 1994. Digital elevation model grid size, landscape representation and hydrologic simulations. *Water Resources Research*, 30: 1019-1028.
- Zhu, X.H., Cai, Y.L. and Yang, X.C., 2004. On fractal dimensions of China's coastlines. *Mathematical Geology*, 36(4): 447-461.
- Zühlsdorff, C., Hanebuth, T.J.J. and Henrich, R., 2008. Persistent quasi-periodic turbidite activity off Saharan Africa and its comparability to orbital and climate cyclicities. *Geo-Marine Letters*, 28(2): 87-95.

## PUBLICATIONS OF THE AUTHOR

### Journals

**Porter-Smith, R.**, Lyne, V.D. and Kloser, R.J., (in prep). Catchment-based classification of Australia's continental slope canyons.

**Porter-Smith, R.**, (in prep). Mesoscale coastal complexity and its relationship to structure and forcing from terrestrial and marine processes.

**Porter-Smith, R.**, Harris, P.T., Heap, A.D., Anderson, O., Coleman, R., Greenslade, D., Jenkins, C.J. & McQuillan, P. (In prep) Classification of the Tasmanian Continental Shelf using multivariate analysis of wave and tide dynamics and physical sediment parameters.

**Porter-Smith, R.**, Harris, P. T., Anderson, O., Coleman, R., & Greenslade, D., & Jenkins, C.J (2004). Classification of the Australian continental shelf based on predicted sediment threshold exceedance due to tidal currents and swell waves. *Marine Geology* Vol 211/1-2 pp 1-20.

**Porter-Smith, R.**, (2003) Bathymetry of the George V<sup>th</sup> Land shelf and slope, *Deep Sea Research Part II*, Vol. 50/8-9 pp 1337 - 1341.

Harris, P. T., Heap, A., Bryce, S., **Porter-Smith, R.**, Ryan, D., & Heggie, D.T. (2002). Classification of Australian clastic coastal depositional environments based upon a quantitative analysis of wave, tidal and river power. *Journal of Sedimentary Research*, Vol. 72, No 6, pp 858-870.

### Conference Abstracts and Papers

**Porter-Smith, R.** and Lyne, V.D. (2007). Regionalisations of the Australian coastal and marine environment: A geophysical perspective. GeoHab, Marine Benthic Habitats of the Pacific and Other Oceans: Status, use and management. Noumea, New Caledonia.

Hayes, D., Fulton, E., Condie, S. A., Rhodes, J., **Porter-Smith, R.**, Astles, K., and Cui, G. (2007). Ecosystem Modelling, a Tool for Sustainable Regional Development. .

MODSIM07 International Congress on Modelling and Simulation : Land, water & environmental management : integrated systems for sustainability : proceedings , Christchurch, New Zealand. Christchurch: Modelling and Simulation Society of Australia and New Zealand.

Last, P. R., Lyne V. D., **Porter-Smith, R.**, Yearsley, G. K., Gomon, M. F., Hayes, D. E., Gledhill, D. C., Rees, A. J. J., and White, W. T. (2006). Application of a demersal regionalization framework to assess faunal structuring on Australias continental shelf and slope and their relationship to deepwater geophysical properties. In: GeoHab Conference, Edinburgh, Scotland.

Lyne V. D., Hayes, D. E., **Porter-Smith, R.**, and Last, P. R. (2006). Application of a demersal regionalization framework to assess faunal structuring on australias continental shelf and slope and their relationship to deepwater geophysical properties. In: GeoHab Conference, Edinburgh, Scotland.

Lyne V. D., Hayes, D. E., **Porter-Smith, R.**, and Last, P. R. (2006). Development and application of a pelagic regionalisation for Australia's marine jurisdiction. In: GeoHab Conference, Edinburgh, Scotland.

Lyne, V. D., Hayes, D. E., **Porter-Smith, R.**, Griffiths, F. B., and Condie, S. A. (2005). Pelagic regionalisation national marine bioregionalisation integration project: summary report. National Marine Bioregionalisation of Australia. Hobart, Tas.: National Oceans Office DVD.

**Porter-Smith, R.**, Harris, P.T., Heap, A.D., Anderson, O., Coleman, R., Greenslade, D., Jenkins, C.J. & McQuillan, P. (2002) Classification of the Tasmanian Continental Shelf using multivariate analysis of wave and tide dynamics and physical sediment parameters. *Proceedings of Annual Conference of the Australian Marine Science Association*, Townsville, Qld. 10-12 July, 2002, p. 106.

**Porter-Smith, R.**, (2002) Bathymetry of the George V<sup>th</sup> Land shelf and slope, *Special workshop, Annual Conference of the Australian Marine Science Association*, Townsville, Qld. 9-10 July.

**Porter-Smith, R.**, Harris, P.T., Andersen, O., Coleman, R., Greenslade, D., and Jenkins, C.J. (2001) Classification of the Australian continental shelf based on predicted sediment threshold exceedance due to tidal currents and swell waves. *Proceedings of Annual Conference of the Australian Marine Science Association*, Townsville, Qld. 3-6 July, 2001, p. 132.

**Porter-Smith, R.**, Harris, P.T., Andersen, O., Coleman, R., Greenslade, D., and Jenkins, C.J. (2001) Classification of the Australian continental shelf based on predicted

sediment threshold exceedance due to tidal currents and swell waves. *COGS 2001-Proceedings Fifth Australian Marine Geoscience Conference*, Hobart, TAS, 27-29 June, 2001, p. 39.

Harris, P.T., **Porter-Smith, R.**, Andersen, O., Coleman, R., & Greenslade, D. (2001) GEOMAT – Modelling of continental shelf sediment mobility in support of Australia's regional marine planning process. *Proceedings of the Geological Association of Canada and Mineralogical Association of Canada Joint Annual Meeting*, St Johns Newfoundland, Canada, 27-30 May, 2001, Vol. 26, p. 59.

Harris, P. T., Heap, A., Bryce, S., **Porter-Smith, R.**, Ryan, D., & Heggie, D. (2001). Classification of Australian coastal depositional environments based upon a quantitative analysis of wave, tidal and fluvial power. *COGS 2001-Proceedings Fifth Australian Marine Geoscience Conference*, Hobart, Tas., 27-29 June, 2001, p. 17

Harris, P. T., Heap, A., Bryce, S., **Porter-Smith, R.**, Ryan, D., & Heggie, D. (2001). Classification of Australian coastal depositional environments based upon a quantitative analysis of wave, tidal and fluvial power. *Proceedings of Annual Conference of the Australian Marine Science Association*, Townsville, Qld. 3-6 July, 2001, p. 156.

Harris, P. T., Heap, A., Bryce, S., **Porter-Smith, R.**, Ryan, D., & Heggie, D. (2001). Classification of Australian coastal depositional environments based upon a quantitative analysis of wave, tidal and fluvial power. *Proceedings of the 21<sup>st</sup> Meeting of the International Association of Sedimentologists*, Davos, Switzerland, 3-5 September, 2001, p. 89.

Harris, P.T., **Porter-Smith, R.**, Heggie, D., Heap, A., Bryce, S., Ryan, D. (2000) Classification of Australian estuaries based on wave, tide and river energy regime. Third International River Management Symposium, Brisbane, Qld., 6-8 Sept., 2000, p. 33.

**Porter-Smith, R.** and Harris, P.T (2002). Improved bathymetric model resulting from WEGA Voyage 5.1, RV TANGAROA. Workshop at Antarctic CRC, Hobart, December 2000.

**Porter-Smith, R.**, Harris, P.T., Anderson, O. and Coleman, R. (1999) Classification of the Australian continental shelf based on predicted sediment threshold exceedance due to tidal currents and swell waves. Fourth Australian Marine Geology Conference. Exmouth, Western Australia, 26 Sept - 1 Oct., 1999, pp. 48-50.

## Reports

- Lyne, V.D., White, W.T., Gledhill, D., Last, P.R., Rees, T. and **Porter-Smith, R.**, 2009. Analysis of Australian continental shelf provinces and biomes based on fish data, CSIRO Marine & Atmospheric Research, Hobart.
- Heap, A., Bryce, S., Ryan, D., Radke, L., Smith, C., **Porter-Smith, R.**, Harris, P., & Heggie, D. (2001). Australian Estuaries & Coastal Waterways: A Geoscience Perspective for Improved and Integrated Resource Management, A Report to the National Land & Water Resources Audit Theme 7: Ecosystem Health. Australian Geological Survey Organisation, Record No. 2001/7.
- Butler, A., Harris, P.T., Lyne, V., Heap, A., Passlow, V. and **Porter-Smith, R.**, 2001. An Interim Bioregionalisation for the continental slope and deeper waters of the South-East Marine Region of Australia.
- Harris, P. T., **Porter-Smith, R.**, Anderson, O., Coleman, R., & Greenslade, D. (2000). GEOMAT - Modelling of Continental Shelf Sediment Mobility in Support of Australia's Regional Marine Planning Process. Australian Geological Survey Organisation Record No. 2000/41.
- Harris, P. T., **Porter-Smith, R.**, & O'Brien, P. E. (1999). Report on BASSLINK cable route in Bass Strait: Seabed geology, bathymetry, and sediment mobilisation. Confidential Report prepared for: William Wood and Associates Pty Ltd, Environmental Management Consultants, Relbia, TAS No. Australian Geological Survey Organisation.